

Chris Done · Marek Gierliński · Aya
Kubota

Modelling the behaviour of accretion flows in X-ray binaries

Everything you always wanted to know about accretion
but were afraid to ask

Received: date

Abstract We review how the recent increase in X-ray and radio data from black hole and neutron star binaries can be merged together with theoretical advances to give a coherent picture of the physics of the accretion flow in strong gravity. Both long term X-ray light curves, X-ray spectra, the rapid X-ray variability and the radio jet behaviour are consistent with a model where a standard outer accretion disc is truncated at low luminosities, being replaced by a hot, inner flow which also acts as the launching site of the jet. Decreasing the disc truncation radius leads to softer spectra, as well as higher frequencies (including QPO's) in the power spectra, and a faster jet. The collapse of the hot flow when the disc reaches the last stable orbit triggers the dramatic decrease in radio flux, as well as giving a qualitative (and often quantitative) explanation for the major hard-soft spectral transition seen in black holes. The neutron stars are also consistent with the same models, but with an additional component due to their surface, giving implicit evidence for the event horizon in black holes. We review claims of observational data which conflict with this picture, but show that these can also be consistent with the truncated disc model. We also review suggested alternative models for the accretion flow which do not involve a truncated disc. The most successful of these converge on a similar geometry, where there is a transition at

C. Done and M. Gierliński
Department of Physics
University of Durham
South Road, Durham, DH1 3LE, UK.
E-mail: Chris.Done@durham.ac.uk, Marek.Gierlinski@durham.ac.uk

A. Kubota
Institute of Physical and Chemical Research (RIKEN),
2-1 Hirosawa, Wako, Saitama 351-019, Japan
Present address: Electronic Information Systems, Shibaura Institute of Technology
307 Fukasaku, Minuma-ku, Saitama-shi, Saitama 337-8570, Japan
E-mail: aya@shibaura-it.ac.jp

some radius larger than the last stable orbit between a standard disc and an inner, jet dominated region, with the X-ray source associated with a mildly relativistic outflow, beamed away from the disc. However, the observed uniformity of properties between black holes at different inclinations suggests that even weak beaming of the X-ray emission may be constrained by the data.

After collapse of the hot inner flow, the spectrum in black hole systems can be dominated by the disc emission. Its behaviour is consistent with the existence of a last stable orbit, and such data can be used to estimate the black hole spin. By contrast, these systems can also show very different spectra at these high luminosities, in which the disc spectrum (and probably structure) is strongly distorted by Comptonization. The structure of the accretion flow becomes increasingly uncertain as the luminosity approaches (and exceeds) the Eddington luminosity, though there is growing evidence that winds may play an important role. We stress that these high Eddington fraction flows are key to understanding many disparate and currently very active fields such as ULX, Narrow Line Seyfert 1's, and the growth of the first black holes in the Early Universe.

Keywords accretion, accretion discs · black hole physics · X-rays: binaries

1 Introduction

Understanding black hole accretion is important for its own sake. However, it also has much wider physical and astrophysical implications. Luminous accretion flows light up their surroundings, regions of strongly curved space-time. The distortions imprinted on the observed spectrum from special and general relativity depend on the velocity and geometry of the luminous material as well as on the shape of the potential (Cunningham 1975; Fabian et al. 1989; Fabian et al. 2000). Thus observational tests of Einstein's gravity depend on understanding these properties of the accretion flow. On larger scales, accretion is now realized to be a key to understanding the growth of structure in the Universe.

Most galaxies have a central black hole, the growth of which is somehow linked to the growth of the galaxy as a whole, as the mass of the stellar bulge on kpc scales correlates with the mass of the black hole on subparsec scales (see e.g. Tremaine et al. 2002). There is strong evidence that the mechanism for this is linked to feedback from the accretion flow, which reheats gas in clusters of galaxies, preventing runaway cooling and so regulating star formation (e.g. di Matteo, Springel & Hernquist 2005). The coeval growth of galaxies and their central black holes is also shown by the similar redshift for peak activity for both quasars and star formation at $z \sim 2$ (e.g. Boyle & Terlevich 1998), while at much higher redshifts the radiation from these first objects (accreting black holes and their host galaxies) re-ionizes the Universe (Fan, Carilli & Keating 2006).

There are many new observational constraints on accretion flows in strong gravity which have led to a revolution in our understanding of these systems. Much of this has come from the RXTE satellite, with its huge database of

X-ray observations of the accretion flow in galactic binary systems. Concurrently there has also been a huge increase in radio data for these objects, tying the jet emission into the accretion flow. Last, but certainly not least, this has driven major advances in our theoretical understanding of these systems. There is now an emerging picture which can provide a framework for understanding the bewildering variety of spectra and variability (including the multiple Quasi Periodic Oscillations, hereafter QPO's) seen from accretion flows in strong gravity. The focus of this review is to describe how these current models of the changing nature and geometry of the accretion flow can give a framework in which to broadly explain the majority of the behaviour seen from these objects.

While this review concentrates on stellar remnant compact objects, the physical processes should be fairly scale invariant. Understanding accretion in strong gravity anywhere should give us pointers to understanding it everywhere, with the accretion flows in Galactic binaries giving a baseline model for the accretion flows onto higher mass black holes in ultra-luminous X-ray sources, active galaxies and quasars.

2 Accretion discs: Spectra and stability

Astrophysical black holes are very simple objects, possessing only mass and spin. In steady state the accretion flow should be completely determined by these parameters, together with the mass accretion rate. Much of the dependence on mass can be removed by scaling the accretion rate to the Eddington accretion rate, as sources emitting at similar fractions of the Eddington luminosity, L/L_{Edd} , should have similar accretion flows. The only other parameters which can affect the observational appearance of these systems are the inclination angle, and any non-stationary effects from variability behaviour. The problem is then simply to determine how the properties of the accretion flow depend on this very restricted physical parameter set.

Mass (and inclination) is potentially observable from the binary orbit. Spin is more difficult to measure. Unlike mass it does not leave a discernable mark on the external spacetime at large distances, making a significant difference only close to the event horizon. Mass accretion rate is also not trivial to observe. The luminosity produced per unit mass accreted depends on the gravitational potential. This depends on spin, as the last stable orbit is dragged inwards for a rotating black hole, but it also depends on the nature of the accretion flow at this point. If gravity is the only force acting then the gravitational energy gained in the region between the last stable orbit and the horizon simply remains with the rapidly infalling material (stress-free boundary assumption: Novikov & Thorne 1973). However, there can be pressure forces and/or magnetic forces which might violate this in a hot and/or magnetically dominated flow (Abramowicz et al. 1988; Agol & Krolik 2000). As well as this uncertainty on the total energy available, there is also the potentially larger uncertainty attached to what fraction of this is radiated as opposed to powering winds and/or a jet and/or being carried along with the material (advected). The observed X-ray luminosity is only a tracer, and

probably a non-linear tracer, of the total mass accretion rate (e.g Kording, Fender & Migliari 2006).

2.1 Steady State Accretion Discs

The structure of the accretion flow is derived by balancing gravitational heating against cooling so depends at the outset on which set of heating/cooling processes are assumed to be important. In the canonical approach of Shakura & Sunyaev (1973), the assumption is that viscous stresses convert the gravitational potential to heat, and that the heat released at a given radius is radiated locally (so advection, winds and jet cooling are neglected). The resulting spectrum is rather robust if the energy thermalizes, so at given radius, $r = R/R_g$ (where R_g is the gravitational radius GM/c^2) the disc emits as a (quasi) blackbody of temperature $T(r) \propto r^{-3/4}$. At smaller radii there is more luminosity generated as gravity is stronger, and this is dissipated over a smaller area, so the temperature increases inwards. This solution gives a geometrically thin disc except at luminosities close to Eddington.

The assumption that the energy thermalizes means that the spectrum is (to zeroth order) independent of the details of the viscosity mechanism. Thus the models can predict the observed disc spectra using only phenomenological descriptions of the stresses, most notably the Shakura–Sunyaev α prescription, where the shear stresses, $t_{r\phi}$, are assumed to be directly proportional to total pressure $P_{tot} = P_{gas} + P_{rad}$, so $t_{r\phi} = \alpha P_{tot}$. A key breakthrough in the last 10 years has been identifying the physical origin of the stress as the magnetic rotational instability (MRI: see e.g. the review by Balbus 2005), a self-sustaining dynamo process. Numerical simulations including this self-consistent heating are still in their infancy but already yield significant insights into the nature of the jet (see Section 8), and promise much future progress (see e.g. Balbus 2005).

2.2 Stability and Time Dependence

The Shakura–Sunyaev disc solution described above is a global solution, i.e. it assumes that the mass accretion rate is *constant* with radius. This is not necessarily true, and in fact Shakura–Sunyaev accretion discs are subject to two major instabilities, one connected to the ionization of hydrogen which is triggered at fairly low luminosities and controls the long term outburst behaviour of the accreting sources, and the other due to radiation pressure, which should occur at higher luminosities.

The accretion flow stability at a given radius is a function of the heating and cooling mechanisms chosen. Generically, the flow is *thermally* unstable if small perturbations in temperature grow i.e. if a small increase in temperature causes a further rise in temperature. Similarly, the flow is *viscously* (or secularly) unstable if a small increase in mass accretion rate, \dot{M} , leads to a larger increase in \dot{M} so that the disc is eaten away at that radius. The timescale for these instabilities to grow are $t_{th} \sim \alpha^{-1} t_{dyn}$ and

$t_{visc} \sim \alpha^{-1}(H/R)^{-2}t_{dyn}$, where H is the vertical scale height of the disc, and the dynamical (orbital) timescale, $t_{dyn} = 4.5 (m/10) (r/6)^{3/2}$ ms for a Schwarzschild black hole of mass mM_{\odot} (see e.g. Frank, King & Raine 2002; hereafter FKR, and Kato, Fukue & Mineshige 1998, hereafter KFM). For a thin disc, the thermal timescale is much faster than the viscous one as $H/R \ll 1$. Hence the thermal instability takes place without there being time to change the amount of material in the disc at that radius if $H/R \ll 1$. Conversely, both timescales are more or less equal for a geometrically thick flow so the disc structure can respond to the changing temperature (FKR, KFM).

2.2.1 Hydrogen Ionization Instability

A Shakura–Sunyaev disc at low mass accretion rates is unstable both thermally and viscously for temperatures around that associated with the ionization of hydrogen, i.e. 10^4 – 10^5 K. For low mass accretion rates, the temperature is low so the material is mostly neutral. The opacity is also low, much lower than predicted by free–free processes as the electrons are bound (see e.g. Cannizzo & Reiff 1982). However, the opacity rises extremely steeply between 10^4 – 10^5 K, so that a small increase in temperature of the material produces a huge increase in opacity as the highest energy photons on the Wien tail of the thermal distribution are able to ionize some of the hydrogen in the disc. This means that these photons are absorbed, so their energy stays in the disc, increasing its temperature, rather than escaping to cool the material. More of the photons can ionize H, so more are trapped in the disc, increasing the temperature still further. This thermal runaway only stops when H is almost completely ionized, so that there is no longer a rapid jump in opacity of the disc to give the rapid decrease of disc cooling and hence the rapid increase in disc temperature (KFM; FKR).

The thermal instability then triggers the viscous instability, as the increased temperature means an increased mass accretion rate through the annulus (as the viscous stresses are proportional to pressure in the Shakura–Sunyaev α prescription). This is now larger than the input mass accretion rate (which was just enough to take the temperature of the annulus to 10^4 K to trigger the instability), so the material in the disc is eaten away at this radius. The pressure decreases, so the heating decreases, so the temperature decreases until hydrogen is able to recombine. This triggers the thermal instability again, this time with the cooling running away until H is mostly neutral again at temperatures below 10^4 K. But this low temperature gives lower mass accretion rate than input so the disc builds up again (KFM; FKR).

This description of the H ionization limit cycle is a purely local instability, i.e. at a single radius in the disc. However, the discontinuous jump in temperature and hence in mass accretion rate means that it will affect the next annulus of disc material. This can have a global impact on the disc structure if the difference in mass accretion rate between the ionized and neutral material is large enough. The whole disc structure can then do limit cycle behaviour between a Shakura–Sunyaev disc with larger mass transfer rate than

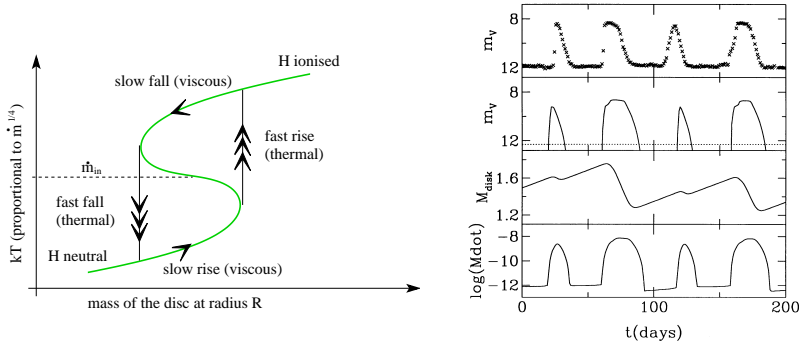


Fig. 1 The hydrogen ionization instability. The figure on the left shows the local effect of the instability, where the mass accretion rate through the disc jumps discontinuously at a given radius. The right hand panel shows results from theoretical models of the effect of this local instability on the global disc structure. The entire disc alternates between periods of outburst and quiescence, matching very well to the observed behaviour of dwarf novae such as SS Cyg, as shown in the top panel. From Cannizzo (1993).

from the companion, so the whole disc is being eaten away on the viscous timescale, to a quiescent disc where H is mostly neutral everywhere. The quiescent disc structure is very unlike that predicted by the Shakura–Sunyaev equations as it does not have constant mass accretion rate at all radii. Instead it has more or less constant temperature, so has mass accretion rate decreasing at smaller radii (e.g. the review by Lasota 2001).

The disc instability model (DIM) of the observed outbursts can be summarized as follows (e.g. Lasota 2001). The quiescent disc builds up from steady mass transfer from the companion. Eventually this gets hot enough to trigger the H ionization instability at some radius. The increased mass accretion rate then increases the mass accretion rate through the next radius in the disc. This triggers the H ionization instability, and a heating wave propagates inwards (and outwards) through the entire disc. This increased mass accretion rate is maintained until the outer disc temperature dips below the H ionization temperature. This propagates a cooling wave, which switches the entire disc back into the quiescent state after only a small fraction of the mass in the disc has been accreted. Such alternating periods of disc outbursts and quiescence are seen in the dwarf novae subclass of disc accreting white dwarf systems (Cataclysmic Variables). The characteristic light curve of the disc is shown in Fig. 1 (KFM, FKR)

However, time-dependent disc codes can only produce this behaviour if the viscosity is dramatically different above and below the H ionization instability. The observed outburst behaviour of accreting white dwarfs (simpler laboratories of disc physics as they are less extreme than neutron stars and black holes: see e.g. reviews by Osaki 1996 and Lasota 2001) can only be produced if the scaling of the stress with total pressure changes by a factor 5–10 (Smak 1984). This may have a physical origin in the behaviour of the MRI. H is neutral in quiescence, so there are very few free electrons to an-

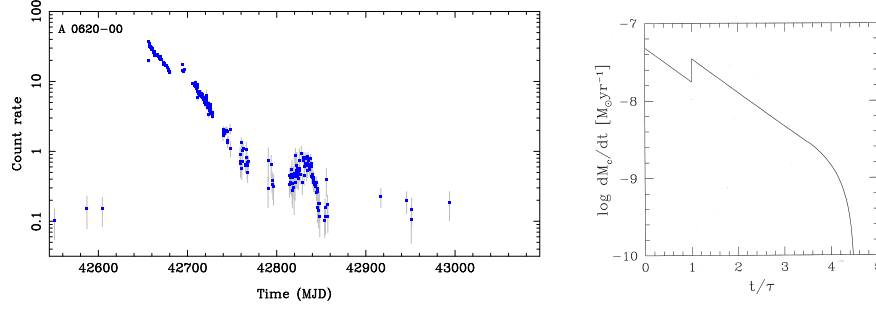


Fig. 2 The left panel shows the X-ray light curve of the BHB A 0620-00 from the Ariel V all sky monitor. The fast rise, followed by an exponential decay (with a reflare) is well matched by theoretical models of the hydrogen ionization instability controlling the fast rise, with irradiation preventing the disc switching back into quiescence, leading to the exponential decay when the irradiation is strong enough to keep the whole disc above the hydrogen ionization temperature, and then to a linear decay as this region shrinks in size (From King & Ritter 1998).

chor the magnetic fields. The MRI may be suppressed, and much less efficient hydrodynamic processes such as spiral waves, probably dominate the stress (Gammie & Menou 1998). This may only be the case in the Galactic binary discs. Supermassive black holes have Shakura-Sunyaev discs with much lower density, so recombination is not so effective at suppressing free electrons from e.g. potassium, iron etc., so even when H is mostly neutral then the MRI may still be able to operate. The disc instability is then purely local, not global, and does not lead to the same outburst/quiescence behaviour (Menou & Quataert 2001) despite the disc temperature crossing the H-ionization regime (Siemiginowska, Czerny, & Kostyunin 1996; Burderi, King & Szuszkiewicz 1998).

The disc instability in neutron star (hereafter NS) and black hole binaries (hereafter BHB) gives very different behaviour to that of the white dwarfs. Fig. 2 shows an example of this. While the quiescent disc and fast rise to outburst can be modelled by the same codes as work for the white dwarf discs, they cannot produce the quasi-exponential decay (KFM; Lasota 2001). This is because the hugely luminous inner disc in these X-ray binary systems means that irradiation is also important, which can keep the disc hot even at large radii (van Paradijs 1996). If the irradiation is strong enough to prevent H recombining then the disc is kept on the hot branch, with a higher mass accretion rate than supplied by the companion. This eats away the disc, pulling its temperature down, reducing the mass accretion rate through the disc which decreases the X-ray irradiation. This gives the characteristic exponential decay if the whole disc is irradiated, but eventually the irradiation becomes weak enough that the outer disc temperature goes below the hydrogen ionization and switches to the cool branch. However, the cooling front is prevented from propagating inwards on the viscous timescale as its innermost radial extent is set by the radius of the irradiated region. This leads to linear decays (King & Ritter 1998; Lasota 2001).

Since we observe such exponential decays (see Fig 2), the disc must be irradiated. The optical light from discs in X-ray binaries is also much brighter than predicted by the Shakura–Sunyaev disc, again pointing to the importance of irradiation (van Paradijs & McClintock 1994). However, the disc shape is probably convex so that it self-shields the outer disc for irradiation from the bright, inner regions (Dubus et al. 1999). One potential way around this is if there is tenuous material above the disc which can intercept some small fraction of the X-ray flux and scatter it down onto the disc (Dubus et al. 2001; Lasota 2001). Such material can clearly be seen in the small subset of systems which are seen almost edge on. In these cases the disc and/or companion star can completely obscure a direct view of the bright inner disc and intrinsic hard X-ray coronal emission (and the boundary layer between the disc and surface in the neutron stars), so that the X-ray source is only seen via scattering in an accretion disc corona (ADC: e.g. Frank, King & Lasota 1987; FKR; see Section 10). The name is somewhat confusing as this material is in all probability some sort of large scale wind/outflow from the outer disc (Begelman, McKee & Shields 1983) and so is physically separate from the intrinsic hard X-ray emitting region which is small, and close to the central object but is also sometimes termed ‘the corona’.

These models of irradiated discs can also explain the distinction in disc stability between BHB in Low Mass X-ray Binaries (hereafter LMXB) and High Mass X-ray Binaries (HMXB) powered (mostly) by Roche lobe overflow such as Cyg X-1, LMC X-1 and LMC X-3. For a given mass black hole, a high mass companion star typically has a much higher mass accretion rate than a low mass one, giving a higher outer disc temperature. This effect more than compensates for the lower temperature expected from the larger outer disc radius from the larger orbit, so the outer edge of the disc is generally above the H ionization instability in HMXB (van Paradijs 1996). All of the 3 known BHB persistent sources (Fig. 5) are HMXB, though it is also possible for LMXB BHB to be persistent at fairly low luminosities (Menou, Narayan & Lasota 1999).

Similarly, these disc models can also explain the difference in stability properties between the neutron star and BHB LMXB. A neutron star primary has lower mass than a black hole, so for a given mass companion overflowing its Roche lobe requires a smaller binary orbit. Smaller orbital separation means a smaller disc due to tidal truncation so the outer disc does not extend to such low temperatures, so is more likely to be stable. Many neutron star LMXB are persistent sources while *all* known LMXB BHB are transient (King, Kolb & Burderi 1996; Dubus et al. 1999). Fig. 6 shows light curves of five neutron star systems. Two of them, 4U 1608–52 and Aql X-1, are recurrent transients, where the systems are known to have large orbital periods. This requires that the companions are somewhat nuclear evolved in order that they fill their Roche lobes, and the resulting large disc can go unstable on its outer edge (King et al. 1997). This is presumably also the case for the other known NS transients, apart from the millisecond pulsars, where the disc is unstable because the orbit is so small rather than so large. These have companions where the mass transfer rate is low enough that the

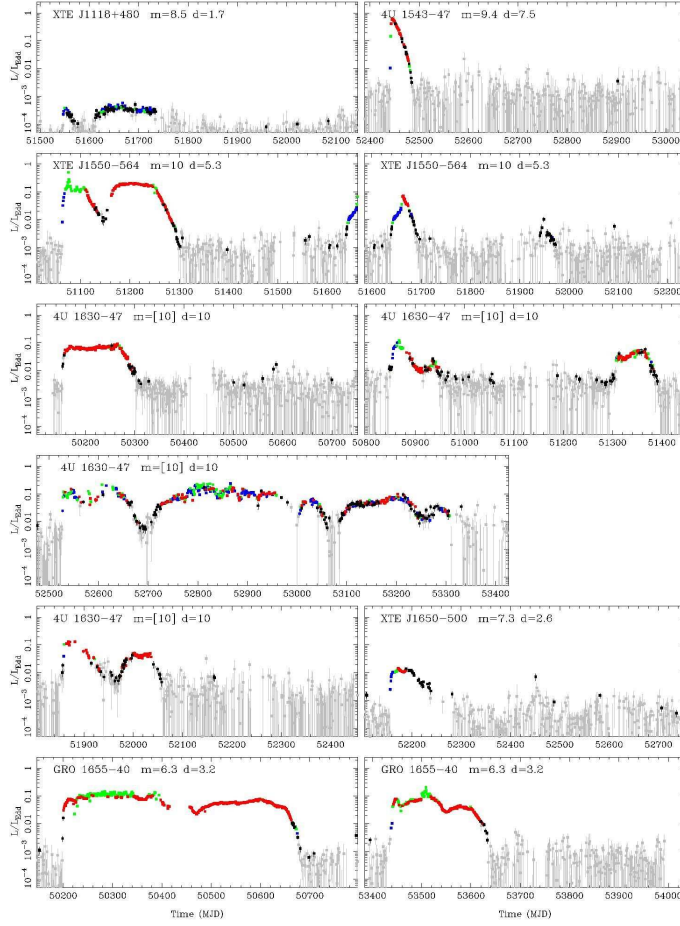


Fig. 3 *RXTE All Sky Monitor* light curves of BHB LMXB showing the outburst behaviour. Blue, green and red points indicate that the spectral hardness corresponds to the hard, very high and soft states, respectively, while black indicates that the uncertainties on the colour are too large to assign a state. Grey points correspond to non-detections (3σ). m is the mass (in M_{\odot}) and d is the distance (in kpc) used for Eddington luminosity estimates (see Gierliński & Newton 2006 for details).

outer disc edge temperature drops below the H-ionization point even though the disc is tiny (Chakrabarty & Morgan 1998; Ergma & Antipova 1999).

While much is now understood, the detailed shape of the light curves of many of the systems still hold some puzzles. In both NS and BHB, the accretion rate through the disc can be *variable* even in persistent systems e.g. 4U 1705-44 and Cyg X-1, while the outburst light curves of many transients,

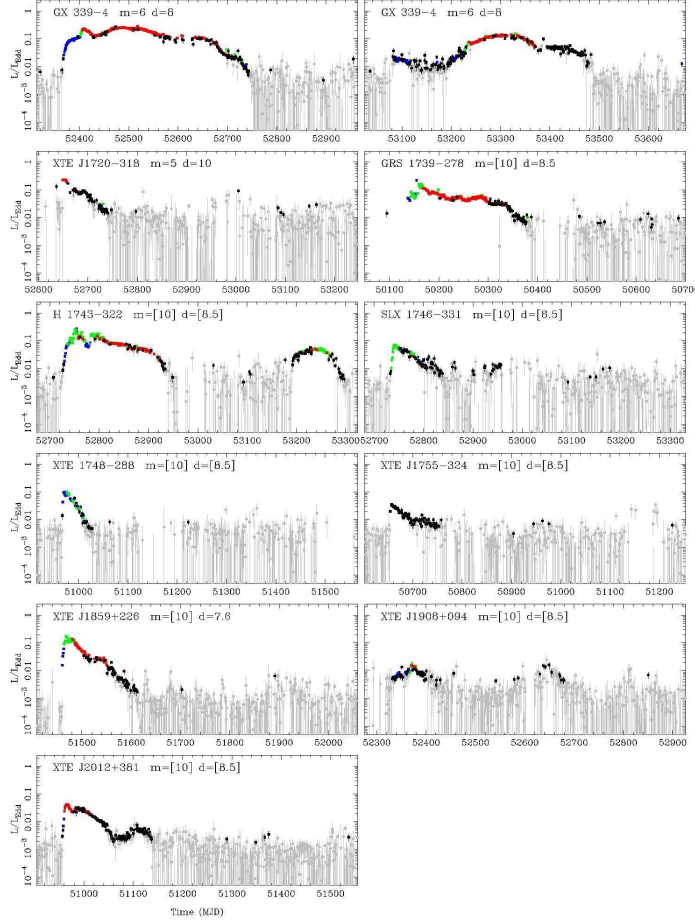


Fig. 4 As for Fig. 3

especially the longer period systems, can be much more complex than simple exponential or linear decays (see Figs. 5, 6). The interplay between the irradiation controlled H-ionization instability and the tidal instability and/or an enhanced mass accretion rate from the irradiated companion may go some way to explaining the variety of light curve behaviour shown in Figs. 3, 4 (e.g. the review by Lasota 2001). Nonetheless, the match between the disc theory and the observed long timescale light curves provide compelling evidence for something very like a Shakura–Sunyaev outer disc in these systems.

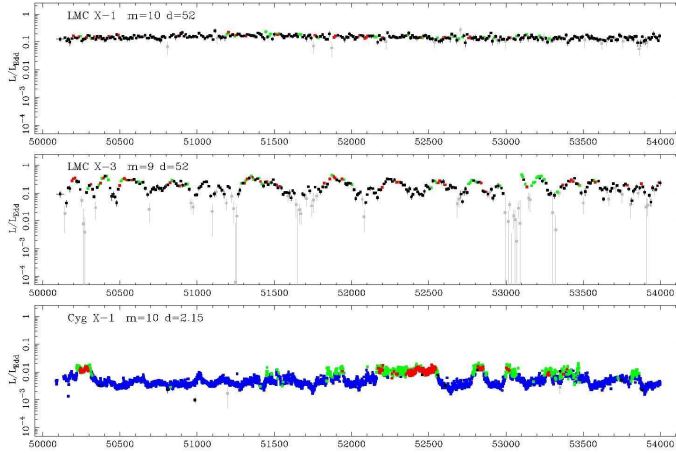


Fig. 5 As for Fig. 3 but for the BHB HMXB. These are all persistent sources due to the high mass transfer rate from the high mass companion star which keeps the whole disc above the hydrogen ionization instability point. However, although they do not show dramatic outbursts, they do show variability, which can lead to spectral transitions. Note the change in X-axis scale from the previous ASM plots.

2.3 The radiation pressure instability

The Shakura–Sunyaev disc is also unstable at high mass accretion rates at small radii due to the rapid increase in heating as the disc goes from being gas pressure dominated ($P_{\text{gas}} = nkT$) to being radiation pressure dominated ($P_{\text{rad}} = \sigma T^4/3c$). A small increase in temperature at this point causes a large increase in pressure, and hence a large increase in heating since the stresses are assumed to be $\propto P_{\text{tot}}$. This gives a large increase in temperature which is not balanced by any correspondingly large decrease in opacity to increase cooling, so there is runaway heating.

In the Shakura–Sunyaev disc equations there is no high mass accretion rate, high temperature stable solution as in the H ionization instability, so the runaway predicts complete disruption of the disc. However, incorporating radial advection into the equations gives an additional cooling process as some fraction of the energy is carried along with the flow into the next annulus as well as there being energy losses through radiation (Abramowicz et al. 1988). This can balance the increased heating, giving a stable upper branch and so the possibility of the same sort of thermal-viscous limit cycle as discussed above for the H ionization instability. However, there are several key differences. Firstly, the disc typically has $H/R \sim 1$ on the advection dominated slim disc branch. Thus viscous and thermal timescales are not so different, so the amount of material in the annulus changes with the temperature. Secondly, there is probably no change in the viscosity mechanism (MRI for both the gas pressure and radiation pressure dominated branches). The

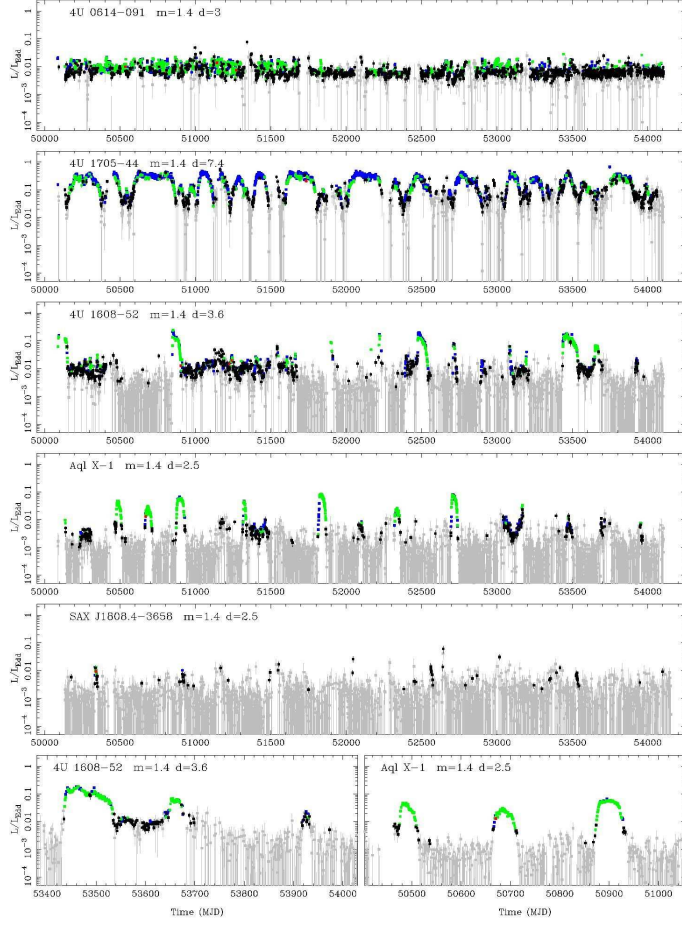


Fig. 6 As for Fig. 3 but for the neutron star LMXB systems (atolls). In contrast to the BHB, most of the known systems are persistent, so are shown on the same X-axis scale as in Fig. 5. Again, they can show smaller scale variability, and this can trigger state transitions. However, there are a few transients, e.g. 4U 1608–52 and Aql X–1, where the secondary is evolved into a (sub)giant, or the millisecond pulsars such as SAX J1808.4–3658 where the companion is almost completely accreted. Selected individual outbursts from 4U 1608–52 and Aql X–1 are shown on the same scale as the transient LMXB BHB outbursts in Figs. 3 and 4 to highlight the similarities in behaviour.

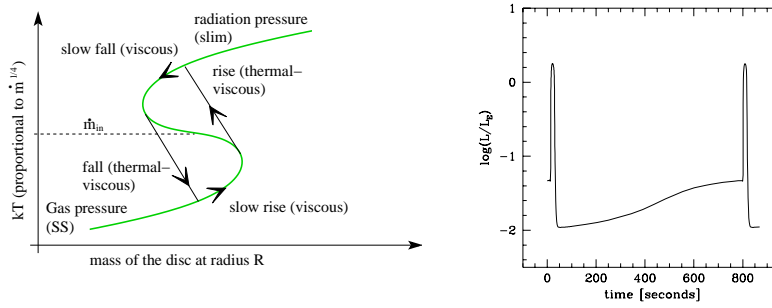


Fig. 7 The radiation pressure instability. The figure on the left shows the local effect of the instability, where the mass accretion rate through the disc jumps discontinuously at a given radius. The right hand panel shows results from theoretical models of the effect of this local instability on the global disc structure with standard Shakura–Sunyaev viscosity ($\alpha = 0.1$), for $L/L_{\text{Edd}} = 0.06$. No BHB shows anything like this behaviour (From Szuszkiewicz & Miller 2001).

combination of these two effects mean that the local instability can propagate, but it is only the radiation pressure dominated part of the disc which becomes globally unstable rather than the entire disc.

However, unlike the H-ionization instability for the outer disc, there is very little evidence that the radiation pressure instability exists as described here. Disc with the classic Shakura–Sunyaev stress prescription become radiation pressure unstable at around $\geq 0.06L_{\text{Edd}}$, and produce limit cycles (Honma, Kato & Matsumoto 1991; Szuszkiewicz & Miller 2001; Merloni & Nayakshin 2006). The inner disc is where most of the gravitational energy is released, so this instability has a dramatic effect on the light curve (see Fig. 7). Yet the spectra of BHB show *stable* disc spectra up to at least $0.7L_{\text{Edd}}$ (see Section 2.1).

This plainly shows that the classic Shakura–Sunyaev stress prescription is wrong! Alternative stress prescriptions with heating proportional to gas pressure only are stable everywhere (Stella & Rosner 1984). However, the super-Eddington BHB GRS 1915+105 *does* show something which looks very much like a limit cycle in some of its light curves (see Section 11). Thus it seems more likely that the effective stress scales somewhat more slowly with temperature than predicted by radiation pressure, but somewhat faster than predicted by gas pressure alone. Analytic estimates of the effective stress produced by the MRI indicate that it may be more appropriate to describe the heating as proportional to the geometric mean of the gas and total pressure (Merloni 2003). Such discs are locally unstable at $L/L_{\text{Edd}} \sim 0.3$, but the effects of advection from neighbouring annuli mean that this is damped out, making this prescription stable to somewhat higher luminosities, around $L/L_{\text{Edd}} \sim 0.4$ (Honma, Kato & Matsumoto 1991; Merloni & Nayakshin 2006). This seems very promising, especially as the exact onset of the instability is quite sensitive to small changes in the effective α prescription around

this point (KFM). Thus a small tweak in stress scaling from the geometric mean could probably give the stability limit beyond ~ 0.5 as observed, followed by the onset of the radiation pressure instability at higher luminosities required to explain the unique limit cycle like behaviour of GRS 1915+105 (see e.g. the review by Fender, & Belloni 2004). This is the only BHB in our Galaxy which spends significant amounts of time at luminosities near Eddington, so plausibly its unique variability is connected to this being the only source with high enough luminosity to trigger the radiation pressure instability (Done, Wardziński & Gierliński 2004, see Section 11).

3 The inner accretion flow

3.1 Spectral states in Cyg X-1

The irradiation controlled H-ionization instability explains much of the observed long term light curve behaviour in both neutron stars and black holes. This is clear evidence for the outer disc having a structure at least something like the (time dependent) Shakura-Sunyaev disc models. However, they do *not* fully explain the spectra. Disc spectra simply change in luminosity and temperature, but maintain their robust, quasi-thermal shape. By contrast, the observed spectra vary tremendously in shape. This has been known since the early days of X-ray astronomy, from the behaviour of the first well studied BHB, Cyg X-1. This shows two very different types of spectra, illustrated in Fig. 8 (Gierliński et al. 1999), plotted in νF_ν so a peak indicates the characteristic photon energy of the source output. As shown in this figure, the alternatively named ‘high’, ‘soft’ or ‘thermal dominant’ state is characterized by a dominant soft component below ~ 10 keV, accompanied by a complex non-thermal tail of emission extending to 500 keV and beyond (Gierliński et al. 1999; McConnell et al. 2000). The soft component is interpreted as thermal emission from an optically thick accretion disc around the black hole, as it can be well reproduced by a multicolour disc model (Dotani et al. 1997 using the DISKBB model; Mitsuda et al. 1984), which approximates the spectrum from a Shakura–Sunyaev disc. However, the tail of emission beyond the disc spectrum which extends to high energies is plainly not explained as part of the standard disc models.

The discrepancy between observations and the disc predictions are even more marked in the other spectral shape seen in Cyg X-1, (see Fig. 8) where a large fraction of the power is emitted in a spectrum which looks entirely unlike a disc. These spectra, alternatively termed ‘low’ or ‘hard’ state, peak instead at ~ 100 keV, though it is accompanied by a low temperature disc component (see Section 4.1).

The varying (and often confusing) nomenclature reflects the growing understanding of these spectra. At first, with observations only covering the classic 2–10 keV bandpass, the difference in count rate of a factor ~ 5 between the two states lead to the ‘high’ and ‘low’ description (see Fig. 5). Increasing spectral coverage showed that the change in bolometric luminosity during the transition is much smaller (e.g. Nowak 1995; Zhang et al. 1997; Gierliński et al. 1999). This, together with the discovery of hysteresis in other

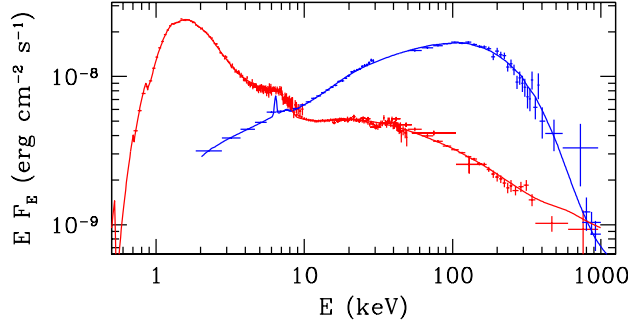


Fig. 8 X/γ-ray spectral states in Cyg X-1. Classical soft (red) and hard (blue) states taken from Gierliński et al. (1999).

BHB (e.g. the review by Nowak 1995; Section 6.1) led instead to the ‘soft’ and ‘hard’ terminology, based on spectral shape rather than intensity. Here we will adopt ‘hard state’ as denoting the low/hard state and ‘soft state’ for the high/soft/thermal dominant state.

Thus both spectral states require that there are two components to the emission from the accretion flow. There is generally some trace of an optically thick disc, which can be dominant (as in the soft state) but this is always accompanied by higher energy emission, which requires that some fraction of the accretion power is dissipated in optically thin material so that the energy does not thermalize to the disc temperature (see e.g. the review of radiative processes in BHB by Zdziarski & Gierliński 2004).

3.2 Optically thin accretion flows: structure

One very attractive possibility for the origin of the optically thin emission component is if the accretion flow itself becomes optically thin. The key assumption for the disc spectra is that the energy thermalizes. This requires that there are multiple collisions between protons and electrons, and multiple collisions between electrons and photons. This is not necessarily the case, especially at low mass accretion rates when the density of the flow becomes low. Early on it was realized that if the flow is hot then it can easily become optically thin to electron-photon collisions. This also implies that the flow is optically thin to electron-proton collisions (e.g. Stepney 1983) which has very important consequences as the protons probably acquire most of the gravitational energy (since gravity acts on mass), yet it is electrons which are by far the more efficient radiators (Shapiro, Lightman & Eardley 1976, hereafter SLE76; Ichimaru 1977; Narayan & Yi 1995). Incomplete thermalization of protons with electrons leads to the formation of a two temperature plasma, where the protons gain most of the gravitational energy and lose very little of it to the electrons, while the electrons gain only a small amount of energy via Coulomb collisions and lose most of it by radiating. Since the flow is optically thin then this radiation is in the form of Comptonization,

bremsstrahlung and/or cyclo-synchrotron rather than blackbody radiation. The proton temperature is close to virial, so the flow has a large scale height, and pressure forces are important as well as centrifugal forces in balancing gravity (SLE76; Ichimaru 1977; Narayan & Yi 1995).

The detailed structure of such hot, optically thin, geometrically thick two temperature flows depends on the conditions assumed. Without advection the properties of the accreting gas are described by SLE76. However, advection of gravitational energy by the protons should always be important for such two temperature flows (Ichimaru 1977; Ion torus: Rees et al. 1982; Advection Dominated Accretion Flow, hereafter ADAF: Narayan & Yi 1995). The classic ADAF solution of Narayan & Yi (1995) is self-similar, imposing a single value for the advected fraction at all radii, with the further assumption that advection is only a cooling process. Yuan (2001) relaxes these assumptions, and shows that the solutions then also include a region at higher luminosities, where the advected fraction is negative (so advection is a heating process) and strongly radially dependent (luminous hot accretion flows, LHAF: Yuan 2001). Both ADAF and the more general LHAF have proton temperatures which are hot enough for the material to be formally unbound, i.e. with positive Bernoulli parameter so can form a wind (Narayan & Yi 1995). The properties of this wind are not well determined, but it can form an advection dominated inflow/outflow solution (ADIOS: Blandford & Begelman 1999) where the mass loss rate probably depends on \dot{M} (Yuan, Cui & Narayan 2005). Convection should also be important in these flows (Blandford & Begelman 1999), and can dominate in the class of models termed convection dominated accretion flows (CDAF: Abramowicz & Igumenshchev 2001).

The full structure of the flow is complex, even in a hydrodynamic description with the Shakura–Sunyaev analytic stress prescription. Yet more complexity should be present with the inclusion of magnetic fields, giving a Magnetically Dominated Accretion Flow (MDAF: Meier 2005) or jets (Jet Dominated Accretion Flow; JDAF: Falcke, K rding, & Markoff 2004). This proliferation of properties for the hot inner flow gave rise to the all inclusive term ?DAF, but numerical simulations which include the self-consistent heating from the magnetic dynamo may be a better guide to the properties of the flow than analytic approximations. These show that in the limit of no radiative losses the structure is something like that predicted by the ADIOS models, but these flows also have a relativistic jet (e.g. Hawley & Balbus 2002). This is very important as it shows that there is no additional physics required to produce the jet: the MRI in a geometrically thick hot, accretion flow in strong gravity is sufficient (see Section 8; Meier 2005).

3.3 Optically thin accretion flows: stability

All the varieties of hot, optically thin flows are quasi-spherical with $H/R \sim 0.3\text{--}0.4$. Thus the thermal timescale is still shorter than the viscous timescale and the stability of the flow at any radius can be assessed assuming that the surface density remains constant as for thin discs (see Section 2.2). In the

SLE76 flows, ion heating by gravity is balanced with ion cooling through Coulomb collisions heating the electrons. The electrons then radiate this energy via bremsstrahlung and Compton scattering (both of which depend only on electron temperature). An increase in ion temperature causes an initial increase in ion cooling as the ions have more energy to give to the electrons. The electron cooling is unaffected so the electrons must heat up. The details of Coulomb coupling mean that this decreases the efficiency of the energy exchange, by a factor which more than offsets the original increase in ion temperature and results in a *lower* rate of cooling of the ions. Thus a small increase in ion temperature leads to a lower energy loss rate of the ions, so the ion temperature increases still further and the flow is thermally unstable (Pringle 1976).

However, for all the flows including advection, ion cooling can be dominated by advective losses rather than Coulomb heating to the electrons. The advective losses scale simply with the ion temperature, so an ion temperature perturbation causes an increase in ion cooling through advection and the system is stable (Narayan & Yi 1995). All the numerical MRI flows are thermally (and viscously) stable also, as is shown by the fact that time dependent simulations reach an equilibrium structure with well defined mean properties (e.g. Hawley & Balbus 2002)

3.4 Two types of accretion flow as the origin of spectral states?

The two types of spectra seen in Cyg X-1 (hard and soft) are rather naturally explained by the existence of two very different stable accretion flow structures, with a hot, optically thin, geometrically thick flow which can exist only at low luminosities, as well as a cool, optically thick, geometrically thin disc. Geometrically, these can be put together into the truncated disc/hot inner flow model which can explain the observed dichotomy of hard and soft spectra. At low L/L_{Edd} , the inner optically thick disc is replaced by an optically thin, hot flow, probably through evaporation (Meyer & Meyer-Hofmeister 1994; Różańska & Czerny 2000; Mayer & Pringle 2007). There are few photons from the disc which illuminate the flow, so Compton cooling of the electrons is not very efficient compared to heating from collisions with protons. This ratio of power in the electrons to that in the seed photons illuminating them, $\mathcal{L}_h/\mathcal{L}_s$, is the major parameter (together with optical depth of the plasma) which determines the shape of a thermal Comptonization spectrum (e.g. Haardt & Maraschi 1993). Physically, $\mathcal{L}_h/\mathcal{L}_s$ sets the energy balance between heating and cooling, and hence sets the electron temperature. Thus $\mathcal{L}_h/\mathcal{L}_s$ is a more fundamental parameter to understand thermal Compton scattering than electron temperature.

In the hard state, the relative lack of seed photons illuminating the hot inner flow means that $\mathcal{L}_h/\mathcal{L}_s \gg 1$, producing hard thermal Comptonized spectra. These can be roughly characterized by a power law in the 5–20 keV band with photon index $1.5 < \Gamma < 2$ where the photon spectrum $N(E) \propto E^{-\Gamma}$ [alternatively the flux $F(E) = EN(E) \propto E^{-\alpha}$ where energy index $\alpha = \Gamma - 1$ and $0.5 < \alpha < 1$]. Conversely, when the mass accretion rate

increases, the flow becomes optically thick, and collapses into a Shakura–Sunyaev disc (see Section 2.1). The dramatic increase in disc flux due to the presence of the inner disc marks the hard-soft state transition (Esin, McClintock & Narayan 1997; Poutanen, Krolik & Ryde 1997), and also means that any remaining electrons which gain energy outside of the optically thick disc material (perhaps from heating in magnetic reconnection events above the disc) are subject to much stronger Compton cooling, with $\mathcal{L}_h/\mathcal{L}_s \leq 1$. This results in Comptonized spectra which are typically much softer, thus the soft state is characterized by a strong disc and soft tail, roughly characterized by a power law index of photon index $\Gamma \geq 2$.

3.5 Yet more Black Hole spectral states

Cyg X-1 actually shows only a very small range of variability, with L/L_{Edd} changing by only a factor ~ 3 on long timescales (e.g. Done & Gierliński 2003). The increase in data from transient BHB in the early 1990's from the *Ginga* satellite showed a further variety of spectral shapes could be observed at high accretion rates. These are similar to the soft state in that their X-ray emission peaks below 10 keV, as expected for a disc. However, the high-energy emission accompanying the disc spectrum can also be very strong, but is much steeper than that seen in either the hard or soft states. These are termed the very high or steep power law dominant state (hereafter very high state; see figure 9b), initially discovered during a bright outburst of GX 339–4 (Miyamoto et al. 1991) and GS 1124–68 (Miyamoto et al. 1993), and now generally seen in the brightest phase of many BHBs including GRS 1915+105 (Reig, Belloni & van der Klis 2003; Done et al. 2004), GRO J1655–40 (Sobczak et al. 1999a; Kubota, Makashima & Ebisawa 2001), XTE J1550–564 (Sobczak et al. 1999b; Kubota & Makishima 2004), and 4U 1630–472 (Abe et al. 2005). Similar spectra with strong disc emission together with a strong steep tail are also seen at lower luminosities, during the transitions, where they are termed Intermediate state (hereafter IS; Ebisawa et al. 1994; Belloni et al. 1996). It has long been realized that these IS spectra share many characteristics of the very high state (Belloni et al. 1996), so here we will treat them both together as very high state (but see Gierliński & Newton 2006).

Figure 9 shows a selection of spectra seen from the BHB, GRO J1655–40, at different mass accretion rates, showing examples of these states (hard, soft, soft with extremely weak tail, sometimes called ultrasoft, and an extreme example of the very high state). As can be seen from this figure, these states are *not* a unique function of mass accretion rate as measured by bolometric luminosity. The hard state seen on the rise is as luminous as the soft state seen later in the outburst (see e.g. XTE J1550–564 in Fig. 3). This lack of one-to-one correspondence between spectral state and L/L_{Edd} is termed hysteresis and is probably due to non-stationary behaviour of the accretion flow associated with the dramatic rise in transient outbursts (see Section 6.1). Since the IS is seen during the transitions, then this likewise can occur over a wide range of luminosities.

However, despite this severe complication, the general picture is now clear that soft and very high states are typically high luminosity states, while

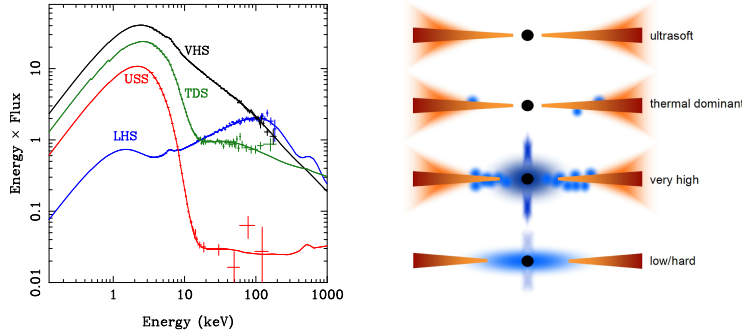


Fig. 9 The left hand panel shows a selection of states taken from the 2005 outburst of GRO J1655–40. The right hand panel shows the proposed accretion flow changes to explain these different spectra, with differing contributions from the disc, hot inner flow and its associated jet, active regions above the disc and a wind.

the hard state is seen at lower luminosities. Comprehensive reviews of the observational properties of these spectral states are given by e.g. Tanaka & Lewin (1995) and Remillard & McClintock (2006).

Thus while we have two theoretical stable accretion flow models, a disc and an optically thin, hot (messy) flow, there are (at least) three different types of spectra to explain. As outlined in Section 3.4, the hot flows plus a truncated disc can generically match the hard state properties (see also Section 4.1), while the spectra seen at high L/L_{Edd} show clear signs of being dominated by the disc. At these high luminosities the disc is likely to extend down to the last stable orbit (see Section 5), but even the soft-state spectra are always accompanied by a high-energy tail. This shows that there must be some sort of optically thin dissipation which can co-exist with the majority of the accretion flow being in the form of a disc. This could be due to some small fraction of the flow in a state analogous to the hot, optically thin (messy) flow seen in the hard state, but with properties modified by the strong Compton cooling (Esin 1997; Janiuk, Życki & Czerny 2000) and thermal conduction (Różańska & Czerny 2000; Liu, Meyer & Meyer-Hofmeister 2005). There are also alternatives to these smooth flows in models where the energy dissipation is instead inherently very inhomogeneous, perhaps due to magnetic reconnection of flux tubes rising to the surface of the disc, as was first suggested by Galeev, Rosner & Vaiana (1979), and finds some support in the inherently variable (in both space and time) dissipation produced by the MRI (e.g. Hawley & Balbus 2002).

One way to put all these mechanisms together into a plausible model for all the spectral states is sketched in Fig. 9b, similar to that first proposed by Esin et al. (1997). In the sections below we will outline how this model works to explain the observed spectra of each state. We discuss alternatives to the truncated disc in Section 4.2.

4 The low/hard state

4.1 Hot inner flow and truncated disc

At low luminosities the spectra peak at 100 keV rather than the expected disc temperature of < 0.5 keV (see Fig. 9). These hard-state spectra clearly show that the structure of emitting region is very different to that expected from a disc. The spectra are broadly fit by thermal Comptonization models, with electron temperatures $kT_e = 75\text{--}110$ keV for the best studied case of Cyg X-1 (Ibragimov et al. 2005). Fig. 10 shows representative spectra for this state. The range of spectral slopes indicate a range in $\mathcal{L}_h/\mathcal{L}_s$ from $\sim 5\text{--}15$ (Ibragimov et al. 2005). This is fairly naturally produced in the context of the truncated disc model. At very low luminosities the disc is truncated far from the hole and there is little overlap between the hot flow and cool disc so few seed photons illuminate the flow, giving $\mathcal{L}_h/\mathcal{L}_s \gg 1$. As the disc moves progressively inwards it increasingly extends underneath the hot inner flow so that there are more seed photons intercepted by the flow, decreasing $\mathcal{L}_h/\mathcal{L}_s$ (as in the geometries sketched in Fig. 10).

The maximum luminosity which can be carried by this flow marks the transition luminosity to the soft state. However, this point is rather unclear both theoretically and observationally! Theoretically the problem is that the structure of the hot flow is not yet well understood. Models of ADAFs show they can only exist up to $L/L_{\text{Edd}} \sim 1.3\alpha^2 \sim 0.01$ for $\alpha = 0.1$ (Esin et al. 1997), though this can be extended up to $L/L_{\text{Edd}} \sim 0.1$ in the LHAFs (Yuan et al. 2007), and potentially further still since these analytic models do not include the magnetic fields produced by the MRI which may give enhanced energy release in the rapid infall region of the flow close to the black hole (Agol & Krolik 2000). Enhanced magnetic pressure due to the collapse of the hot flow may also be important in increasing the maximum luminosity (Machida, Nakamura & Matsumoto 2007). Observationally, the problem is that the transition happens at a range of luminosities, even in a single object! The best studied case is that of XTE J1550–564, where the transition occurs from $L/L_{\text{Edd}} \sim 0.2$ to $L/L_{\text{Edd}} = 0.003$ (Done & Gierliński 2003). This range can be suppressed by considering only the soft-to-hard state transition on the decline, ignoring the hard-to-soft transitions on the rapid rise to outburst which are typically at higher L/L_{Edd} . The transitions on the slow decline pick out a fairly constant value of $L/L_{\text{Edd}} \sim 0.02$ (Maccarone 2003) but there are exceptions even here, with the 1998 outburst of XTE J1550-564 staying in the soft state down to $L/L_{\text{Edd}} \sim 0.003$ (Gierliński & Done 2003). This variety of luminosities for the transition is one manifestation of hysteresis, where the same source can show different spectra at the same luminosity (see Section 6.1). Nonetheless, the properties of the hard state are well matched by a model of a hot flow with a truncated disc which progressively moves inwards as the mass accretion rate increases.

The behaviour of the intrinsic emission from the disc itself is harder to track as the disc temperature is below 0.5 keV. This means that it cannot be easily observed with the *RXTE* PCA instrument (3–20 keV), which has by far the most data on BHBs. Instead of multiple monitoring observations

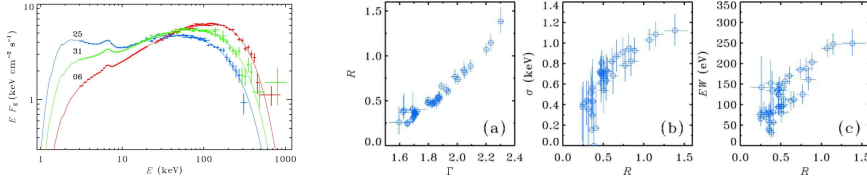


Fig. 10 Range of (absorbed) low/hard state in Cyg X-1, together with the correlated changes in spectral index and (neutral) reflected fraction, reflected fraction and amount of smearing of the associated iron line, and reflected fraction and equivalent width of the iron line. These all change in a manner qualitatively consistent with the disc extending down further into the hot inner flow (from Ibragimov et al. 2005).

there are only occasional snapshots with satellites covering the softer X-ray bandpass (*ASCA*, *BeppoSAX*, *Chandra* and *XMM-Newton*) and these data are also often heavily absorbed by the considerable interstellar column seen towards many BHB as they are in the plane of our Galaxy. Nonetheless there are some indications that the disc behaves as predicted by these truncated disc models. The most convincing of these is the BHB XTE J1118+480, one of the few sources at high Galactic latitude. The very low galactic column to this object gives the best view of the EUV/soft X-ray region where the disc should peak. This is also a transient where the outburst peak luminosity was very low, at $L/L_{\text{Edd}} \sim 10^{-3}$, so it remains clearly in the hard state during the entire outburst (see Fig. 3). Multiwavelength campaigns (IR–optical–UV–X-ray) show that the disc has very low maximum temperature of $\sim 10\text{--}40$ eV, well fit with a truncation radius of $\sim 100\text{--}300 R_g$ (e.g. Esin et al. 2001; Frontera et al. 2001; Chaty et al. 2003, see Fig. 11). The total spectrum also points to the geometry being inhomogeneous. The hard X-ray spectrum clearly shows that the X-ray source is illuminated by rather few seed photons i.e. that $\mathcal{L}_h/\mathcal{L}_s \gg 1$. However the total spectrum has the soft and hard luminosities about equal (Fig. 11). This is consistent with the disc subtending rather a small solid angle at the source of energetic electrons, also as predicted by the truncated disc models (see Fig. 9).

No other BHB in the hard state has comparable data, but there are snapshot observations of the soft component in Cyg X-1 at $L/L_{\text{Edd}} \sim 0.01\text{--}0.02$. Here the disc temperature is of order $0.1\text{--}0.2$ keV (Bahucińska-Church et al. 1995; Ebisawa et al. 1996; Di Salvo et al. 2001), consistent with a truncated disc where the inner radius is more like $50 R_g$ (di Salvo et al. 2001). Again, there is roughly as much power in this disc spectrum as there is in the hard X-ray component, yet the hard X-ray spectrum implies that the source is photon starved, with $\mathcal{L}_h/\mathcal{L}_s \gg 1$. However, these broadband data also show that the soft spectrum is more complex than expected from simple disc plus Comptonization and its (mainly neutral) reflection. There is spectral curvature which can be modelled as an additional, higher temperature soft component or as a slightly steeper power law which contains 5–10 per cent of the total X-ray power (Ebisawa et al. 1996; di Salvo et al. 2001; Ibragimov et al. 2005 see Fig. 11; Makishima et al. 2007). GX 339–4 also shows

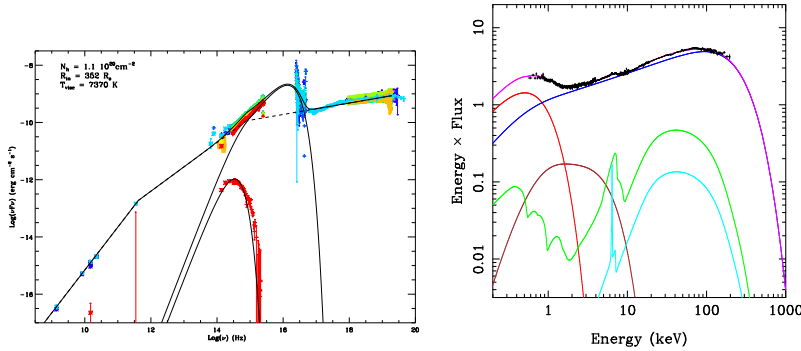


Fig. 11 The soft component in the hard state. left panel: the disc in XTE J1118+480 at $L/L_{\text{Edd}} \sim 10^{-3}$ (Chaty et al. 2003). Right panel: the disc in Cyg X-1 at $L/L_{\text{Edd}} = 0.02$ (after di Salvo et al. 2001). The disc spectrum (red) is accompanied by a small tail to higher energies (brown), producing a soft excess which is around 10 per cent of the total soft emission and at somewhat higher temperature. The other components of the model are thermal Comptonization (dark blue), smeared (green) and narrow (light blue) reflection.

a similarly complex soft component in the hard state (Wilms et al. 1999), as does GRO J1655-40 (Takahashi et al 2007). The origin of this is not well understood. It could be connected to a warm layer or hot spots on the disc (di Salvo et al. 2001), or to uncertainties in reflection modelling (Done & Nayakshin 2001), or could be an artifact of intrinsic curvature of the Comptonized continuum (such as can be produced by anisotropic Comptonization from a sphere rather than planar geometry: Haardt & Maraschi 1993) or to time averaging over a variable shape Comptonization component (Poutanen & Fabian 1999; Revnivtsev, Gilfanov & Churazov 1999). Whatever its origin, this component means that extracting the true disc temperature from limited bandpass data is difficult. In general, a small, hot ‘disc’ spectrum is more likely to be indicating this unknown component than the true disc spectrum. This may be the origin of the apparently untruncated disc seen in the hard state in GX 339-4 (Miller et al. 2006, see Section 4.3 below).

The hard X-ray continuum is seen together with some reflected emission from the accretion disc which is generally not highly ionized. Both the solid angle subtended by this reflecting material and the amount of relativistic smearing increase as the hard state spectrum steepens (e.g. Gilfanov, Churazov, & Revnivtsev 1999) although there is some systematic uncertainty in the amount of reflection which is produced due to the poorly understood spectral curvature of the complex soft excess (Ibragimov et al. 2005). However, the trend for an increasing reflected fraction with steeper spectra is plainly qualitatively consistent with the geometries sketched in Fig. 10 where the increasing penetration of the cool disc into the inner hot flow gives more seed photons to cool the flow. This decrease in $\mathcal{L}_h/\mathcal{L}_s$ results in steeper continua spectra, together with a larger solid angle subtended by the disc and larger relativistic effects. This can give both a good qualitative *and* quantitative description of the spectral index–reflection correlation seen in the data,

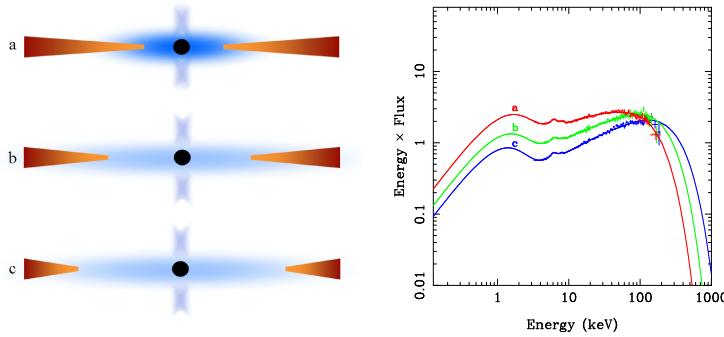


Fig. 12 Range of low/hard state geometries in the truncated disc model, together with their predicted spectra. When the disc is truncated far from the black hole, few disc photons are intercepted by the hot flow. Thus the Comptonized spectrum is hard, while a large fraction of disc photons are seen directly. As the disc extends further underneath the hot flow the larger fraction of disc photons intercepted means the spectrum becomes softer as the electron temperature is cooler, while the disc is hotter but less distinct.

(Zdziarski, Lubinski & Smith 1999; Zdziarski et al. 2003) especially given the uncertainties in determining the amount of reflection. As well as being dependent on details of how the continuum is modelled (Wilson & Done 2001; Ibragimov et al. 2005) there are also theoretical uncertainties on the shape of the reflected spectrum when the material is ionized. Low energy line emission contributes to the spectrum as well as simple electron scattering of the incident continuum as the material is heated and ionized by the X-ray illumination (Ross & Fabian 1993; Życki & Czerny 1994). Compton upscattering in the upper, X-ray heated layers of the disc can give additional broadening to the spectral features (Ross, Fabian & Young 1999) and there should also be a range of ionization states present, from both radial and vertical stratification, and this can be highly complex if the disc is in hydrostatic balance (Nayakshin, Kazanas & Kallman 2000).

By contrast, the properties of the thermal Comptonizing region are more robust. Fig. 12 shows a series of models for the hard state which quantify the effect of the geometry changes, where the disc extends progressively further inwards as a function of \dot{M} and the fraction of disc flux intercepted by the hot flow also progressively increases (based on the EQPAIR code of Coppi 1999). These models have the disc inner radius decreasing by a factor 2, while the covering fraction of the hot flow increases from 0.2 to 0.6. The optical depth in the hot flow is fixed at unity, and $\mathcal{L}_h/\mathcal{L}_s$ decreases from 15 to 2.5. This model incorporates Compton (and Coulomb) cooling self consistently, and predicts electron temperatures dropping from 110 keV to 70 keV. This bears a strong resemblance to the observed hard-state spectra shown in Fig 10.

4.2 Alternative Geometries for the hard state

Alternative geometries which include an untruncated disc and (mostly) isotropic source emission have significant problems in matching the observed features of the hard-state spectra. The continuum spectral shape rules out slab corona models as the spectra all peak at high energies. Such hard spectra from thermal Comptonization are only possible if the luminosity in seed photons within the X-ray region is less than that in the hot electrons i.e. $\mathcal{L}_h/\mathcal{L}_s \gg 5$. A disc extending underneath an isotropically radiating hot electron region would intercept around half the Comptonized emission in a slab corona geometry. Part of this emission can be reflected, but reflection cannot be efficient at 100 keV (where the spectrum peaks) due to electron recoil. The maximum albedo of the disc even for completely ionized reflection is around 0.3 for the hardest spectra, so the rest of the illuminating flux is thermalized in the disc. In a slab geometry all this thermalized emission is seen by the hot electrons, giving $\mathcal{L}_h/\mathcal{L}_s \leq 2/0.7 = 2.8$ (corresponding to photon indices of $\Gamma > 2$), much smaller than that required to fit the hardest spectra (with $\Gamma \sim 1.5$) of $\mathcal{L}_h/\mathcal{L}_s > 10$ (Haardt & Maraschi 1993; Stern et al. 1995; Malzac, Dumont & Mouchet 2005).

A patchy corona, perhaps made up of individual magnetic flares, allows part of the reprocessed flux to escape without re-illuminating the hot electron region, so it can produce the required hard spectra. However, the one advantage of a slab corona is that the reflected flux is also intercepted by the disc, and hence Comptonized into continuum flux. This suppresses the amount of recognizable reflected emission, so that $\Omega/2\pi < 1$ as observed in the hard state (Haardt et al. 1994; Petrucci et al. 2001). A patchy corona allows the reprocessed flux to escape, but this also allows the reflected flux to escape, so $\Omega/2\pi \rightarrow 1$ for the hardest spectra, in direct conflict with the observations (Malzac, Beloborodov & Poutanen 2001; Malzac et al. 2005). A patchy corona can only be retrieved if the disc has an extremely ionized skin, making a completely reflective layer, while the observed near-neutral reflection is produced deeper in the disc. Such complex ionization structure, with a rapid transition between ionized and neutral material, can be produced by hard X-ray illumination (Nayakshin et al. 2000). However, the extreme ionization reflection produced by the skin is only indistinguishable from the continuum at low energies. The reflection albedo at high energies is independent of the ionization state of the material, and electron recoil in the disc means the reflected emission must drop at ~ 100 keV. Thus a spectrum with a large contribution from extremely ionized material should be steeper in the 50–100 keV band than the 5–20 keV band. This is not observed (Maccarone & Coppi 2002; Barrio, Done & Nayakshin 2003).

A disc extending down to the last stable orbit cannot be ruled out completely though. Firstly, the predicted steepening of the 50–200 keV spectrum in ionized reflection models could be counterbalanced by a flattening in the underlying high energy continuum, though it seems contrived that this should cancel out to look like an unbroken power law. Secondly and perhaps more plausibly, the continuum source could be connected to the jet, and be in motion along the jet axis, expanding away from the disc at moderately rel-

ativistic velocities. Mild beaming of the X-ray emission could result in a reflected fraction of ~ 0.3 as observed, even if an untruncated disc were present. Similarly the beaming suppresses the soft seed photon flux from the disc so that the resulting continuum spectrum is hard. The observed increase in reflected fraction with spectral slope shown in Fig. 10 could be explained if the expansion velocity decreases with luminosity (Beloborodov 1999; Malzac et al. 2001), and perhaps this change in beaming pattern also produces increased illumination of the inner disc, giving the observed increase in smearing (Fig. 10). However, this is *opposite* to the increase in jet velocity at the transition inferred from radio data (Fender, Belloni & Gallo 2004; see Section 8). An increase in jet velocity is also required for the internal shock models to explain the dramatic radio flares seen on the hard-to-soft (but *not* on the soft-to-hard) transitions, as these require that faster jet from the brighter, softer hard state collides with the previous, slower jet material (Fender, Belloni & Gallo 2004; see Section 8).

Models where the X-rays are produced directly in the jet were proposed by Markoff et al. (2001). These produce the hard X-rays by synchrotron emission from the high-energy extension of the same non-thermal electron distribution which gives rise to the radio emission. However, the observed shape of the high-energy cutoff in the hard state is very sharp, and cannot be easily reproduced by synchrotron models (Zdziarski et al. 2003). These jets are also generally radiatively inefficient, yet the observed luminosity change at the hard-soft state transition where the flow changes to a radiatively efficient disc is not large (less than a factor of a few, see Fig. 8: Maccarone 2005). Instead, there are now composite models where the X-rays are from Comptonization by thermal electrons at the base of the jet, while the radio is from non-thermal electrons accelerated up the jet (Markoff et al. 2005). The base of the jet expands at weakly relativistic speeds, and the resulting weak beaming away from the disc is similar to that proposed by Beloborodov (1999), though the model of Markoff et al. (2005) has this in the centre of a truncated disc. Given that the hot inner flow probably relates physically to the base of the jet (see Section 8), then this model converges on the truncated disc/inner hard X-ray source geometry shown in Fig. 12, though with some additional weak beaming of the hard X-rays as in the Beloborodov (1999) model.

The magnetized accretion–ejection models of Ferreira et al. (2006) have a similar outer disc–inner jet structure, though here the inner, optically thick disc is still present down to the last stable orbit. However, its properties are very different from the standard Shakura–Sunyaev disc in that the angular momentum of the infalling material is transported self-consistently by the jet. The transition radius between this jet dominated disc and the standard accretion disc is variable, producing the range of behaviour seen in the hard state spectra in a similar way to the truncated disc/hot inner flow models.

However, all these alternative models require that the X-ray source is mildly beamed away from the disc. This is challenged by the observation that the hard state BHB show no trend in their properties as a function of inclination (Fender et al. 2004; Narayan & McClintock 2005). Systematic studies of hard state properties over a sample of BHB at various inclinations

should constrain the amount of beaming (e.g. amount of reflection or spectral slope versus low frequency QPO) and show whether these models are allowed by the data.

Thus all currently viable models for the hard state converge on a geometry where the standard disc extends down only to some radius larger than the last stable orbit, with the properties of the flow abruptly changing at this point. The only alternative to a hot inner flow for the origin of the X-ray emission is a mildly relativistic outflow, where the velocity decreases as the source brightens to produce the observed softer spectra and higher reflected fraction. This is probably inconsistent with the very attractive internal shock models for the bright radio flares at the hard-to-soft transitions, and may also be at odds with the observed uniformity of hard state properties across BHB with different inclinations.

4.3 Challenges to the truncated disc geometry for the hard state

While the alternative flows discussed above face some observational challenges, there is also current controversy over the truncated disc/hot inner flow models over claims that the data show evidence for an *untruncated disc* in the hard state. Firstly, there are occasional observations of extremely smeared iron line and reflection features in this state in XTE J1650–500 (Miller et al. 2002; Minutti et al. 2004) and in GX 339–4 (Miller et al. 2006). These are fairly bright hard states (XTE J1650–500 is close to an intermediate state) so while the truncated disc models do predict that the inner radius is not at the last stable orbit, there is no requirement for it to be very recessed. However, the claimed broadening is such that the disc extends down to the innermost stable orbit for a fast rotating black hole, in conflict with the truncated disc models. For XTE J1650–500, Done & Gierliński (2006) refit the data to show that the smearing can be significantly reduced to a level compatible with a truncated disc if there is also resonance iron K line *absorption* from an outflowing disc wind (see Section 10 for more on outflows and winds). While this has yet to be explicitly demonstrated for the GX 339–4 data, the same spectral degeneracy probably occurs in all moderate resolution CCD data. Higher resolution grating or bolometer data is required to unambiguously show the presence or absence of such absorption features, and hence reveal the shape of the underlying continuum and reflection components. Further ambiguity comes from the shape of the reflected emission, as it is plainly ionized in these data. All current ionized reflection models are calculated for conditions appropriate to AGN discs (e.g. Ballantyne, Ross & Fabian 2001), where the intrinsic thermal emission is in the UV/EUV, so that ionization of heavy elements is determined only by photoionization. Yet for BHB the disc is at soft X-ray temperatures, so collisional processes are also important in setting the ion populations, reducing the irradiation required. This changes the shape of the reflected spectrum due to changing the vertical temperature structure and hence the amount of internal Comptonization (Ross, Fabian & Young 1999). The vertical structure also depends on the illumination, especially if the disc is in hydrostatic equilibrium (Nayakshin et al 2000; Done & Nayakshin 2007). Thus both better data and better reflection models are

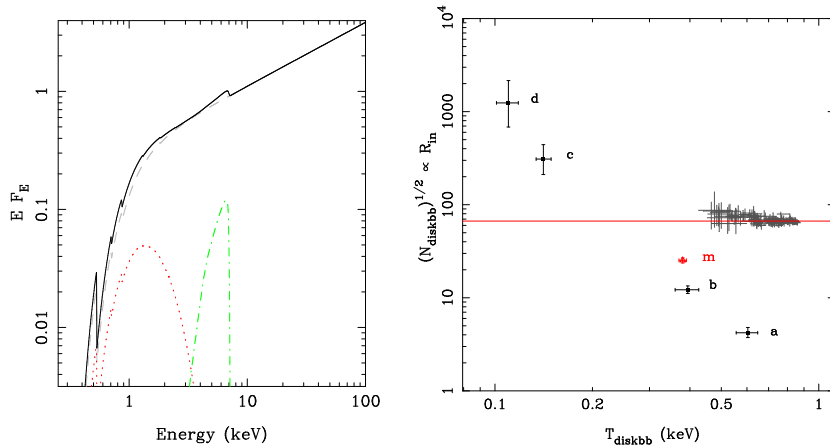


Fig. 13 The left hand panel shows a bright hard state ($L_{\text{bol}}/L_{\text{Edd}} \sim 0.02$, assuming mass of $6 M_{\odot}$, distance of 4 kpc) model spectrum of GX 339–4 from simultaneous *XMM-Newton* and *RXTE* data (first model in table 1 of Miller et al. 2006). The disc is shown in dotted red curve, the Gaussian line in dash-dotted green curve and the power law in dashed grey curve. The disc contribution to the 0.1–100 keV flux is only 2.5 per cent ($L_{\text{disc}}/L_{\text{Edd}} \sim 6 \times 10^{-4}$), so its parameters are dependent on the continuum model. The right panel shows the square root of the DISKBB model normalization, which is proportional to its inner radius. The red point (marked *m*) corresponds to the observation in the left panel. The derived inner radius is smaller than the approximately constant radius seen in disc-dominated spectra from *RXTE* monitoring (grey points, red line shows the mean; after Gierliński & Done 2004). This is also seen in archival *ASCA* data in the hard state when the disc is determined against a simple power law (*a*), or Comptonized continuum (*b*). However, a more complex spectral form, modelled with an additional power law (*c*) or Comptonization component (*d*) gives the opposite result. The disc is then larger than that seen in the high/soft state, consistent with a truncated geometry.

required before the broad iron line results can be claimed to clearly rule out the truncated disc geometry (Done & Gierliński 2006). Nonetheless, this is an important goal, as it is possibly the only way to detect a non-radiative, weakly illuminated, optically thick inner disc (e.g. Beloborodov 1999; Malzac et al. 2001; Ferreira et al. 2006) and hence understand the nature of the inner accretion flow.

There is a further challenge to the hot inner flow models, from the residual disc emission in the sources with only moderate galactic absorption ($< 0.5 \times 10^{22} \text{ cm}^{-2}$). These show spectra with a rise at low energies, which can be fit by disc models with luminosity and temperature indicating that the disc extends down close to the black hole (GX 339–4: Miller et al. 2006; SWIFT J1753.5–0127: Miller, Homan & Miniutti 2006; XTE J1817–330: Rykoff et al. 2007). However, disc luminosity and temperature are very difficult to uniquely determine unless the disc is the dominant spectral component (see Section 5 and 5.2). These apparent disc components typically carry less than 5–10 per cent of the flux in the instrument bandpass, so details of how the tail is modelled become very important.

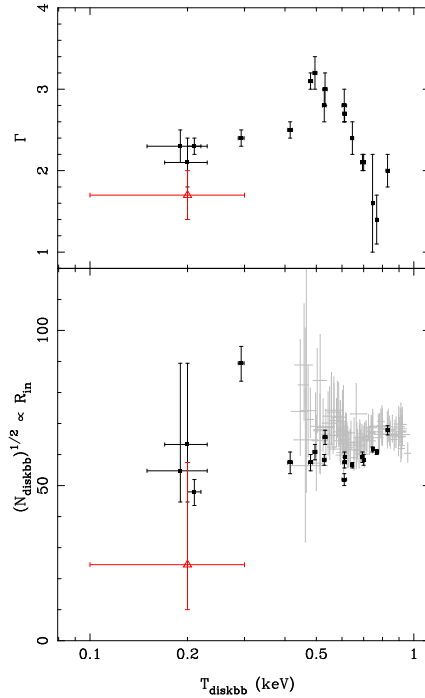


Fig. 14 The outburst of XTE J1817–330, with data fit to a disc plus power law model. The upper panel shows the power-law spectral index while the lower panel shows square root of DISKBB normalization ($\propto R_{\text{in}}$). The black points are the *SWIFT* best-fit results from table 3 in Rykoff et al. (2007) while the grey data show results from *RXTE* monitoring of this outburst (soft state only). Both *SWIFT* and *RXTE* data give similar results for the inner radius of the disc-dominated state, and show that this is approximately constant. The *SWIFT* data show that the source is always in the disc-dominated or intermediate state apart from one potential observation in the hard state (red triangle). This has large uncertainties (so may be an intermediate state rather than hard state) but is consistent with a disc which extends down to the same or smaller inner radius than that seen in the disc-dominated data. This result is similar to the apparently small radii discs seen in simple fits to hard state data in GX 339–4 (see Fig. 13). Hence, its properties depend on the detailed model of the hard-state continuum used, and a soft excess/low-energy continuum curvature will allow a truncated disc fit to these data.

We show this explicitly for the GX 339–4 data of Miller et al. (2006) in Fig. 13 (left panel), where one of their model fits to the data (an absorbed disc, power law and broad line) is shown as a deconvolved νF_ν spectrum. The contribution of the disc is extremely weak, less than 20 per cent of the total flux even at its peak energy, and it carries less than 1 per cent of the bolometric luminosity. Plainly the derived parameters of this component will be very dependent on the detailed modelling of the spectrum at soft energies. We illustrate this using archival data from GX 339–4 in its 1995 September 12 hard state observation from *ASCA* (Wilms et al. 1999). The right hand panel of Fig. 13 shows the square root of DISKBB normalization ($\propto R_{\text{in}}$) from these

data assuming that the continuum is given by an absorbed disc plus power law (a) or Comptonized (b) spectrum. Both these give a disc which is *smaller* than the disc seen in the same object in *RXTE* observations of its high/soft, disc dominated spectra (see Section 5). This is directly opposite to the predictions of the truncated disc model. However, there are clear indications that the soft spectrum in the hard state is more complex (see Fig. 11 and Section 4.1; Ebisawa et al. 1996; Wilms et al. 1999; di Salvo et al. 2001; Ibragimov et al. 2005; Takahashi et al. 2007; Makishima et al. 2007). Fitting a more complex form, so that the non-disc continuum is either a broken power law (c) or low temperature Comptonization plus the harder power law (d) gives a *larger* inner radius than that seen in the disc dominated states, consistent with the truncated disc models. These derived radii will all increase if the disc normalisation is corrected for the photons scattered into the Comptonised spectrum (Kubota et al. 2001; Kubota & Makishima 2004; Kubota & Done 2004; Done & Kubota 2006; Makishima et al. 2007).

Thus the derived disc radii in hard-state spectra are sensitive to the assumed continuum shape. A power law or downwards curving continuum (soft deficit) at low energies gives an inner disc radius which is much smaller than that derived from an upwards curving (soft excess) continuum. The red point in Fig. 13 (right panel, marked as *m*) shows DISKBB normalization from the power-law continuum fit to *XMM-Newton*/*RXTE* data of Miller et al. (2006). While these data have not yet been fit to more complex continua, it seems likely that increasing the non-disc continuum at low energies would force the residual disc emission to be at lower temperature and larger radius. These uncertainties in the underlying spectral shape clearly preclude any definitive measure of the disc in these data, and there are also further uncertainties in the spectral modelling of the disc spectrum in the low/hard state as the stress-free inner boundary condition is probably not appropriate and the disc may also be significantly heated by irradiation and/or conduction.

Rykoff et al. (2007) also claim that the evolution of the disc component in an outburst of XTE J1817–330 is incompatible with the truncated disc models. We replot their results from multiple *SWIFT* observations in Fig. 14 for the disc plus power law models, where the upper panel shows the power-law spectral index, and the lower panel the derived disc radius. This outburst was also followed by the *RXTE* satellite, and we include DISKBB normalization as derived from the PCA data as the grey points in Fig. 14. The two instruments give results which are consistent, and the combined datasets show clearly that the disc-dominated state has a well defined, approximately constant radius. However, the *SWIFT* spectral indices show that the Rykoff et al. (2007) data contain only one possible spectrum in the hard state ($\Gamma < 2$), and that its signal-to-noise is limited. Thus their data do not put any strong constraints on the disc in the hard state, contrary to their conclusions. The point lies below the constant radius inferred from the disc dominated data (though its large uncertainty means it is also consistent with this value), similar to the simple continuum fits to the hard state GX 339–4 data shown in Fig. 13b. We have re-extracted these data and find that a more complex continuum form, with upwards curvature, allows a much larger disc, consistent with the truncation models.

Thus there are no observations which unambiguously conflict with the truncated disc models, while there are a tremendous amount of data which can be fit within this geometry, including spectra, rapid variability characteristics (see Section 9) and jet properties (see Section 8). While the truncated disc model is indeed currently a very simplified version of what must be a more complex reality, nonetheless the range of data it can qualitatively (and sometimes quantitatively) explain gives confidence that it captures the essence of the hard state.

5 High mass accretion rates: thermal dominant and very high states

5.1 Disc spectra in the soft state

The spectra in Fig. 9 which are dominated by a thermal component and where the tail is only a small fraction of the total bolometric luminosity (soft state) show convincing evidence for a disc. However, this is actually surprising as the classic Shakura–Sunyaev disc is unstable at high luminosities when radiation pressure starts to dominate the total pressure (see section 2.3), pointing to the heating being somewhat different than assumed (Section 2.3). Nonetheless, this uncertainty in stress prescription has very little impact on the zeroth order predicted disc spectra. The fact that the observed soft-state spectra are so close to the expectation of an optically thick, geometrically thin disc means that the accretion structure is understood at some level, so the disc spectra can be used to probe the dramatically curved space-time in the vicinity of the black hole. In particular, in the Shakura–Sunyaev models the emitting disc only extends down to the last stable orbit round the black hole, and then free falls rapidly to the event horizon. The lack of stress at the last stable orbit gives a clear inner edge to the disc, and so provides an observational diagnostic of the spin from the observed temperature and luminosity of the disc spectrum (see Section 2.1).

Simple spectral fitting for the soft component is based on the DISKBB model which ignores any inner disc boundary condition, describing the disc local temperature as $T(r) = T_{\text{in}} \cdot (r/r_{\text{in}})^{-3/4}$ (Mitsuda et al. 1984). The DISKBB model is parameterized by T_{in} and r_{in} , the maximum observed disc temperature and the apparent disc inner radius, respectively, where the disc bolometric luminosity L_{disc} can be related to these two spectral parameters as $L_{\text{disc}} = 4\pi r_{\text{in}}^2 \sigma T_{\text{in}}^4$. However, several corrections are required to derive the true inner disc radius from these measured parameters. In order of importance these include the stress-free inner boundary condition (which means the temperature drops to zero at the innermost stable orbit, so the peak temperature is from larger radii and hence is lower: Gierliński et al. 1999; Kubota et al. 2001; Gierliński et al. 2001), spectral hardening due to incomplete thermalization of the escaping radiation (colour temperature correction: Shimura & Takahara 1995; Merloni et al. 2000; Davis et al. 2005), and relativistic corrections (which can either increase or decrease the observed temperature depending on inclination: Cunningham 1975; Zhang, Cui, Chen 1997).

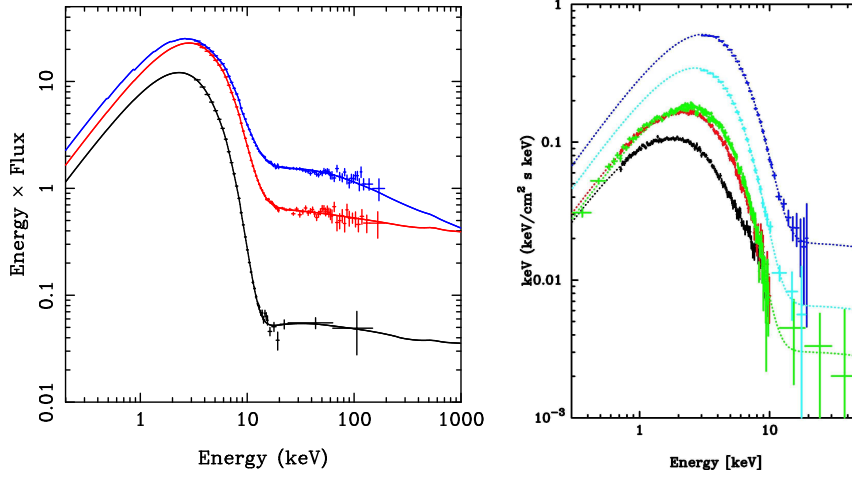


Fig. 15 A range of soft-state spectra at different luminosities from the BHB 4U 1655-40 from RXTE PCA and HEXTE data showing that the hard tail is indeed negligible in this state (left). The right panel shows LMC X-3 from ASCA (black and red), BeppoSAX (green) and RXTE PCA (cyan and blue) data. The disc peak is clearly well covered by the instruments with softer response, and these give results which are consistent with those derived from RXTE data (Davis et al. 2006).

Nonetheless, irrespective of the true disc radius, compelling evidence for the standard disc formalism is given by the *observation* that the value of r_{in} is usually observed to remain constant in the soft state as L_{disc} changes significantly (Ebisawa et al. 1991; 1993; 1994). An alternative, even more direct way to present the same result is to plot the observed disc luminosity and temperature against each other for multiple observations (Kubota et al. 2001; Kubota & Makishima 2004; Kubota & Done 2004; Gierliński & Done 2004; Davis et al. 2006; Shafee et al. 2006, see Fig. 15). Fig. 16 shows this for the BHB with soft-state spectra which span the largest range in luminosity. Clearly these sources are consistent with an approximate $L \propto T^4$ relation over factors of 10–50 change in disc luminosity, as predicted for a constant inner radius for the accretion disc. This is exactly the behaviour predicted by General Relativity at the last stable orbit, so these data confirm that gravity is consistent with Einstein’s predictions even in the strong field limit. This is fantastic—but also highlights the fact that the point at which corrections due to GR become large is below the last stable orbit! Given that the closeness of this to the event horizon, this shows that observational tests of newer theories of gravity will be very challenging (Gregory et al. 2004).

5.1.1 Black hole spin

Assuming GR is indeed the correct theory, these data also give a way to measure the spin of the black hole assuming there are some constraints on distance, mass and inclination from the binary parameters. However, then the

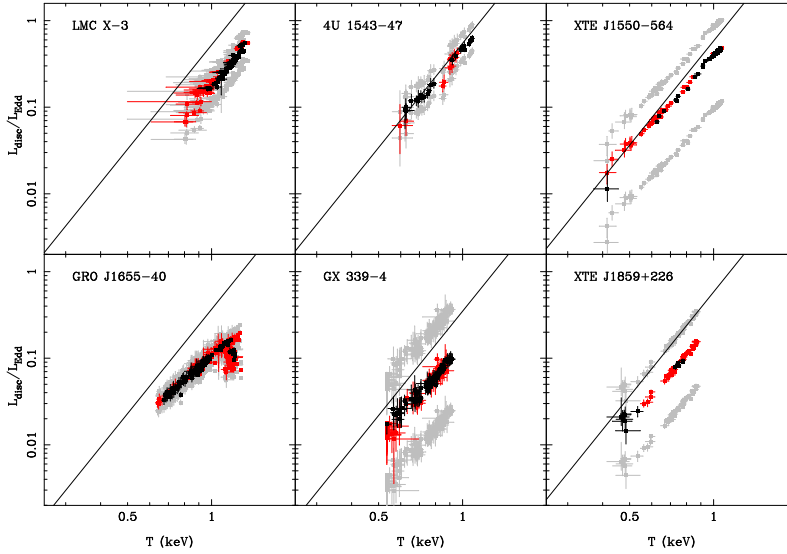


Fig. 16 Luminosity–temperature relations for the black holes with disc dominated spectra fit with DISKBB for those which span the largest range in luminosity. Grey points show the range of uncertainty due to mass and distance estimates.

details of the corrections discussed above are a key issue. Several attempts have been made to assess each of these separately. Gierliński et al. (2001) and Kubota et al. (2001) address the stress free inner boundary correction, while Zhang et al. (1997) tabulated the general relativistic correction factors affecting the escaping radiation from the disc around a Schwarzschild and maximal Kerr black hole. Both these effects are calculable from first principles. However, this is not the case for the colour temperature correction, as this depends on the disc opacity as a function of both frequency and vertical depth in the disc. This means that the calculations are sensitive to the (unknown) stress prescription. In general, opacity is a strongly decreasing function of frequency, so the lower energy radiation can thermalize while the emission at higher energies does not. Thus the emission is a blackbody only up to the frequency at which the true opacity becomes small. To get the same amount of energy out with incomplete thermalization requires that the emission extends out to higher energies as a blackbody is the most efficient emission process at a given temperature. This modifies the blackbody radiation, in a way which depends on the vertical density and temperature structure of the disc (Shakura & Sunyaev 1973).

The difference between the temperature inferred from the high-energy rollover of the thermal emission, and that expected from a true blackbody is termed a colour temperature correction, f_{col} . Calculations using the vertical structure predicted by a Shakura–Sunyaev α disc show that this is remarkably constant with both radius and L/L_{Edd} , with $f_{\text{col}} \sim 1.8$ predicted over the range $0.005 \leq L/L_{\text{Edd}} \leq 0.5$ (Shimura & Takahara 1995). This robustness was challenged by Merloni et al. (2000), who found much larger f_{col}

at small mass accretion rates. However, the origin of this discrepancy may be that Merloni et al. (2000) assumed a constant vertical density profile. This is only appropriate for a radiation pressure dominated disc and breaks down at low \dot{M} where the disc is gas pressure dominated and has stronger density/temperature gradients (Gierliński & Done 2004).

These results are now superseded by calculations which include full metal opacities. The Shakura–Sunyaev models assume that the only sources of opacity are free–free and electron scattering, yet bound–free (photoelectric absorption edge) opacity is important even at fairly high temperatures (Davis et al. 2005). These new models also directly incorporate the stress free inner boundary condition, and self-consistently propagate the escaping radiation through the curved spacetime (Davis et al. 2005; Davis & Hubeny 2006). These confirm that the colour temperature correction can remain fairly constant over large changes in luminosity (Davis et al. 2005), and fits to soft-state spectra give estimates for spin ranging from 0.1–0.8 for the 5 BHB with the best data (Davis, Done & Blaes 2006; Shafee et al. 2006; Middleton et al. 2006). Such moderate (as opposed to maximal) spins also match with the theoretical predictions for the birth spin distribution of black holes, as the pre-supernovae core before stellar collapse is slowly rotating, and spin up from captured fallback of material is countered by angular momentum loss in gravitational waves during the formation process (see e.g. the review by Gammie, Shapiro & McKinney 2004). Spin-up through accretion during the lifetime of the binary is limited in most systems as the companion mass in LMXB is smaller than the black hole mass (King & Kolb 1999).

5.1.2 Deviations of soft-state spectra from $L \propto T^4$

Fig. 16 shows overwhelmingly that the disc dominated, soft-state spectra do follow a $L \propto T^4$ relation, as predicted from simple models of a constant radius, constant colour temperature correction disc. However, mild deviations from this sometimes occur at high luminosities, for example GRO J1655–40 and to a lesser extent in XTE J1550–564 (Fig. 16) all bend away from the $L \propto T^4$ relation at temperatures of 0.9–1.2 keV. These ‘apparently standard’ spectra are similar to the simple soft state, in that they are still dominated by a strong thermal component, and the tail to higher energies is weak. However they vary slightly differently in that the disc luminosity increases rather more slowly with temperature, more like T^2 than T^4 (Kubota & Makishima 2004). Thus either the disc colour temperature correction is increasing, and/or its inner radius is decreasing, and/or the disc temperature structure is different from the Shakura–Sunyaev prediction that $T(r) \propto r^{-3/4}$.

The new models of disc spectra do predict an increase in colour temperature correction at high luminosities (Davis et al. 2006). Beyond temperatures of 0.9–1 keV even metals become completely ionized, and there is very little true opacity, giving an increasing f_{col} . The size of this effect depends on the optical depth of the disc i.e. on α (Fig 17) as large stresses mean that the disc is very efficient in transporting material, so the underlying disc is less dense. Recombination is less effective so the photosphere is more highly ionized and runs out of true opacity at lower L/L_{Edd} than for smaller effective viscosity.

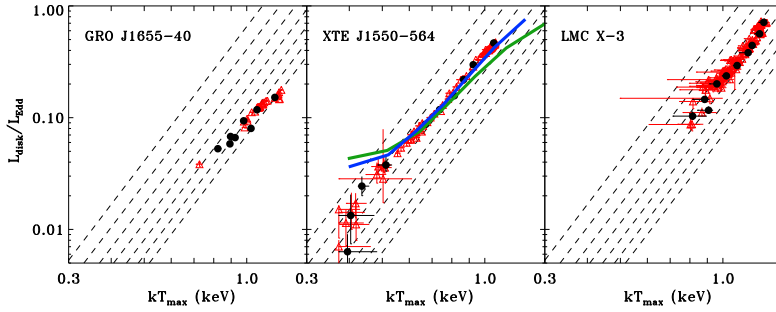


Fig. 17 Luminosity–temperature relations for the black holes with disc dominated spectra spanning the largest range in luminosity fit to the newest models of disc spectra. The blue and green lines superimposed on XTE J1550–564 show the disc model solutions of Davis et al. (2006) for viscosity of $\alpha = 0.01$ and 0.1 , respectively. A larger viscosity scaling gives a disc which is less massive, so it becomes optically thin at lower luminosity/temperature. This bends the relation away from the purely thermal $L \propto T^4$.

While the models with $\alpha \sim 0.01$ do match the bend in XTE J1550–564, this is not a particularly convincing explanation. Firstly, the rapid rise to outburst requires $\alpha \sim 0.1$ (Lasota 2001), which is inconsistent with the observed bend (Fig 17). Secondly, the bend seen in GRO J1655–40 has a somewhat different shape, and LMC X-3 (and to a lesser extent 4U 1543–47 see Fig. 16) have no bend at all but cover the same temperature–luminosity range (Davis et al. 2006).

Optically thick advection (radiation trapping) can also cause a deviation in the L – T relation. This is neglected in the Davis et al. (2005) models but should be important in a Shakura–Sunyaev disc at high L/L_{Edd} (see Section 2.3). The immense energy released close to the plane of the disc does not have time to escape to the photosphere before being swept along with the flow to smaller radii. This is more important at smaller radii so preferentially suppresses the luminosity of the hottest parts of the disc. For a disc temperature distribution parameterized as a power law, with $T(r) \propto r^{-p}$, these models predict that p goes from 0.75 in the standard regime to 0.5 when advection dominates the inner regions (e.g. Watarai et al. 2000). This matches very well to the behaviour seen (Kubota & Makishima 2004; Kubota et al. 2001), making these models attractive. Nonetheless, this is a global physical mechanism so should apply to all BHB, so again this fails to adequately address why there is no such effect seen in LMC X-3. A further argument against this bend being from the onset of advection is that this is predicted to change the observed behaviour only at $L/L_{\text{Edd}} \sim 1$, rather higher than the luminosities inferred here.

Instead, the difference in behaviour of different sources at the same inferred temperature and luminosity might be explained by different inclinations as these deviations are most noticeable for highly inclined sources. Both GRO J1655–40 and XTE J1550–564 are at $\sim 70^\circ$, and a further source 4U 1630–47 where the bend is also seen (Abe et al. 2005, not included here

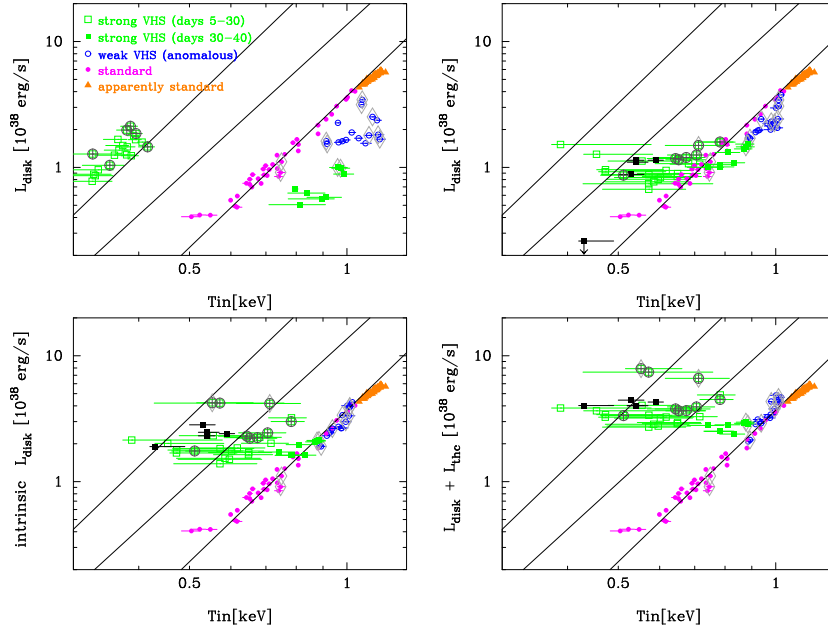


Fig. 18 Luminosity – temperature relations for XTE J1550–564 as derived from model fits of (a) a disc plus power law tail (b) an additional steep thermal Comptonization component. This illustrates the importance of fitting physical models for the tail when it is energetically dominant (very high state) though when the tail is weak (soft state) this has little effect. (c) shows the reconstructed disc luminosity assuming that all the energy in the Comptonized tail was derived from the disc, while (d) shows the reconstructed disc luminosity assuming that all the photons in the tail came from the disc. Plainly, there are some extremely Comptonized very high-state spectra which cannot be matched easily to an untruncated disc geometry (Kubota & Done 2004).

as the interstellar absorption is very high) is also likely to be at similarly high inclinations (Tomsick, Lapshov & Kaart 1998). Conversely, 4U 1543–47 is at fairly low inclination (Orosz et al. 1998), and LMC X-3, while not well determined, must be less than $\sim 70^\circ$ (Cowley et al. 1983). Inclination could affect the observed spectrum in several ways, perhaps by the disc starting to become geometrically thick and self-shielding part of its inner regions, and/or that an equatorial wind from the disc (see Section 10) starts to become optically thick, with $\tau_T > 1$ so that the luminosity seen at high inclinations is only $\exp(-\tau)$ (plus some geometry dependent contribution from scattering into the line of sight) of the intrinsic flux seen at low inclinations.

5.2 Disc spectra in the very high state

Much larger deviations from the standard $L \propto T^4$ relation are seen in soft states where the spectra are no longer disc dominated, and the tail carries

more than ~ 30 per cent of the luminosity. The importance of the tail underneath the disc emission in these very high/intermediate-state spectra means that details of how this is modelled can affect the derived parameters of the disc. A simple and often used approximation for the shape of the tail is a power law. However, if the tail is produced by Compton scattering of disc photons then there is a low energy break at energies close to the seed photons. This gives a much lower continuum flux underneath the disc spectrum, so leads to a larger inferred disc luminosity (Poutanen et al. 1997; Done, Życki & Smith 2002). This effect recovers the expected untruncated disc properties in spectra where the Comptonized component is less than 50 per cent of the bolometric flux (Kubota et al. 2001; Kubota & Done 2004). Additional effects then become important, as Comptonization conserves photon number. When the number of photons in the Comptonized spectrum is not negligible compared to those in the disc then the intrinsic disc spectrum is brighter than observed (Kubota & Makishima 2004; Kubota & Done 2004). This helps recover the expected untruncated disc in even more strongly Comptonized spectra, but for the most extreme very high state the disc still appears distorted (Done & Kubota 2006; see Fig. 18 and Section 5.3.1).

This supports the idea that there are two types of very high state geometry, one where Comptonization is stronger than in the soft state, but where the disc extends down to the last stable orbit, and one where the Comptonization is so strong that the underlying disc structure starts to change (Done & Kubota 2006). This is similar to the suggested distinction between the intermediate and very high states of Esin et al. (1997).

5.3 The high-energy tail in the soft and very high states

The soft state is always accompanied by a small fraction of emission in a tail extending to much higher energies. The shape of this tail can be roughly modelled by a power law of photon index $\Gamma \sim 2 - 2.2$ extending out beyond 500 keV (Gierliński et al. 1999). This index remains remarkably constant in the soft state irrespective of whether the tail carries 1 or 10 per cent of the total power. If the tail was produced by thermal Comptonization then this would imply that $\mathcal{L}_h/\mathcal{L}_s$ is fairly constant at ~ 2 in the energetic electron region, which is easy to arrange if the seed photons are produced predominantly by reprocessing (Haardt & Maraschi 1993). Since the intrinsic disc flux is high then this implies that the X-ray regions cover only a very small section of the disc, motivating the magnetic flare geometry sketched in Fig. 9 (Poutanen et al. 1997).

However, the high-energy tail is *not* produced by thermal Comptonization. To extend out to 500 keV and beyond requires a very high temperature, so the X-ray region must have a rather small optical depth in order to give $\Gamma \sim 2$. This leads to a bumpy spectrum, with individual Compton scattering orders separated rather than merging into an approximate power law (Gierliński et al. 1999). The observed smooth spectrum can instead be produced by Compton scattering on a non-thermal electron population, where the index is set predominantly by the shape of the electron distribution rather than $\mathcal{L}_h/\mathcal{L}_s$. This removes the constraints on geometry, since there is now

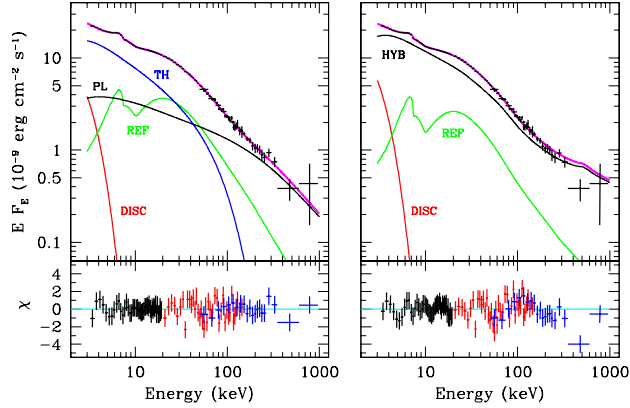


Fig. 19 Two possible spectral decompositions of the extreme very high state seen in XTE J1550–564. The left hand panel shows the fit assuming that there are two regions of energetic electrons, one thermal, connected to the hot inner flow (blue: TH), and one non-thermal (black: PL). The power-law distribution of electrons does not necessarily give a power-law photon spectrum. The right panel assumes there is only one region, where the electron distribution is a hybrid, being thermal at low Lorentz factors and non-thermal at higher ones. The reflection of the intrinsic spectrum (green: REF) is always required to highly ionized and hence is somewhat uncertain (from Gierliński & Done 2003).

no requirement for the seed photons to be reprocessed. Instead, the observed constancy of the spectral index implies some mechanism for fine tuning the electron acceleration process which is not yet understood.

While the tail is clearly non-thermal, it is not well fit in detail by a power law spectrum and its reflection (Gierliński et al. 1999; Zdziarski et al. 2001). While some of this may be due to uncertainties in modelling ionized reflection (see Section 4.1) the continuum shape should also be complex. The self consistent electron spectrum is set by a balance between the accelerative heating with cooling. The acceleration process may produce a power law electron distribution, but the cooling is more complex. High-energy electrons will cool via Compton scattering (which does produce a power law distribution) but electron–electron (Coulomb) collisions are more important than Comptonization for the low energy electrons. This is a collisional process so produces a thermal distribution. Thus the self consistent electron distribution is hybrid, being thermal at low energies with a non-thermal tail to high energies (Coppi 1999). This produces complex curvature in the Compton scattered spectrum, with a mixture of thermal and non-thermal features which fit very well to the observed soft-state spectra, with the inclusion of ionized reflection (Gierliński et al. 1999; Ibragimov et al. 2005).

The very high state tail is qualitatively similar, showing a mix of thermal and non-thermal features, but this dual nature can be seen more clearly than for the soft state. Simple power law fits do not give even a fair approximation to the shape of the tail as shown e.g. Sobczak et al. 1999b, who used different power law indices to fit the 3–20 keV and 20–200 keV data from this state

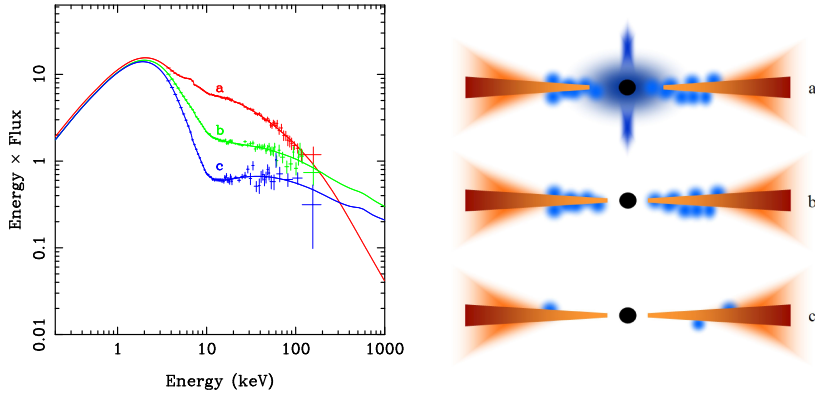


Fig. 20 Left: Extreme very high-state spectrum (a) merging smoothly onto less Comptonized very high (b) and then into a soft-state spectrum (c). All data taken from XTE J1550–564. Right: A range of geometries which can smoothly connect between extreme very high and soft states.

in XTE J1550–564. The shape of the tail is somewhat different from the soft state also: the non-thermal high energy tail is steeper, and the thermal low energy Comptonization carries a larger fraction of the total power (Zdziarski et al. 2001; Gierliński & Done 2003). Ionized reflection again adds to this continuum complexity.

Fig. 19 shows a range of possible models which can fit the tail seen in an extreme very high-state spectrum. It can be described either by two separate regions, one where there is low temperature, moderate optical depth ($\tau \sim 2$), thermal Compton scattering, together with a separate non-thermal electron region (which is again a hybrid rather than simple power law). Alternatively the thermal and non-thermal electrons can be co-spatial, but where not all the intrinsic acceleration is non-thermal. Some fraction of the power has to directly heat the electrons in order for the thermal Comptonization to be as important as observed (Gierliński & Done 2003).

5.3.1 Geometry of electron acceleration region in soft and very high states

The geometry of the electron region can be constrained from the spectra, and from the spectral evolution. Fig. 20 shows that the very high state can smoothly connect onto the soft state. The shape of the soft state spectra, with the disc being dominant, clearly shows that few of these seed photons are intercepted by the hot electrons. This can be made more quantitative. The electrons scatter only a fraction $C_f[1 - \exp(-\tau)]$ where C_f is the covering fraction of the energetic electron regions over the disc and τ is their optical depth. Thus either C_f or τ must be small in the soft state.

This is plainly not true in the extremely Comptonized very high state spectra, where the disc spectrum merges smoothly into the Comptonized emission. Both C_f and τ must be large in these spectra, though for the more weakly Comptonized very high state the disc is more visible, requiring that

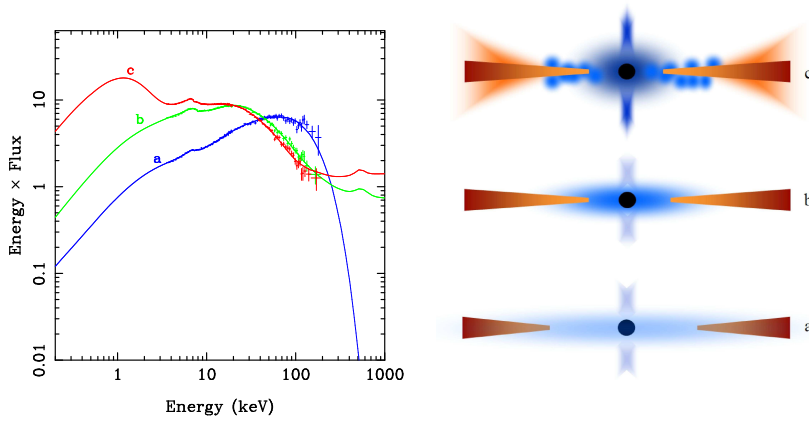


Fig. 21 Left: hard-state spectrum (a) merging smoothly onto less Comptonized very high state (b) and then into an extreme very high-state spectrum (c) during the rapid rise to outburst. All data taken from XTE J1550–564. Right: A range of geometries which can smoothly connect between the hard state and extreme very high-state spectra.

at least one of C_f or τ decreases from the extreme very high state through to the soft state (Fig. 20).

A further constraint comes from the fact that the very high state is seen to merge smoothly into the hard state on the rise to outburst (see Fig. 21). Given that the extreme very high-state spectra indicate both thermal and non-thermal electrons then it is plausible that the thermal component is from the remains of the hot inner flow, while the non-thermal is from magnetic flares above the disc (see also Fig. 19). A detailed analysis of the disc spectrum also supports the idea that the disc is slightly truncated in these extreme very high state (Done & Kubota 2006), though there are substantial uncertainties in the models of disc spectra at this point. Nonetheless, the range of very high state geometries shown in Fig. 20 and 21 match all current constraints, and form a bridge between the hard and soft states.

6 Spectral evolution

The previous sections outlined a physically motivated model in which spectral changes (particularly the hard-soft spectral transition) are driven by a changing geometry. There now exists an enormous amount of data from the X-ray binary systems which can be used to test this. Done & Gierliński (2003) systematically analyzed all the available spectra from many black hole systems, using broad band ‘colours’ to get an overview of the source behaviour. They fit physically motivated spectral models to the data in order to get intrinsic fluxes i.e. corrected for absorption and the detector response. Ratios of these fluxes roughly relate to the mean spectral slope across the given energy bands. Many black holes can then be plotted on the same diagram,

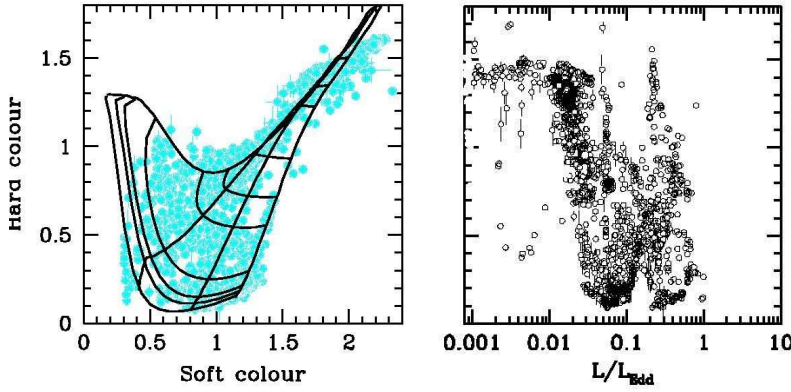


Fig. 22 Left: Colour-colour diagrams of BHBs (after Done & Gierliński 2003), overlaid with model tracks which incorporate the changing geometry of the disc, hot flow and corona. Right: Colour-luminosity plot of BHB showing how the same spectrum is seen at very different luminosities. This scatter is seen in individual objects, where the characteristic hard-to-soft spectral transition occurs at higher luminosity on the rapid rise to outburst than on the decline.

as shown in Fig. 22. *All* the black holes are consistent with the *same* spectral evolution track on these colour-colour diagrams, and this colour evolution can be well matched by Comptonization models which are based on the geometry changes described in the sections above (black lines superposed on the colour-colour data in Fig. 22; Done & Gierliński 2003).

6.1 Hysteresis

Fig. 22 shows that this well ordered behaviour in terms of the evolution of spectral shape does *not* uniquely correlate with L/L_{Edd} . Many different spectral states can be seen at a given L/L_{Edd} , or conversely, a given spectral transition e.g. hard-to-soft can be seen at multiple values of L/L_{Edd} .

This is not just due to uncertainties in distance, mass etc. The *same* black hole can show a *different* transition luminosity at different times (see e.g. Remillard & McClintock 2006). There is no one-to-one mapping between spectral state and L/L_{Edd} in most BHB. This is the well known hysteresis effect (e.g. Nowak 1995, Maccarone & Coppi 2003), which is most obvious in terms of the luminosity at which the major hard-to-soft transition takes place, with hard state having larger luminosities on the rapid rise to outburst in the hard/very high/soft state transition than the reverse on the slow decline. This effect occurs in *all* BHB with high enough signal-to-noise to track the transition except for Cyg X-1 (e.g. Maccarone & Coppi 2003). Thus hysteresis is suppressed in some way in this system, and there are two plausible potential candidate mechanisms for this, and both are based on the fact that Cyg X-1 is the only bright HMXB BHB source. The first possibility is that hysteresis is caused by the dramatic changes in accretion flow during

the H ionization instability. The high mass companion to Cyg X-1 has such a large mass transfer rate that the disc is above the H ionization temperature everywhere (see Section 2.1) so does not show the violent instability. Alternatively, since the companion does not completely fill its Roche lobe, it may be accreting low angular momentum material from the stellar wind, so forming a rather different accretion flow (Smith, Heindl & Swank 2002; Maccarone & Coppi 2003). A comparison with the neutron star LMXB favours the former explanation as the only two systems to show large scale hysteresis are also the only two in which the disc shows the dramatic H ionization instability (Gladstone, Done & Gierliński 2007). The consequent dramatic change in mass accretion rate takes much longer to propagate through the thin disc than through the hot inner flow (Smith, Heindl & Swank 2002), allowing the system to access non-equilibrium states. This is a rather different model for the observed behaviour than those which assume there are two potential steady state solutions at a given mass accretion rate, where the solution chosen depends on the past history of the flow (e.g. Zdziarski & Gierliński 2004)

7 Neutron star spectra

Black holes and neutron stars have very similar gravitational potentials as neutron star radii are of the order of three Schwarzschild radii, the last stable orbit of material around a black hole. Thus the gravitational potential in which the accretion flow is embedded is very similar between the two objects, and the models developed for the black holes should simply carry over to the neutron star systems.

However, there is a fundamental difference between the two classes of objects. Neutron stars have a solid surface, while black holes do not. Surface processes such as X-ray bursts (from nuclear burning of the accreted material onto the surface), or coherent pulsations (from a residual magnetic field) are unique signatures of neutron stars. These are a sufficient but not necessary condition for a surface: not all neutron star systems show these (e.g. the review by Lewin, van Paradijs & Taam 1993)

By contrast, the boundary layer between the accretion flow and the surface should *always* be present. In Newtonian gravity an accretion disc can radiate only half of the gravitational potential energy with the other half stored as kinetic energy of the rotating material. This kinetic energy is all radiated at the surface in a boundary layer if the surface is stationary. In General Relativity the energy in the boundary layer is even larger, about twice that of the disc (Sunyaev & Shakura 1986; Sibgatullin & Sunyaev 2000). Neutron stars can of course be rapidly rotating, but even the fastest confirmed millisecond pulsar PSR J1748–2446ad (at 716 Hz) is rotating at only approximately half the Keplerian period (Hessels et al. 2006), where the energy released in the boundary layer should still be as much as that in the disc (Sibgatullin & Sunyaev 2000).

Thus the expectation is that accreting neutron stars with low magnetic fields ($B < 10^{8-9}$ G, so that this does not affect the dynamics of the accretion flow) should have accretion flows which are similar to black holes at the

same L/L_{Edd} , but with the addition of a boundary layer with luminosity comparable to that of the disc.

Low magnetic fields are found only in the LMXB NS systems. There are no known NS HMXB with low fields, nor are there any known NS LMXB with high fields. This can plausibly be explained as dissipation of the high birth field of $\geq 10^{12}$ G in accretion torques during the long term evolution of the binary to Roche lobe overflow (see e.g. the review by Bhattacharya & Srinivasan 1995). However, even within the LMXB NS there are a range of B fields. The accreting millisecond pulsars must have fields around $\sim 10^8$ G in order for the magnetic pressure to dominate over the ram pressure of the $L/L_{\text{Edd}} \sim 0.05$ flow and hence produce the eponymous X-ray pulsations (Chakrabarty & Morgan 1998). The rest of the LMXB NS systems must have lower surface fields, or they too would produce similar pulsations during periods of similarly low mass accretion rate (Vaughan et al 1994; Maccarone & Coppi 2003). This range of surface field can be explained from the differences in *long term* mass accretion rates. The millisecond pulsars are unstable to the disc instability, and are bright only during short outbursts (see Fig. 6). Their mean mass accretion rate is much lower than all the other NS LMXB (e.g. Gladstone, Done & Gierliński 2007), and this is insufficient to bury their surface field under the accretion flow, where it can only diffuse out on timescales of ~ 100 years (Cumming, Zweibel & Arras 2001).

Neutron star LMXBs fall into two categories: atolls (including all the millisecond pulsars: e.g. Van Straaten, van der Klis & Wijnands 2005) and Z sources (Hasinger & van der Klis 1989). These differ in luminosity (as well as several other aspects, see Section 11.2), with the Z sources being typically brighter ($>0.5 L_{\text{Edd}}$) while the atolls are seen over the same range of luminosities as the black holes discussed in the previous sections (from $< 10^{-3}$ up to $\sim L_{\text{Edd}}$). Thus here we consider only the atolls and millisecond pulsars, as these form a matched luminosity sample to compare with the BHB.

The most obvious point of similarity is that the atolls switch between two distinct spectral states (e.g. Gierliński & Done 2002; Maccarone & Coppi 2003): the soft ‘banana’ and the hard ‘island’, so named from the shapes they make on a colour–colour diagram. Sources which show transitions between these states trace out a C (or atoll) shaped path from the hard island state at the top right of the C down to the lower banana branch at the bottom of the C and then curving slightly upwards and to the right (bottom right hand end of the C, termed the upper banana branch) as the source luminosity increases further (see e.g. Hasinger & van der Klis 1989). The corresponding spectra are shown in Fig. 23, and the correlation with the BHB soft–hard transition is clear, with the island state corresponding to the hard state and the banana branch corresponding to the soft states (soft/very high).

7.1 Spectral evolution in atolls

The left panel of Fig 24 shows this hard–to–soft spectral transition even more clearly in the colour–colour and colour–luminosity diagrams for a sample of millisecond pulsars and atolls (Gladstone et al 2007). These colours are

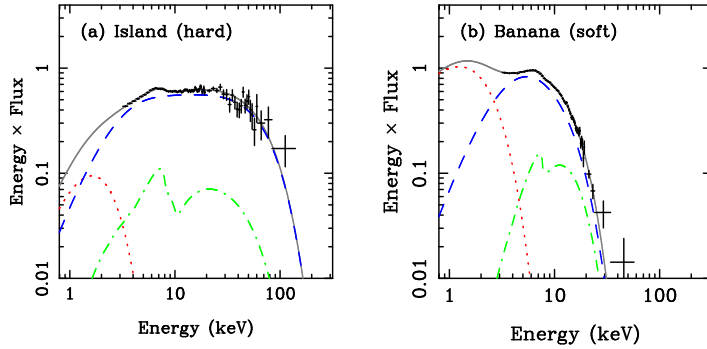


Fig. 23 Two spectral states of an atoll 4U 1705–44 from *RXTE*. The panels show unfolded and unabsorbed X-ray spectra, together with the best-fitting models extrapolated below the lower PCA bandwidth limit (3 keV) in order to demonstrate the soft component. (a) the hard (island) state (observation id. 40051-03-12-00) fitted by a blackbody (dotted red curve), its thermal Comptonization (dashed blue) with reflection (dash-dot green). (b) the soft (banana) state (observation id. 40051-03-14-00) fitted by a disc blackbody (dotted red), thermal Comptonization of unseen seed photons hotter than the disc (dashed blue) and reflection (dash-dot green).

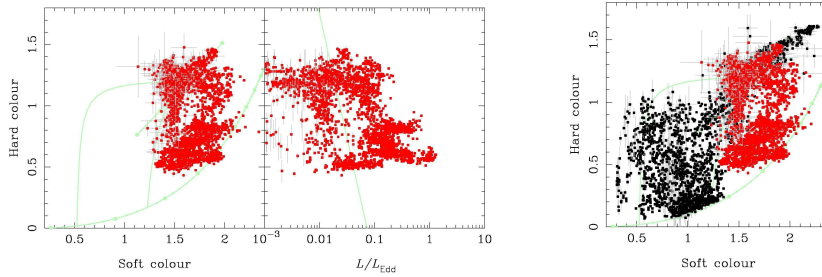


Fig. 24 Left: Colour–colour and colour–luminosity diagrams for all low column atolls and millisecond pulsars in Gladstone et al (2007). Right: a comparison of BHB (black) and neutron star (red) spectral evolution. Plainly there are significant differences between these two types of object, consistent with the existence of an event horizon in black holes, in contrast with the known surface of the neutron star (after Done & Gierliński 2003).

exactly equivalent to the ones used for the BHB in Fig. 22, so can be directly compared (Done & Gierliński 2003, right panel of Fig 24). The very similar gravitational potential and very similar range in L/L_{Edd} give rise to very different spectral evolution between BHB and neutron stars.

This difference can be interpreted by using the same truncated disc model, outlined in Secs. 3.4 and 6, but taking into account the presence of the solid surface (see Gierliński & Done 2002; Done & Gierliński 2003). This can impact the spectrum in two separate ways, firstly through its direct

thermal emission, and secondly through the additional energy released in the boundary layer.

The truncated disc model for the lowest mass accretion rates in BHB has few seed photons from the disc illuminating the inner hot flow. The resulting spectrum has weak disc emission, and a hard Comptonized spectrum. In the NS at correspondingly low accretion rates, the disc should be similarly truncated, while the hot inner flow joins smoothly onto the optically thin boundary layer (Medvedev & Narayan 2001; Medvedev 2004). Thus the hot flow is (at least) twice as luminous as before, so might be expected to be harder than in BHB. However, the neutron star surface provides an additional source of seed photons as it is heated by irradiation and/or conduction. Since these are at the centre of the hot flow then they form the dominant seed photon flux. For the expected quasi-spherical geometry then only a fraction $1 - e^{-\tau}$ are seen uncomptonized. Nonetheless, these residual surface photons can be the source of the soft component seen in the island state (Gierliński & Done 2002b), as the disc is at lower energies due to truncation and (similarly to the BHB, see Section 4.1) it is made more difficult to see by the often high Galactic absorption column.

The additional source of seed photons from the NS surface means that NS spectra are never quite as hard as the hardest BHB (Done & Gierliński 2003). It also changes the evolution of the spectrum as a function of luminosity compared to the BHB: NS move horizontally to the right on a colour-colour diagram, when brightness increases (Gierliński & Done 2002a; Muno, Remillard & Chakrabarty 2002), whereas the BHB move diagonally (see Section 6). This can be explained by the increasing temperature of the neutron star surface as accretion rate (and optical depth of the hot flow) increases. With the seed photon temperature rising, the energy at which the Comptonized spectrum rolls over at its low-energy end increases, and the contribution of the uncomptonized soft photons from the NS surface decreases. Therefore, the soft X-ray part of the spectrum becomes harder and the soft colour increases. Since the seed photons are from the neutron star surface rather than from the disc then the disc truncation radius makes little difference to the spectrum. The seed photon geometry does not change, nor does the ratio of seed photon to hot electron luminosity since the seed photon luminosity is tied to that of the hot flow (via irradiation and/or conduction). Thus the Comptonized spectrum remains the same at high energies, away from the seed photons so the hard colour stays the same, and the source moves horizontally on the colour-colour diagram (Gierliński & Done 2002a, 2002b; Done & Gierliński 2003).

With further increasing accretion rate the disc eventually moves in and the hot inner flow collapses into a thin disc. The increased mass accretion rate is now all concentrated in the equatorial plane and the boundary layer (or a spreading layer which has similar properties: Inogamov & Sunyaev 1999; Suleimanov & Poutanen 2006) becomes optically thick to electron scattering, but not yet thick enough to completely thermalize into a blackbody (Popham & Sunyaev 2001). Thus the boundary layer spectrum changes dramatically from hot, optically thin Comptonization to much lower temperature (only slightly higher than expected for complete thermalization), optically thick

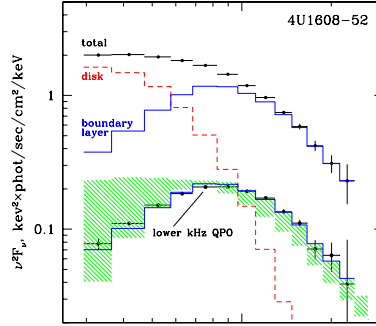


Fig. 25 Fourier-frequency resolved spectra of the boundary layer in the atoll 4U 1608 at high L/L_{Edd} (banana branch). The lower kHz QPO ν_l has the same spectrum as that inferred from fitting the ‘Eastern’ model to the total spectrum (black) i.e. where the disc (red) is at lower energies and the Comptonized boundary layer (blue) contributes at higher energies. (from Gilfanov, Revnivtsev & Molkov 2003).

Comptonization, giving a correspondingly dramatic drop in hard colour from the island state to the banana branch. The decrease in the inner disc radius is consistent with increasing frequencies in power spectra as the source makes a transition from the island state to banana branch (see e.g. the review by van der Klis 2004; Section 9).

However, detailed X-ray spectral fitting of the soft/banana state shows that unambiguously decomposing the smooth curved shape into disc and boundary layer components is difficult. Historically, there were two different approaches to the spectra. In the Eastern model (Mitsuda et al. 1989) the soft and hard components were identified with the disc and Comptonized boundary layer, while in the Western model (White, Stella & Parmar 1988) they were attributed to blackbody from the surface/boundary layer and a Comptonized disc, respectively. However, this ambiguity is now resolved, most compellingly by variability studies which show that the spectrum of the variable component is hard. Since the most rapid variability should be associated with the BL rather than the disc (as is also the case in BHB: Churazov, Gilfanov & Revnivtsev 2001), then this is clear evidence for the ‘Eastern model’ with a lower temperature disc and hotter, Comptonized BL (Gilfanov, Revnivtsev & Molkov 2003; Revnivtsev & Gilfanov 2006; see Fig. 25). Better spectral models of Comptonization which include the low energy turn-down of the Comptonized emission close to the seed photon energy also break the spectral degeneracy, and show clearly that even the spectra alone favour this model (Di Salvo et al. 2000; Gierliński & Done 2002b).

Thus there is strong evidence for the identification of the cooler component on the banana branch as the disc, while the hotter one is the boundary layer (Eastern model). There is clear, though indirect, spectral evidence for the NS surface emission as well from the fact that the seed photon energy is higher than the observed disc spectrum (Di Salvo et al. 2000; Gierliński & Done 2002b; Falanga et al. 2006). All three components can only be seen

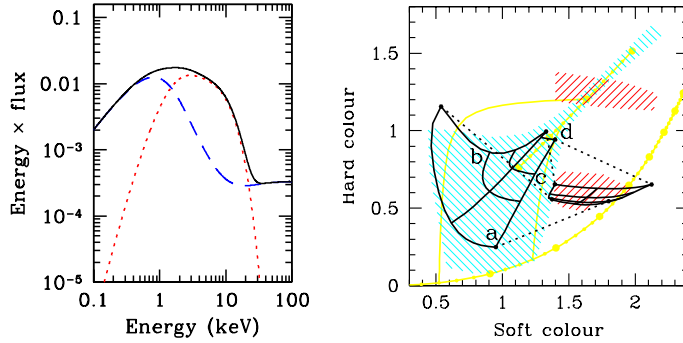


Fig. 26 The effect of the boundary layer. Left: The dashed blue curve represents a soft-state spectrum of a black hole with disc emission and a hard power-law tail. The red dotted curves show additional emission from the boundary layer with luminosity equal to that of the original spectrum. The total spectrum (solid curve) represents a typical soft-state spectrum from a neutron LMXB. A weak tail to higher energies, observed in many neutron star sources (Paizis et al. 2006), may be a direct counterpart of the non-thermal Comptonization in black holes. Right: Colour-colour diagram showing the areas occupied by black holes (top left to bottom right cyan hatched area) and atolls (top right to bottom left red hatched area). The grid on the left represents a range of models (disc + hybrid Comptonization) which describe the range of soft states from black holes. Point *b* on the grid corresponds to the black hole model on the left panel (dashed blue curve). Adding a boundary layer transforms the entire grid into the area covered by the banana state of atolls.

directly around the transition, where the disc has high enough temperature to contribute to the X-ray bandpass, while the boundary layer is not yet completely optically thick so as to Comptonize all the NS surface photons (Fiocchi et al. 2007).

As the luminosity increases along the banana branch then the disc becomes more luminous and hotter. This should also follow a luminosity $\propto T^4$ relation while the disc maintains a constant inner radius, but decomposing the curvy spectra to this accuracy is difficult (Done & Gierliński 2002b; Takahashi & Makishima 2006; Lin, Remillard & Homan 2007). The shape of the Comptonization also changes, in a way which is consistent with it becoming more optically thick as the accretion rate increases, and hence becoming more saturated, approaching a blackbody (Gierliński & Done 2002b; Revnivtsev & Gilfanov 2006). This competes with the expected increase in temperature of the BL due to increased luminosity, as more complete thermalization leads to a lower effective temperature. Thus the BL temperature can remain constant or even drop as the mass accretion rate increases (Gierliński & Done 2002b; Revnivtsev & Gilfanov 2006), giving a fairly constant hard colour, while the soft colour (set by the disc) increases along the banana branch.

Fig. 26 shows how the addition of the boundary layer to the variety of soft states (soft and very high) BHB accretion flow models reproduces the colour evolution along the banana branch. Thus the NS LMXB are consistent with the same accretion flow models as the BHB, where the major spectral evolu-

tion is driven by the decreasing truncation radius of the disc with increasing accretion rate, but with the addition of the boundary layer expected from the NS surface. Conversely, the fact that there is a clear difference between the spectral evolution of BHB and NS LMXB is consistent with the existence of an event horizon in BHB, the most extreme strong gravity prediction of Einstein's General Relativity (see e.g. the review by Narayan 2003 for other evidence for a black hole event horizon).

8 Linking jets to the hot inner flow

Another major area of progress in the last few years has been in terms of understanding the link between accretion flows and jets. Like everything else, the radio emission strongly correlates with spectral state in BHB. The low/hard state has a steady jet, with radio luminosity $L_R \propto L_x^{0.7}$ (e.g. Corbel et al. 2003; Gallo, Fender & Pooley 2003). This can be quantitatively matched by an ADAF-like hot inner flow producing the X-ray emission, and acting as the base of the jet which produces the correlated radio flux (Heinz & Sunyaev 2003). This can also explain the apparently much weaker radio emission seen in neutron star systems. The ADAF-like flow is inefficient in BHB, so the X-ray emission is weaker for the same accretion flow than in neutron stars where the advected energy is released at the surface (Kording et al. 2006).

However, this relation abruptly changes during transitions to the soft state, where the radio emission is strongly suppressed (Tananbaum et al. 1972; Fender et al. 1999b; Corbel et al. 2001; Gallo et al. 2003). The very high/intermediate state is much more complex, as it is the transition state between the low/hard to high/soft states, i.e from a bright steady jet to strongly suppressed radio emission (the 'jet line', which seems to correspond to the ejection of the last remaining portion of the hot inner flow: Vadawale et al. 2001; 2003). The rapid changes in the jet are not limited to this apparent collapse. This state is also characterized by transient outbursts of the radio emission, some of which can be directly resolved into bright blobs moving away from the source at relativistic speeds (e.g. Mirabel & Rodriguez 1994; Hjellming & Rupen 1995; Fender et al. 1999a).

All these events can be unified into the picture for the outbursts outlined above, and given an outline theoretical basis in terms of our current (limited) understanding of jet production. Meier (2005) describes the two requirements for producing a jet as a strong, ordered magnetic field, and some means of getting mass onto this field. A large scale-height flow offers the means to do both of these. Thus any state in which there is a large scale-height inner flow should produce a jet, while that from a geometrically thin disc is expected to be much weaker, as observed. Transient bright events during the state transitions can be phenomenologically explained if the jet Lorentz factor increases as the accretion disc moves inwards (Vadawale et al. 2003; Fender, Belloni & Gallo 2004; 2005). During the rise to outburst the faster jet catches up with the slower moving ejected material, and the resulting shocks provide local energy dissipation and acceleration of particles. This explains why such transient radio brightenings are *not* seen in intermediate states when the source *declines* from high/soft to low/hard state - the disc

is moving outwards, so the jet speed decreases, so there is no possibility for the slower jet to interact with the faster one (Fender et al. 2005). Again, this can be connected to the theoretical jet models which predict a terminal speed related to the escape velocity of the foot-point of the magnetic field. As the disc moves inwards, compressing the radial extent of the hot flow and/or anchoring the large scale height magnetic field, the escape velocity increases so the jet speed increases.

While this gives a very attractive picture, significant problems remain. One obvious question is what ultimately powers the jet, whether it predominantly taps the gravitational potential or whether it predominantly taps the spin energy, plausibly via the Blandford–Znajek mechanism. The possibility of spin powered jets has given rise to persistent speculation in the literature that relativistic jets require a maximally spinning black hole. This is open to observational constraints! Spin in BHB is measurable, though currently controversial. If the BHB have a *range* of spins from $a_* = 0.1$ – 0.8 as suggested by accretion disc fitting to the disc dominated high/soft-state spectra (Davis, Done & Blaes 2006; Shafee et al. 2006; Middleton et al. 2006) then this clearly rules out a very strong dependence of jet power on spin since they are all consistent (though with large uncertainties) with the *same* $L_R \propto L_X^{0.7}$ relation (Middleton et al. 2006). This would favour a predominantly gravity powered jet.

MRI simulations of large scale-height accretion flows offer some independent suggestions. These include the self-consistent, magnetically generated stresses and produce jets and outflows without additional physics. These show in general that the jet has *two* components, a matter dominated, funnel wall jet and an electromagnetic Poynting flux jet (McKinney 2005; Hawley & Krolik 2006). The electromagnetic jet is probably highly relativistic and is very strongly dependent on a_* , indicating that this may be partly (or perhaps even mostly) powered by the black hole spin (McKinney & Gammie 2004). By contrast, the funnel wall outflow is less relativistic and is much less dependent on black hole spin (McKinney 2005; Hawley & Krolik 2006). While we caution again that the simulations do not currently include radiation, so cannot yet be unambiguously connected to observations, it seems that the funnel wall, matter dominated jet, powered predominantly by the gravity of the accretion flow, matches rather well to the properties of the jets in Galactic black hole binaries (see McKinney 2005). By contrast, the spin powered electromagnetic jet should be strongly beamed, making it hard to detect unless observed within 5 – 10° of their rotation axis. There are no known LMXB systems at such low inclination angles. However, the inner disc can be misaligned with the binary orbit, in which case the jet *may* be close to the line of sight in the BHB V4641 Sgr (Maccarone 2002).

9 Variability Power Spectra

The variability power density spectra (PDS) likewise change dramatically as a function of L/L_{Edd} , correlating strongly with spectral state (see e.g. the reviews by van der Klis 2004 and Remillard & McClintock 2006). Here we show how the major features of the power spectra can be explained in

the truncated disc model, though we also stress that there is much more complexity which is not currently well understood.

9.1 PDS from the low/hard (BHB) and island (NS) states

One of the most confusing aspects of the power spectral literature is the multiple components and variety of nomenclature used. Again, similarly to spectral states, this reflects the evolution of the field driven by the growing signal-to-noise and concomitant understanding of the power spectral shapes. The left panel of Fig. 27 shows a power spectrum from GX 339-4 in one of its hard states. With poor data this can be described as band limited noise, with a ‘flat top’ in $\nu P(\nu)$, so represents a power spectrum with equal variability power per decade in frequency, i.e. $P(\nu) \propto \nu^{-1}$. This extends between a low and high frequency break, ν_b , below which the PDS is $\propto \nu^0$, and ν_l , above which the spectrum steepens to $\propto \nu^2$. However, with good data it is apparent that this band limited noise is bumpy, and not well represented by a (twice broken) power law (Belloni & Hasinger 1990). Instead, it is much better described by a series (generally 4–5) of peaked noise components (Lorentzians), where the peak frequency, width and normalization are free to vary (Psaltis, Belloni & van der Klis 1999; Nowak 2000; Belloni, Psaltis & van der Klis 2002). In this description the ‘flat top’ is made from 2–3 Lorentzians, with the lowest and highest frequency components typically having roughly equal power, giving a broad peak in $\nu P(\nu)$ between ν_b (also sometimes called ν_{low} or ν_0) and ν_l . In between these there is another component, peaking at ν_h , which is associated with (or sometimes replaced by) the low frequency QPO at ν_{LF} , which can have very complex harmonic structure. At the highest frequencies there is sometimes a weak component peaking at ν_u , forming a small bump in the dimmest hard state, but this is soon lost in the noise as the source spectrum softens.

Neutron stars in the island state have long been known to show very similar power spectra to black holes in the hard state (e.g. Yoshida et al 1993). In the newer language of Lorentzians as described above then there are clear similarities to the BHB, with these systems showing the *same* sorts of Lorentzian components (see the right panel Fig. 27), which show the *same* correlations between frequencies as for the black holes (Psaltis et al. 1999; Wijnands & van der Klis 1999; Belloni et al. 2002; van der Klis 2004). However, there are also clear differences. Their smaller mass gives faster timescales, but even allowing for this there is more high frequency power in the neutron stars than in the black holes (Sunyaev & Revnivtsev 2000). Fig. 27 shows power spectra from a neutron star and a black hole (which are matched in ν_b , scaled by the mass difference). It is clear that the major difference is simply in normalization of the highest frequency component ν_u . This can be explained as turbulence at the boundary layer giving additional high frequency noise to excite whatever resonance produces the component at ν_u (Sunyaev & Revnivtsev 2000).

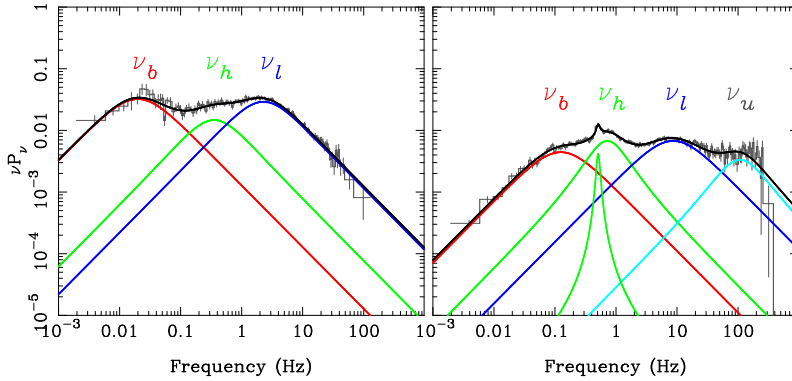


Fig. 27 The right panel shows a PDS from the hard state of GS 339-4, together with its decomposition into 3 Lorentzian components peaking in $\nu P(\nu)$ at ν_b , ν_h , and ν_l , respectively. The left panel shows a PDS from the neutron star 4U 0614+091, showing the same components (with two Lorentzians around ν_h), but with a higher frequency component, ν_u , consistent with there being additional noise power from turbulence at the surface at the shortest timescales.

9.2 Evolution of the PDS during BHB transitions

The evolution of the power spectrum in Cyg X-1 is shown in the panels of Fig. 28 (after Axelsson, Borgonovo & Larsson 2005), with these individual Lorentzians superposed. It is clear that these components are linked together, so that their frequencies all increase as the spectrum softens from the dimmest to the brightest hard state through to the soft state (see e.g. van der Klis 2004). The most obvious correlations are that the LF QPO (or ν_h if the QPO is not seen as a clear component) and low frequency break in the continuum noise power change such that $\nu_{LF} \sim 5\nu_b$ (Wijnands & van der Klis 1999), while $\nu_l \sim 10\nu_{LF}$ (Psaltis et al. 1999; Belloni et al. 2002). There is much less data on the weak high frequency component, but including results from neutron star systems (see below) gives $\nu_u \sim 30\nu_l^{1/2}$ (Belloni et al. 2002). However, there are also systematic correlations in the width and rms of these components, such that as each component approaches ~ 5 Hz its amplitude and width drops (Pottschmidt et al. 2003; Kalemci et al. 2004; Belloni et al. 2005; Axelsson et al. 2005; Kalemci et al. 2006).

Even without a clear model for the origin of the variability, these data give strong support for the truncated disc model. The existence of characteristic frequencies in the PDS shows that some particular radius is picked out by the variability, and that fact these frequencies *move* (by up to a factor 50; Cui et al. 1999) shows that this radius must also move, as predicted by the truncated disc/hot inner flow models. This is a significant success of these models, since the changing geometry picture was developed to explain the spectral transitions.

This can be made more quantitative in a variety of ways. Physically, the truncated disc model has several characteristic frequencies. The lowest of these would probably be the viscous timescale of the inner edge of the

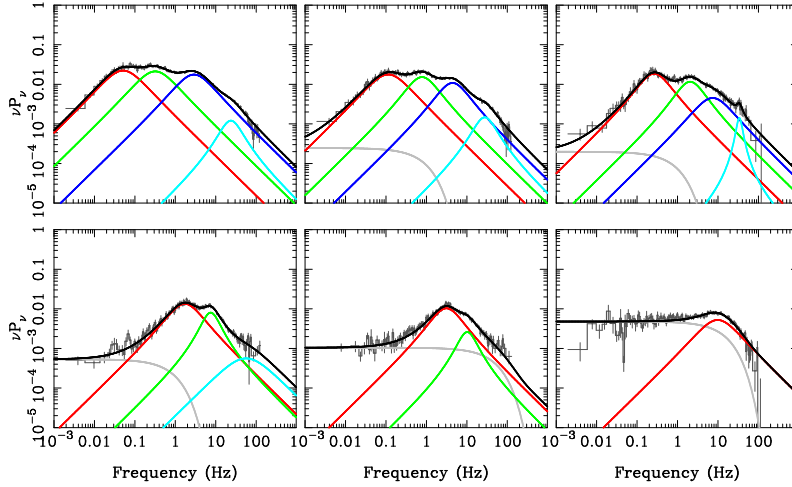


Fig. 28 The evolution of the PDS in Cyg X-1 as it makes a transition from the hard to the soft state, together with the individual Lorentzian components. The major feature is that all frequencies increase together, and that each component is strongly suppressed as it approaches ~ 5 Hz (after Axelsson et al. 2005). The additional noise component shown as the grey line is not seen in transient BHB.

thin disc. This acts as a low pass filter, suppressing any faster fluctuations in the mass accretion rate through the disc due to the inability of the disc to respond to these (Psaltis & Norman 2000, Churazov et al. 2001). This predicts $\nu_b \sim \nu_{visc} = (H/R)^2 \alpha \nu_\phi$ (see section 2.2), so for $H/R \sim \alpha \sim 0.1$ (as appropriate for the thin disc) this gives $\nu_{LFB} \sim 0.2(r/6)^{-3/2}(m/10)^{-1}$ Hz, where $m = M/M_\odot$ is the compact object mass. This predicts that ν_b sweeps from 0.03 to 0.2 Hz as observed during transitions from the hard to very high/soft state if r decreases from 20 to $6 r_g$.

A different way to determine the disc truncation radius is through the low frequency QPO. There is as yet no clear consensus on the origin of this feature, though the relativistic precession model (Stella & Vietri 1998; 1999; Stella, Vietri & Morsink 1999) has many attractions (see e.g van der Klis 2004). Nonetheless, whatever the origin, any characteristic timescale should be longer than the Keplerian orbital period. The QPO itself is not very constraining due to the long timescales implied by its low frequency. However, using ν_{LF} with the correlations described above to predict ν_u even when it is not seen give much tighter constraints on the disc radius. These relations again imply that the inner disc radius moves from $\sim 20 R_g$ in the faintest hard state where the LF QPO is seen to $\sim 4 - 6 R_g$ in the weakest very high state (almost soft state) (Di Matteo & Psaltis 1999).

Thus two independent ways to use the frequencies contained in the PDS give the same radius for the inner edge of the truncated disc and these radii are *quantitatively* as predicted by the changing geometry model for *spectral* transitions, with the disc extending down to the last stable orbit only in the soft state. While there is as yet no wideranging study of these model pre-

dictions across all the BHB, Chaty et al. (2003) note that the large radius of the truncated disc inferred from the hard state spectrum of the dim transient XTE J1118+480 (see Fig. 11) is qualitatively consistent with the longer characteristic PDS timescales seen in this object.

The truncated disc picture can even explain to some extent the evolution of the PDS *shape* during the transitions, not just the evolution of the characteristic frequencies. The left hand panel of Fig. 29 shows that while the frequencies change dramatically, the power at high frequencies remains remarkably constant (Gierliński, Nikolajuk & Czerny 2007). The truncated disc geometry implies that whatever fluctuations are produced at the truncation radius (ν_b , ν_{LF} , and possibly ν_l and ν_u) have to propagate down through the hot flow. This is especially clear in the hard state, where the truncation radius can be much larger than the last stable orbit, yet the luminosity must be predominantly produced in the region of maximum gravitational energy release, i.e. concentrated close to the black hole. Thus the truncation radius produces a spectrum of fluctuations, but these are further modulated by being propagated through the hot flow. In particular, the viscous timescale at the inner edge of the hot flow (i.e. the last stable orbit or below) acts as a low pass filter at frequency ν_{\max} . The observed power spectrum is then given by multiplying the power spectrum of the intrinsic fluctuations with the power spectrum of the low pass filter. This acts to form a high frequency ‘barrier’ at ν_{\max} .

The right hand panel of Fig. 29 shows the effect of this for $\nu_{\max} = 5$ Hz on an intrinsic spectrum of 4 equal rms Lorentzian components with frequencies ν_b , ν_h , ν_l and ν_u all correlated as described above. As the disc inner radius moves inwards, all its characteristic frequencies increase, but fluctuations faster than the viscous timescale at the inner radius of the hot flow are strongly damped. Each component in turn is affected as it approaches ν_{\max} . First the high frequency section of each Lorentzian is trimmed, making it asymmetric, and then as its peak frequency moves through ν_{\max} , the rms of that component is strongly suppressed.

Thus filtering by a hot flow keeps the power spectrum above ~ 5 Hz remarkably constant, as seen in the data. Since all the other frequencies are increasing, this leads to a narrowing of the observed power spectrum, again as seen in the data (Fig. 29). The frequency $\nu_{\max} \sim 5$ Hz also matches quantitative expectations of the viscous timescale at the last stable orbit of a hot inner flow ($H/R \sim 0.3$). With $\alpha \sim 0.1$ this gives a predicted dynamical timescale of ~ 2 ms, close to the ~ 4 ms expected for the last stable of a $10 M_\odot$ black hole (Gierliński et al. 2007; Done & Gierliński 2007).

9.3 Propagation models

The model described above, where a set of characteristic frequencies are produced at the inner disc edge (perhaps excited by the turbulence generated at the disc/hot flow interface) and then propagated down across the hot flow, has yet to be modelled in detail. Instead, the models in the literature mostly incorporate the propagating fluctuation model of Lyubarskii (1997) which makes the broad range of frequencies to describe the continuum ‘flat top

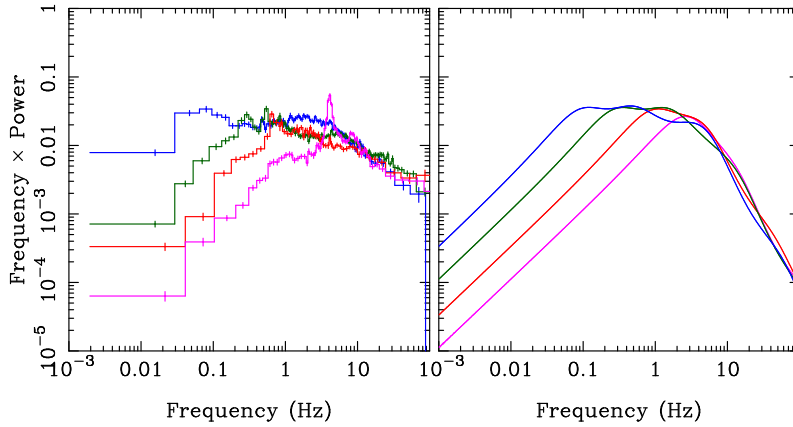


Fig. 29 Left: a range of PDS from XTE J1550–564 during a transition. The major features are that the power spectrum narrows as the spectrum softens, but the power above 5 Hz remains remarkably constant. Right: a model showing how the PDS evolves if an initial spectrum of fluctuations (consisting of 4 Lorentzians with equal power, and correlated frequencies as described in the text) is filtered through a hot inner flow. The viscous timescale at the last stable orbit acts as a low pass filter at fixed frequency $\nu_{\text{max}} = 5$ Hz. As the initial fluctuations move to higher frequencies, more and more of the initial power spectrum is suppressed by the filtering, leading to a narrowing of the observed PDS, and to a remarkably constant spectrum above ν_{max} .

noise’ from a broad range of radii. In the original model, random viscosity fluctuations at some radius (such as would be produced by the time and spatially variable MRI viscosity: Balbus 2005) give random mass accretion rate fluctuations on the viscous timescale at that radius. These affect the emission of the ring at that time, but this is a negligible fluctuation on the total luminosity if the radius is large. More importantly, this fluctuation in mass accretion rate affects the next radial zone in, modulating its random fluctuations. This has the effect that the fluctuations at each radius are the *product* of the fluctuations from all previous radii, forming a fluctuation power spectrum $P(\nu) \propto \nu^{-1}$ down to the inner boundary of the flow, so modulating the region where most of the energy is released. Thus the propagation models make the broad power spectrum from a broad range of radii, while model described above gives a broad range of frequencies from a single radius, and then propagates these down through the extended hot inner flow.

Nonetheless, these pure propagation models explain another puzzling aspect of the variability which points to a deep interconnectedness of its properties. The size of the rms fluctuations, σ , is linearly related to the source flux, F , such that that σ/F remains constant (Uttley & McHardy 2001). This is more or less equivalent to saying that the fluctuations have a log-normal distribution (Uttley, McHardy & Vaughan 2005). There is no way to do this in any model of variability which takes a *sum* of independent events, so all shot noise models are ruled out (Uttley et al. 2005). This also rules out self organized criticality models (e.g. Mineshige, Takeuchi & Nishimori 1994), despite

them also having some radial connections. In these models the variability is propagated inwards only once the accretion flow at that radius crosses some critical threshold in properties. This produces a power law rather than log-normal distribution of fluctuations, pointing to the propagation being truly diffusive rather than triggered abruptly as in the SOC models.

9.4 Propagation in a truncated disc geometry

However, it is plain that these models do need to be coupled to the truncated disc geometry in order to produce the noise power (including all QPO's) in the *Comptonized* spectrum, not in the disc (Rodriguez et al. 2004; Revnivtsev & Gilfanov 2006; Sobolewska & Życki 2006). Such coupling can give a qualitative match to the changes in power spectra seen in the hard-to-soft state transition in Cyg X-1 (Churazov, Gilfanov & Revnivtsev 2001). It can also explain the otherwise utterly puzzling behaviour of the time lags between different frequency bands. Thermal Comptonization models build up the spectrum from repeated scatterings. To produce higher energy photons requires more scatterings, so these should lag behind the lower energy photons by the light crossing timescale. This is a very short timescale, of order milliseconds for the BHB, and should be independent of variability timescale for a uniform region. Instead, the observed lags are smaller for rapid flux changes, and can be as long as a second (Miyamoto & Kitamoto 1989). A non-uniform density profile over an enormous emission region can match these aspects of the data (Kazanas, Hua & Titarchuk 1997). However, as well as being physically unlikely given the small size scale of the gravitational energy release, this can be ruled out as it predicts longer timescales for variability at higher energies, opposite to that observed (Maccarone, Coppi & Poutanen 2000). Instead the lags are much more likely to be associated with spectral variability, where the spectrum evolves from soft to hard (Poutanen & Fabian 1999). This can be produced in the propagating fluctuation model using the *same* geometry as sketched in Fig. 10. The fluctuations start at large radii, where the disc and hot flow overlap. This gives a soft spectrum as there are many seed photons from the disc (due either to intrinsic emission or reprocessed hard X-rays) which illuminate the flow. As this fluctuation propagates inwards then it goes into the region where there is no disc underneath the flow, so fewer soft photons and hence a harder spectra with a smaller amount of reflection (Revnivtsev, Gilfanov & Churazov 1999). Thus the spectrum changes from soft to hard during the rapid variability. This can match the energy and time dependence of the time lags, as well as the broad band power spectral shape and rms-flux relation (Kotov, Churazov & Gilfanov 2001; Arevalo & Uttley 2006).

9.5 Unsolved Problems

This section has not touched on how the frequencies at the truncation radius are generated, nor on the more complex behaviour of the neutron star island-banana transition, where ν_l and ν_u suddenly morph into (or are replaced by?)

the ‘twin peak’ narrow kHz QPO’s, nor the weak narrow high frequency (3:2 harmonic?) QPO’s occasionally seen in the BHB in the very high state (van der Klis 2004). Nonetheless, a model where the truncated disc produces a spectrum of characteristic frequencies which then propagate into the hot inner flow to modulate its Comptonized emission plainly captures the essence of the behaviour. Further investigations, looking at modes of this hot flow (Rezzolla et al 2003; Giannos & Spruit 2004; Blaes, Fragile & Arras 2006) and how it interacts with the surface should surely give insights into these remaining issues.

10 Accretion disc winds

The previous sections have shown how the combination of a fairly standard Shakura–Sunyaev disc and a hot inner accretion flow can explain the major spectral transitions seen in BHB and the disc accreting NS in the range $10^{-3} < L/L_{\text{Edd}} < 0.5$. However, there are also indications that the disc structure *changes* at high mass accretion rates, and that winds become very important. Thus to understand systems at $L/L_{\text{Edd}} > 0.5$ we need more than the simple disc and hot flow picture, we need to understand the impact of winds and outflows on the disc structure.

In recent years, a growing number of X-ray binaries have been found to exhibit absorption lines from highly ionized elements, most often He and H-like Fe at 6.67 and 6.95 keV. These systems range from microquasars such as GRO J1655–40 (Ueda et al. 1998; Yamaoka et al 2001; Miller et al. 2006) and GRS 1915+105 (Kotani et al. 2000; Lee et al. 2002) to atolls (see e.g. the review by Diaz Trigo et al. 2006 and references therein). Where multiple absorption lines are seen then this gives an excellent probe of the physical conditions in the wind (e.g. Ueda et al. 2004; Miller et al. 2006), and these spectra indicate the presence of significant amounts of highly ionized material which is generally outflowing at moderate velocities ($\sim 500 \text{ km s}^{-1}$ in both BHB and NS).

The common features of these systems is that they are all viewed at fairly high inclination angles: most of the atolls are also dippers (Boirin et al. 2005; Diaz Trigo et al. 2006). Thus the absorption is almost certainly due to material driven from the accretion disc, and then photoionized by the strong X-ray illumination from the innermost regions of the accretion flow. The reprocessed emission and scattered flux from this extended material can be seen directly in the accretion disc-corona sources, where the intrinsic X-rays are obscured (e.g. Kallman et al. 2003), but for the majority of highly inclined sources the wind material is seen in absorption against the much brighter intrinsic central X-ray source. This persistent absorption, seen at all orbital phases, can be dramatically enhanced during ‘dip’ events, where there is more material above the disc due to the impact between the accretion stream and disc (e.g. Boirin et al 2005; Diaz Trigo et al. 2006).

Another common feature is that these objects are all in the soft or very high states for the BHB and banana branch for the atolls, so they all possess an inner disc. This could imply that the inner disc is the origin of the wind material, or that radiation from the inner disc is necessary for launching or

driving the wind. A less direct link could be through photoionization, where the soft disc spectrum means that iron is not completely stripped, rendering the material invisible. Alternatively, the wind and untruncated inner disc need not have any causal connection, simply both being consequences of high L/L_{Edd} . Winds are certainly predicted to become stronger at higher L/L_{Edd} , so are most likely to be observed from high L/L_{Edd} sources i.e. those which also have an inner accretion disc.

We first review potential theoretical models for the origin of the wind, and then use the observed properties to show that the most likely is a thermal wind from the outer accretion disc.

10.1 Theoretical models of winds

Accretion discs can potentially power several different kinds of outflow. Radiation pressure on electrons becomes dynamically important as L approaches L_{Edd} , reducing the effective gravity by a factor $\sim 1 - L/L_{\text{Edd}}$. This can be made much more efficient if the cross-section for interaction between the matter and radiation is enhanced by line opacity. There are multiple line transitions in the UV region of the spectrum, so discs where the luminosity is predominantly in the UV region of the spectrum can drive a powerful wind at luminosities far below Eddington. Such line driven disc winds are seen in CV's and are probably also responsible for the broad absorption line (BAL) outflows seen in AGN (e.g. Pereyra, Hillier & Turnshek 2006). However, the disc temperature for black hole binaries means their spectra peak in the soft X-ray regime, with little luminosity in the UV region where line driving is most important (Proga & Kallman 2002). While these winds in binaries are generally observed via the lines, the momentum absorbed in these ion transitions is very small, completely insufficient to drive the wind.

Another type of outflow from a disc is a thermally driven wind (Begelman, McKee & Shields 1983). Here again the central illumination is important, but the process is less direct. The illumination heats the upper layers of the disc to a temperature of order the Compton temperature, T_{IC} . This will expand due to the pressure gradient, and at large enough radii the thermal energy driving the expansion is larger than the binding energy, leading to a wind from the outer disc, while at smaller radii the material forms an extended atmosphere (corona) above the disc. Simple estimates of the transition radius between the static corona and outflowing wind give $R = 3 \times 10^4 \cdot (T_{\text{IC}}/10^8 \text{ K})^{-1} R_g$ (Begelman et al. 1983), while a more careful analysis shows this is an overestimate, and that thermal winds are launched at a radius a factor 5–10 smaller than this (Begelman et al. 1983; Woods et al. 1996). The column density of the wind and its outflow velocity all increase with luminosity, reaching $\sim 3 \times 10^{23} \text{ cm}^{-2}$ and 720 km s^{-1} for $L/L_{\text{Edd}} = 0.3$ at an inclination of 70° (Woods et al. 1996). At even higher luminosities the combination of radiation pressure to thermal driving results in an even more powerful wind (Proga & Kallman 2002).

The last type of outflow is a magnetically driven wind. These are much harder to quantitatively study as the magnetic field configuration is not

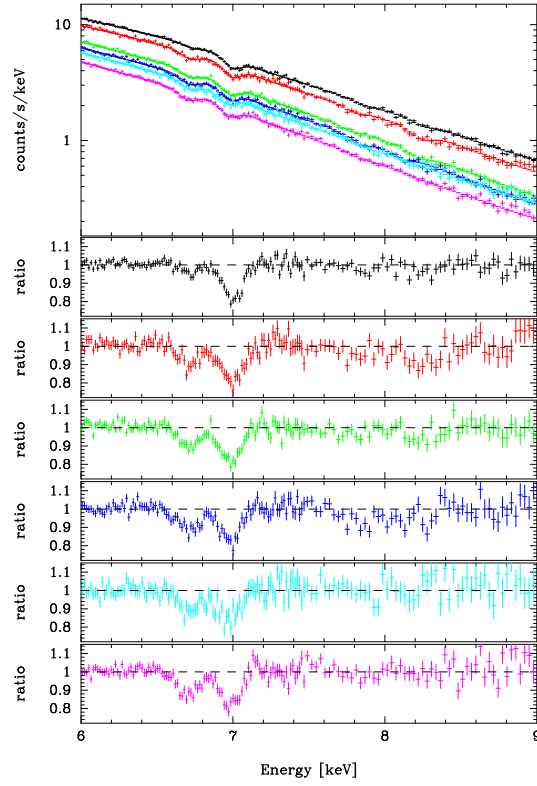


Fig. 30 Evolution of absorption lines on the outburst decay of 4U 1630-47 (Kubota et al. 2006)

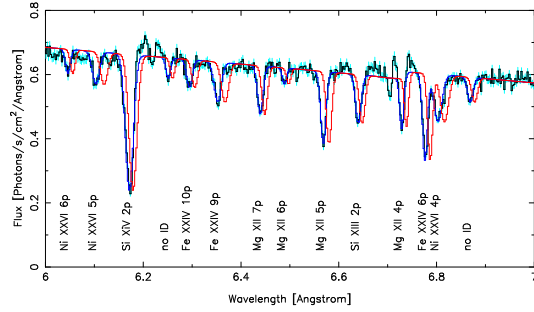


Fig. 31 Absorption lines found in GRO J1655-40 (Miller et al. 2006)

known, yet they are almost certainly present at some level as the underlying angular momentum transport is known to be due to magnetic fields. Winds and jets are clearly present in magnetohydrodynamical (MHD) simulations which include these magnetic stresses self consistently (e.g. Balbus 2005). However, as yet these calculations generally neglect radiative cooling, so describe hot, geometrically thick flows rather than the cool, geometrically thin disc appropriate here. Proga (2000, 2003) make some calculations of magnetic winds from a geometrically thin disc, but imposed an external field geometry. The mass loss rates depend on this field configuration, but in general the winds can be substantially enhanced, and can be launched from any radius. This lack of diagnostic power means that they can be reliably identified only when all other potential mechanisms for a wind are ruled out.

10.2 The nature of the wind in XRB

For all sources the inferred properties of the persistent (non-dip) ionized absorption are very close to those expected from the detailed thermal models of Woods et al. (1996). These models include calculations of the ionization state expected from the material, and *predict* that iron is predominantly H and He-like at the highest luminosity, while the absorption also includes lower ionization species at lower L/L_{Edd} . Such a decrease in the ionization state of the absorber is seen in the multiple spectra taken during the decline from outburst of the BHB transient 4U 1630–47 (Kubota et al. 2007; see Fig. 30). This all makes a compelling case for this material to be predominantly formed from irradiation driven mass loss from the disc.

However, there is one potential requirement for significant magnetic driving from the beautiful Chandra grating data on the ionized absorber seen in the BHB GRO J1655–40 (Miller et al. 2006, see Fig. 31). Here the launching radius inferred for the absorber is much smaller than that of the thermal wind, requiring magnetic fields (Miller et al. 2006). Given the continuity of properties seen between the wind in GRO J1655–40 and in the other BHB and NS systems, this would argue for magnetic fields to be important in all these systems. However, Netzer (2006) shows that the small launch radius is not a unique interpretation of the data, so it seems likely that the material is predominantly thermally driven in all systems, and that its column, outflow velocity and ionisation increase with L/L_{Edd} .

11 Super-Eddington accretion flows

Winds should become even more powerful as the luminosities approach (and go beyond) Eddington as radiation pressure reduces the effective gravity to $1 - L/L_{\text{Edd}}$. This means the outflows can be launched from closer to the black hole and this mass loss may also be important in terms of changing the underlying disc structure. Plainly though this does *not* limit the source luminosity to $\leq L_{\text{Edd}}$ as both BHB and NS can show luminosities above this. The super-Eddington BHB include V404 Cyg and V4641 Sgr near the peak of their outbursts, together with GRS 1915+105 which probably oscillates

between 0.3 and 3 L_{Edd} , and (probably) the HMXB SS 433 which accretes at hyper Eddington rates ($> 1000\times$ higher than those required to radiate at L_{Edd} ; Begelman, King & Pringle 2006; Poutanen et al. 2007). For LMXB NS, all the Z source subclass (Hasinger & van der Klis 1989) have $L \sim L_{\text{Edd}}$, except for the peculiar Z source Cir X-1 which can reach 10 L_{Edd} (Done & Gierliński 2003)!

This handful of sources show some clear trends in their binary parameters. The disc instability model predicts that the peak luminosity is roughly proportional to the size of the disc involved in the outburst (King & Ritter 1998). Only systems with relatively long orbital periods have a large enough disc to potentially reach L_{Edd} , as observed (Shahbaz, Charles & King 1998), and these generally require an evolved and/or high mass donor in order to fill the Roche lobe at such separations (King et al. 1997).

11.1 Black hole binaries

BHB give the cleanest picture of the accretion flow itself, and these show clearly that there is some sort of instability present above $L/L_{\text{Edd}} \sim 1$. V404 Cyg and V4641 Sgr both showed evidence for disruption of the accretion flow near the peak of their outbursts at $L/L_{\text{Edd}} \sim 2 - 3$, with ejected material forming a dense outflow which completely obscured the source (Tanaka & Lewin 1995; Życki, Done & Smith 1999; Revnivtsev et al 2002). This dramatic disruption of the disc may be connected to the transient nature of these sources rather than showing the quasi-steady nature of the accretion flow. However the only such flow at Eddington luminosities is GRS 1915+105 (e.g. Done, Wardziński & Gierliński 2004), and this show unique variability, strongly reminiscent of limit cycle behaviour (e.g. Belloni et al. 2000). If this is a true limit cycle, then this implies the presence of another stable branch at $L > L_{\text{Edd}}$. One obvious candidate for this is the optically thick advective branch (see Section 2.3). However, the clear signatures of mass loss seen from this system (Kotani et al. 2000; Lee et al. 2002) also point to additional cooling from winds being important, as expected for $L \geq L_{\text{Edd}}$ (e.g. Shakura & Sunyaev 1973; Begelman et al 2006; Ohsuga 2006; 2007; Poutanen et al. 2007). There are also powerful jet ejections linked to the limit cycle variability, which can act as another cooling channel (Janiuk, Czerny & Siemiginowska 2002). At even higher quasi steady mass accretion rates (SS 433), the outflow forms an optically thick shroud around the source, which may control the angle of the precessing jet (Begelman et al. 2006). We caution that the accretion structure at such high L/L_{Edd} is almost certainly impacted by the effect of jets and outflows rather than just being described by standard (with or without advection) disc equations.

11.2 Neutron stars

The super Eddington NS systems (Z sources) look subtly different from the atoll systems. Firstly their evolution on a colour-colour diagram is different. The atolls show a transition to the hard (island) state at low luminosities.

This is not present in the Z sources, as their high luminosity means they are always in the soft state. Thus they can be generally be fit by two components, a disc at low energies and (optically thick) Comptonization with seed photons from the (unseen) NS star surface at higher energies. Due to this spectral similarity, Z sources occupy similar area in the colour-colour diagram to the upper banana branch of atolls (Done & Gierliński 2003). However, the way the two categories of sources move in the diagram is markedly different. Z sources move faster and make a small (mostly) Z-shaped track while the atolls move more slowly along the upper banana branch (e.g. Hasinger & van der Klis 1989).

The topological similarity of the Z source track to the full atoll track makes some sort of truncated disc model very attractive. However, the accretion flow cannot be optically thin at such high luminosities, so the disc cannot be truncated by the usual ‘evaporation to a hot inner flow’ mechanism. Instead the disc could be truncated by a residual magnetic field which is finally overcome by the increasing ram pressure of the flow at around Eddington (Gierliński & Done 2002a). The idea that Z sources differ from atolls in more than just accretion rate was suggested at the onset by Hasinger & van der Klis (1989). However, closer examination of the Z track shows that it can sometimes have a further branches at high luminosity which look like another Z off the flaring branch (e.g. Gilfanov et al. 2003). If the horizontal to flaring branch transition is driven by the disc reaching the NS surface, then what causes the additional branches? A better model for these very high mass accretion rate flows might be where the inner disc is truncated by mass loss processes in a wind and/or jet (Takahashi & Makishima 2006). Some evidence for this model comes for the fact that spectral decomposition shows that while the accretion disc luminosity increases monotonically along the Z track, the boundary layer contribution decreases along the normal branch, from roughly equal to that of the disc at the top (close to the horizontal branch) to around zero on the flaring branch (Done, Życki & Smith 2002; Revnivtsev & Gilfanov 2006; Takahashi & Makishima 2006). Alternatively, this could instead indicate that the boundary layer is progressively obscured by the accretion disc thickening.

The link between Z sources and atolls will soon become much clearer, with the recent discovery of the first *transient* Z source, XTE J1701–462 (Homan et al. 2007). As this source declines from its peak (it was still bright at the time of writing this review) then it should transform into a bright atoll (banana branch) and then into a hard (island) state if mass accretion rate is the only distinction between Z and atoll sources. The peculiar Z source Cir X-1 is similarly fading (Saz Parkinson et al. 2003), so again should show whether the only real difference between atolls and Z sources is their mean accretion rate, rather than additional complexity such as a surface magnetic field. This source reached an unprecedented $\sim 10 L_{\text{Edd}}$ (Done & Gierliński 2003), where its spectrum was extremely soft, much softer than expected from the NS models. This is plausibly due to the emission being thermalized in a wind from the disc which is so strong that it becomes optically thick. The observed ~ 1 keV temperature from Cir X-1 at $10 L_{\text{Edd}}$ requires reprocessing from a large region, with radius around $100 R_g$. Direct evidence for a wind in

this system is seen through the detection of X-ray P Cygni profiles (Brandt & Schulz 2000).

Irrespective of what the Z source spectra imply about the nature of the accretion flow, it is obvious that these sources *do not* show the same limit cycle instability as GRS 1915+105. However, their variability on the flaring branch is very rapid and complex, hinting at some sort of instability. Our understanding of such high mass accretion rate flows is extremely rudimentary, yet it is such super-Eddington flows which most probably power the ULX, and certainly power the growth of supermassive black holes in the early Universe.

12 Conclusions

This review illustrates how the multitude of observations of accreting black holes and neutron stars can fit into a model of a changing accretion flow structure as a function of mass accretion rate. The long term light curves of these binary systems give clear evidence for an outer disc with properties like those predicted by the time dependent version of the Shakura–Sunyaev disc structure equations, but the spectra only show evidence for such a disc in the inner regions at (generally) high luminosity $L/L_{\text{Edd}} \geq 0.1$. At lower luminosities, there is extensive evidence that the inner disc is simply not present, with the outer disc making a transition into a hot inner accretion flow. Decreasing this disc truncation radius with increasing mass accretion rate until the disc extends down to the last stable orbit gives the major hard-to-soft spectral transitions seen in these systems. This geometry can also explain the correlated variability power spectral evolution, with the decreasing disc radius giving increasing characteristic frequencies which are then propagated down through the hot flow, and hence filtered on the viscous timescale of the hot flow at its (fixed) inner radius at (or below) the last stable orbit. Even the jet behaviour can be (qualitatively) understood in this picture, as a large scale height flow is probably required for jet formation, so the collapse of the inner flow as the disc reaches its minimum radius at the last stable orbit triggers a similar collapse of the radio emission.

While much can be explained in such models, there is also much left to be understood. A proper model for the variability, including QPO formation, is perhaps soon within reach, while detailed predictions of the jet properties and their impact on the accretion flow may take somewhat longer. Nonetheless, the full numerical simulations of the magnetic stresses which form the physical basis for viscosity are making tremendous progress, and starting to incorporate radiative processes which mean they can be applied to observations. Such simulations (the full MRI stresses, plus full radiation processes) may also point to the nature of the accretion flow at high luminosities, $\geq 0.5L/L_{\text{Edd}}$, where the disc is no longer a simple Shakura–Sunyaev structure but powers substantial winds. Such flows are important not only to explain the observations of high mass accretion rate flows in the local universe (GRS 1915+105, ULX's, narrow line Seyfert 1's) but also have cosmological significance. These are the flows required in the early Universe to

quickly build up mass into the first quasars, and these winds can play an important role in quasar feedback on galaxy formation.

While such an optimistic assessment of the potential progress may seem unrealistic, the tremendous breakthroughs outlined in this review seemed equally unlikely 10 years ago. Advances in instrumentation coupled to new theoretical models and improved numerical simulations hold out a tantalizing glimpse of understanding accretion flows in strong gravity.

Acknowledgements We would like to thank everyone who gave comments on the first draft, especially Thierry Courvoisier, Tom Maccarone and Andrzej Zdziarski. CD and MG acknowledge support from a Particle Physics and Astronomy Research Council Senior and Standard Fellowship, respectively.

References

- . Abe Y., Fukazawa Y., Kubota A., Kasama D., Makishima K., (2005), Three Spectral States of the Disk X-Ray Emission of the Black-Hole Candidate 4U 1630–47, *PASJ*, 57, 629–641
- . Abramowicz M. A., Czerny B., Lasota J. P., Szuszkiewicz E., (1988), Slim accretion disks *ApJ*, 332, 646–658
- . Abramowicz M. A., Igumenshchev I. V., (2001), How Dim Could Accreting Black Holes Be?, *ApJ*, 554, L53–L54
- . Agol E., Krolik J. H., (2000), Magnetic Stress at the Marginally Stable Orbit: Altered Disk Structure, Radiation, and Black Hole Spin Evolution, *ApJ*, 528, 161–170
- . Arévalo P., Uttley P., (2006), Investigating a fluctuating-accretion model for the spectral-timing properties of accreting black hole systems, *MNRAS*, 367, 801–814
- . Axelsson M., Borgonovo L., Larsson S., (2005), Evolution of the 0.01–25 Hz power spectral components in Cygnus X-1, *A&A*, 438, 999–1012
- . Balbus S. A., (2005), Numerical Simulations of the MRI and Real Disks, *ASPC*, 330, 185–196
- . Ballantyne D. R., Ross R. R., Fabian A. C., (2001), X-ray reflection by photoionized accretion discs *MNRAS*, 327, 10–22
- . Bałucińska-Church M., Belloni T., Church M. J., Hasinger G., (1995), Identification of the soft X-ray excess in Cygnus X-1 with disc emission, *A&A*, 302, L5–L8
- . Begelman M. C., King A. R., Pringle J. E., (2006), The nature of SS433 and the ultraluminous X-ray sources, *MNRAS*, 370, 399–404
- . Begelman M. C., McKee C. F., Shields G. A., (1983), Compton heated winds and coronae above accretion disks. I Dynamics, *ApJ*, 271, 70–88
- . Belloni T., Hasinger G., (1990), Variability in the noise properties of Cygnus X-1, *A&A*, 227, L33–L36
- . Belloni T., Psaltis D., van der Klis M., (2002), A Unified Description of the Timing Features of Accreting X-Ray Binaries, *ApJ*, 572, 392–406
- . Belloni T., Klein-Wolt M., Méndez M., van der Klis M., van Paradijs J., (2000), A model-independent analysis of the variability of GRS 1915+105, *A&A*, 355, 271–290
- . Belloni T., Homan J., Casella P., van der Klis M., Nespoli E., Lewin W. H. G., Miller J. M., Méndez M., (2005), The evolution of the timing properties of the black-hole transient GX 339-4 during its 2002/2003 outburst, *A&A*, 440, 207–222
- . Beloborodov A. M., (1999), Plasma Ejection from Magnetic Flares and the X-Ray Spectrum of Cygnus X-1, *ApJ*, 510, L123–L126
- . Bhattacharya, A., Srinivasan, M. K., (1995), in *X-ray Binaries*, eds. W. H. G. Lewin, J. van Paradijs, and W. P. J. van den Heuvel, Cambridge University Press

-
- . Blaes O. M., Arras P., Fragile P. C., (2006), Oscillation modes of relativistic slender tori MNRAS, 369, 1235-1252
 - . Blandford R. D., Begelman M. C., (1999), On the fate of gas accreting at a low rate on to a black hole, MNRAS, 303, L1-L5
 - . Boirin L., Méndez M., Díaz Trigo M., Parmar A. N., Kaastra J. S., (2005), A highly-ionized absorber in the X-ray binary 4U 1323-62: A new explanation for the dipping phenomenon, A&A, 436, 195-208
 - . Boyle B. J., Terlevich R. J., (1998), The cosmological evolution of the QSO luminosity density and of the star formation rate, MNRAS, 293, L49-L51
 - . Brandt W. N., Schulz N. S., (2000), The Discovery of Broad P Cygni X-Ray Lines from Circinus X-1 with the Chandra High-Energy Transmission Grating Spectrometer, ApJ, 544, L123-L127
 - . Burderi L., King A. R., Szuszkiewicz E., (1998), Does the Thermal Disk Instability Operate in Active Galactic Nuclei?, ApJ, 509, 85-92
 - . Cannizzo J. K., Reiff C. M., (1992), Accretion disks in active galactic nuclei - Vertically averaged models, ApJ, 385, 87-93
 - . Chakrabarty D., Morgan E. H., (1998), The two-hour orbit of a binary millisecond X-ray pulsar, Natur, 394, 346-348
 - . Chaty S., Haswell C. A., Malzac J., Hynes R. I., Shrader C. R., Cui W., (2003), Multiwavelength observations revealing the evolution of the outburst of the black hole XTE J1118+480, MNRAS, 346, 689-703
 - . Churazov E., Gilfanov M., Revnivtsev M., (2001), Soft state of Cygnus X-1: stable disc and unstable corona, MNRAS, 321, 759-766
 - . Coppi P. S., (1999), The Physics of Hybrid Thermal/Non-Thermal Plasmas, ASPC, 161, 375-403
 - . Cowley, A. P., Crampton, D., Hutchings, J. B., Remillard, R., & Penfold, J. E. (1983), Discovery of a massive unseen star in LMC X-3, ApJ, 272, 118-122
 - . Cui W., Zhang S. N., Chen W., Morgan E. H., (1999), Strong Aperiodic X-Ray Variability and Quasi-Periodic Oscillation in X-Ray Nova XTE J1550-564, ApJ, 512, L43-L46
 - . Cumming A., Zweibel E., Bildsten L., (2001), Magnetic Screening in Accreting Neutron Stars ApJ, 557, 958-966
 - . Cunningham C. T., (1975), The effects of redshifts and focusing on the spectrum of an accretion disk around a Kerr black hole, ApJ, 202, 788-802
 - . Davis S. W., Blaes O. M., Hubeny I., Turner N. J., (2005), Relativistic Accretion Disk Models of High-State Black Hole X-Ray Binary Spectra. ApJ, 621, 372-387
 - . Davis S. W., Done C., Blaes O. M., (2006), Testing Accretion Disk Theory in Black Hole X-Ray Binaries, ApJ, 647, 525-538
 - . Davis S. W., Hubeny I., (2006), A Grid of Relativistic, Non-LTE Accretion Disk Models for Spectral Fitting of Black Hole Binaries, ApJS, 164, 530
 - . Díaz Trigo M., Parmar A. N., Boirin L., Méndez M., Kaastra J. S., (2006), Spectral changes during dipping in low-mass X-ray binaries due to highly-ionized absorbers, A&A, 445, 179-195
 - . Di Matteo T., Springel V., Hernquist L., (2005), Energy input from quasars regulates the growth and activity of black holes and their host galaxies, Natur, 433, 604
 - . Di Matteo T., Psaltis D., (1999), Quasi-Periodic Variability and the Inner Radii of Thin Accretion Disks in Galactic Black Hole Systems, ApJ, 526, L101-L104
 - . Di Salvo T., Iaria R., Burderi L., Robba N. R., (2000), The Broadband Spectrum of MXB 1728-34 Observed by BeppoSAX, ApJ, 542, 1034-1040
 - . Di Salvo T., Done C., Życki P. T., Burderi L., Robba N. R., (2001), Probing the Inner Region of Cygnus X-1 in the Low/Hard State through Its X-Ray Broadband Spectrum, ApJ, 547, 1024
 - . Done C., Gierliński M., (2003), Observing the effects of the event horizon in black holes, MNRAS, 342, 1041-1055
 - . Done C., Gierliński M., (2006), Truncated disc versus extremely broad iron line in XTE J1650-500, MNRAS, 367, 659-668
 - . Done C., Kubota A., (2006), Disc-corona energetics in the very high state of Galactic black holes, MNRAS, 371, 1216-1230

- . Done C., Nayakshin S., (2001), Observational Signatures of X-Ray-irradiated Accretion Disks, *ApJ*, 546, 419-428
- . Done C., Nayakshin S., (2007), Can the soft excess in AGN originate from disc reflection? *MNRAS*, 377, L59-L63
- . Done C., Wardziński G., Gierliński M., (2004), GRS 1915+105: the brightest Galactic black hole, *MNRAS*, 349, 393-403
- . Done C., Życki P. T., Smith D. A., (2002), The X-ray spectrum of Cyg X-2, *MNRAS*, 331, 453-462
- . Dotani T., et al., (1997), ASCA Observation of Cygnus X-1 in the Soft State: Mass of the Compact Object, *ApJ*, 485, L87-L90
- . Dubus G., Lasota J.-P., Hameury J.-M., Charles P., (1999), X-ray irradiation in low-mass binary systems, *MNRAS*, 303, 139-147
- . Ebisawa K., Mitsuda K., Hanawa T., (1991), Application of a general relativistic accretion disk model to LMC X-1, LMC X-3, X1608-522, and X1636-536, *ApJ*, 367, 213-220
- . Ebisawa K., Makino F., Mitsuda K., Belloni T., Cowley A. P., Schmidtke P. C., Treves A., (1993), Spectral variations of LMC X-3 observed with GINGA, *ApJ*, 403, 684-689
- . Ebisawa K., et al. (1994), Spectral evolution of the bright X-ray nova GS 1124-68 (Nova MUSCAE 1991) observed with GINGA, *PASJ*, 46, 375-394
- . Ebisawa K., Ueda Y., Inoue H., Tanaka Y., White N. E., (1996), ASCA Observations of the Iron Line Structure in Cygnus X-1, *ApJ*, 467, 419-434
- . Ergma E., Antipova J., (1999), An evolutionary model for SAX J1808.4-3658, *A&A*, 343, L45-L48
- . Esin A. A., McClintock J. E., Narayan R., (1997), Advection-dominated Accretion and the Spectral States of Black Hole X-Ray Binaries: Application to Nova MUSCAE 1991, *ApJ*, 489, 865-889
- . Esin A. A., McClintock J. E., Drake J. J., Garcia M. R., Haswell C. A., Hynes R. I., Munro M. P., (2001), Modeling the Low-State Spectrum of the X-Ray Nova XTE J1118+480, *ApJ*, 555, 483-488
- . Esin A. A., (1997), Heating and Cooling of Hot Accretion Flows by Nonlocal Radiation, *ApJ*, 482, 400-413
- . Fabian A. C., Rees M. J., Stella L., White N. E., (1989), X-ray fluorescence from the inner disc in Cygnus X-1, *MNRAS*, 238, 729-736
- . Fabian A. C., Iwasawa K., Reynolds C. S., Young A. J., (2000), Broad Iron Lines in Active Galactic Nuclei, *PASP*, 112, 1145-1161
- . Falanga M., Götz D., Goldoni P., Farinelli R., Goldwurm A., Mereghetti S., Bazzano A., Stella L., (2006), The X-ray spectrum of the bursting atoll source 4U 1728-34 observed with INTEGRAL, *A&A*, 458, 21-29
- . Falcke H., Körtling E., Markoff S., (2004), A scheme to unify low-power accreting blackholes. Jet-dominated accretion flows and the radio/X-ray correlation, *A&A*, 414, 895-903
- . Fan X., Carilli C. L., Keating B., (2006), Observational Constraints on Cosmic Reionization, *ARA&A*, 44, 415-462
- . Fender R., Belloni T., (2004), GRS 1915+105 and the Disc-Jet Coupling in Accreting Black Hole Systems, *ARA&A*, 42, 317-364
- . Fiocchi M., Bazzano A., Ubertini P., Zdziarski A. A., (2007), The First Detection of Compton Reflection in the Low-Mass X-Ray Binary 4U 1705-44 with INTEGRAL and BeppoSax, *ApJ*, 657, 448-452
- . Frank J., King A. R., Lasota J.-P., (1987), The light curves of low-mass X-ray binaries, *A&A*, 178, 137-142
- . Frank J., King A., Raine D., (1992), *Accretion Power in Astrophysics*, (Cambridge: Cambridge Univ. Press)
- . Frontera F., et al., (2001), A Measurement of the Broadband Spectrum of XTE J1118+480 with BeppoSAX and Its Astrophysical Implications, *ApJ*, 561, 1006-1015.
- . Galeev A. A., Rosner R., Vaiana G. S., (1979), Structured coronae of accretion disks, *ApJ*, 229, 318-326

-
- . Gammie C. F., Menou K., (1998), On the Origin of Episodic Accretion in Dwarf Novae, *ApJ*, 492, L75-L78
 - . Gammie C. F., Shapiro S. L., McKinney J. C., (2004), Black Hole Spin Evolution, *ApJ*, 602, 312-319.
 - . Giannios, D., & Spruit, H. C. (2004), Excitation of low-frequency QPOs in black hole accretion, *A&A*, 427, 251-261
 - . Gierliński M., Done C., (2002a), A comment on the colour-colour diagrams of low-mass X-ray binaries, *MNRAS*, 331, L47-L50
 - . Gierliński M., Done C., (2002b), The X-ray spectrum of the atoll source 4U 1608-52, *MNRAS*, 337, 1373-1380
 - . Gierliński M., Done C., (2003), The X-ray/gamma-ray spectrum of XTE J1550-564 in the very high state, *MNRAS*, 342, 1083-1092
 - . Gierliński M., Done C., (2004), Black hole accretion discs: reality confronts theory, *MNRAS*, 347, 885-894
 - . Gierliński M., Newton J., (2006), X-ray spectral transitions of black holes from RXTE All-Sky Monitor, *MNRAS*, 370, 837-844
 - . Gierliński M., Maciolek-Niedźwiecki A., Ebisawa K., (2001), Application of a relativistic accretion disc model to X-ray spectra of LMC X-1 and GRO J1655-40 *MNRAS*, 325, 1253-1265
 - . Gierliński M., Nikolajuk M., Czerny, B., (2007), The power spectra of low/hard state black hole binaries, *MNRAS*, submitted
 - . Gierliński M., Zdziarski A. A., Poutanen J., Coppi P. S., Ebisawa K., Johnson W. N., (1999), Radiation mechanisms and geometry of Cygnus X-1 in the soft state, *MNRAS*, 309, 496
 - . Gilfanov M., Revnivtsev M., Molkov S., (2003), Boundary layer, accretion disk and X-ray variability in the luminous LMXBs, *A&A*, 410, 217-230
 - . Gilfanov M., Churazov E., Revnivtsev M., (1999), Reflection and noise in Cygnus X-1, *A&A*, 352, 182-188
 - . Gladstone J., Done C., Gierliński M., (2007), Analysing the atolls: X-ray spectral transitions of accreting neutron stars, *MNRAS*, 378, 13-22
 - . Gregory R., Whisker R., Beckwith K., Done C., (2004), Observing braneworld black holes, *JCAP*, 10, 13-20
 - . Haardt F., Maraschi L., (1993), X-ray spectra from two-phase accretion disks, *ApJ*, 413, 507-517
 - . Hawley J. F., Balbus S. A., (2002), The Dynamical Structure of Nonradiative Black Hole Accretion Flows, *ApJ*, 573, 738-748
 - . Hasinger, G., & van der Klis, M. (1989), Two patterns of correlated X-ray timing and spectral behaviour in low-mass X-ray binaries, *A&A*, 225, 79-96
 - . Heinz S., Sunyaev R. A., (2003), The non-linear dependence of flux on black hole mass and accretion rate in core-dominated jets, *MNRAS*, 343, L59-L64
 - . Hessels J. W. T., Ransom S. M., Stairs I. H., Freire P. C. C., Kaspi V. M., Camilo F., (2006), A Radio Pulsar Spinning at 716 Hz, *Sci*, 311, 1901-1904
 - . Homan J., et al., (2007), Rossi X-Ray Timing Explorer Observations of the First Transient Z Source XTE J1701-462: Shedding New Light on Mass Accretion in Luminous Neutron Star X-Ray Binaries, *ApJ*, 656, 420-430
 - . Honma F., Kato S., Matsumoto R., (1991), Nonlinear oscillations of thermally unstable slim accretion disks around a neutron star or a black hole, *PASJ*, 43, 147-168
 - . Ibragimov A., Poutanen J., Gilfanov M., Zdziarski A. A., Shrader C. R., 2005, *MNRAS*, 362, 1435
 - . Ichimaru S., (1977), Bimodal behavior of accretion disks - Theory and application to Cygnus X-1 transitions, *ApJ*, 214, 840-855
 - . Inogamov N. A., Sunyaev R. A., (1999), Spread of matter over a neutron-star surface during disk accretion, *AstL*, 25, 269-293
 - . Janiuk A., Czerny B., Siemiginowska A., (2002), Radiation Pressure Instability Driven Variability in the Accreting Black Holes, *ApJ*, 576, 908-922
 - . Janiuk A., Życki P. T., Czerny B., (2000), The role of advection in the accreting corona model for active galactic nuclei and Galactic black holes, *MNRAS*, 314, 364-374

- . Kalemci E., Tomsick J. A., Rothschild R. E., Pottschmidt K., Kaaret P., (2004), A Close Look at the State Transitions of Galactic Black Hole Transients during Outburst Decay, *ApJ*, 603, 231-241
- . Kalemci E., Tomsick J. A., Rothschild R. E., Pottschmidt K., Corbel S., Kaaret P., (2006), The Galactic Black Hole Transient H1743-322 during Outburst Decay: Connections between Timing Noise, State Transitions, and Radio Emission, *ApJ*, 639, 340-347
- . Kazanas, D., Hua, X.-M., & Titarchuk, L. (1997), Temporal and Spectral Properties of Comptonized Radiation and Its Applications, *ApJ*, 480, 735-740
- . King A. R., Kolb U., (1999), The evolution of black hole mass and angular momentum, *MNRAS*, 305, 654-660
- . King A. R., Kolb U., Burderi L., (1996), Black Hole Binaries and X-Ray Transients, *ApJ*, 464, L127-L130
- . King A. R., Frank J., Kolb U., Ritter H., (1997) Transients among Binaries with Evolved Low-Mass Companions, *ApJ*, 484, 844-847
- . K rding E. G., Fender R. P., Migliari S., (2006), Jet-dominated advective systems: radio and X-ray luminosity dependence on the accretion rate, *MNRAS*, 369, 1451-1458
- . Kotani T., Ebisawa K., Dotani T., Inoue H., Nagase F., Tanaka Y., Ueda Y., (2000), ASCA Observations of the Absorption Line Features from the Superluminous Jet Source GRS 1915+105, *ApJ*, 539, 413-423
- . Kotov O., Churazov E., Gilfanov M., (2001), On the X-ray time-lags in the black hole candidates, *MNRAS*, 327, 799-807
- . Kubota A., Makishima K., Ebisawa K., (2001), Observational Evidence for Strong Disk Comptonization in GRO J1655-40, *ApJ*, 560, L147-L150
- . Kubota A., et al., (2007), Suzaku Discovery of Iron Absorption Lines in Outburst Spectra of the X-Ray Transient 4U 1630-472, *PASJ*, 59, 185-198
- . Kubota A., Makishima K., (2004), The Three Spectral Regimes Found in the Stellar Black Hole XTE J1550-564 in its High/Soft State, *ApJ*, 601, 428-438
- . Kubota A., Done C., (2004), The very high state accretion disc structure from the Galactic black hole transient XTE J1550 - 564, *MNRAS*, 353, 980-990
- . Lasota J.-P., (2001), The disc instability model of dwarf novae and low-mass X-ray binary transients, *NewAR*, 45, 449-508
- . Lee J. C., Reynolds C. S., Remillard R., Schulz N. S., Blackman E. G., Fabian A. C., (2002), High-Resolution Chandra HETGS and Rossi X-Ray Timing Explorer Observations of GRS 1915+105: A Hot Disk Atmosphere and Cold Gas Enriched in Iron and Silicon, *ApJ*, 567, 1102-1111
- . Kuulkers, E., & van der Klis, M. (1996), GX340+0 with EXOSAT: its correlated X-ray spectral and timing behaviour., *A&A*, 314, 567
- . Lewin W. H. G., van Paradijs J., Taam R. E., 1995, in *X-ray Binaries*, eds. W. H. G. Lewin, J. van Paradijs, and W. P. J. van den Heuvel, Cambridge University Press
- . Lin D., Remillard R. A., Homan J., (2007), Evaluating Spectral Models and the X-ray States of Neutron-Star X-ray Transients, *ApJ*, accepted, (astro-ph/0702089)
- . Liu B. F., Meyer F., Meyer-Hofmeister E., (2005), Spectral state transitions in low-mass X-ray binaries - the effect of hard and soft irradiation, *A&A*, 442, 555-562
- . Lyubarskii, Yu. E., (1997), Flicker noise in accretion discs, *MNRAS*, 292, 679-685
- . Maccarone T. J., (2002), On the misalignment of jets in microquasars, *MNRAS*, 336, 1371-1376
- . Maccarone T. J., (2003), Do X-ray binary spectral state transition luminosities vary? *A&A*, 409, 697-706
- . Maccarone T. J., (2005), Constraints on jet X-ray emission in low/hard-state X-ray binaries, *MNRAS*, 360, L68-L72
- . Maccarone T. J., Coppi P. S., Poutanen J., (2000), Time Domain Analysis of Variability in Cygnus X-1: Constraints on the Emission Models, *ApJ*, 537, L107-L110

- . Maccarone T. J., Coppi P. S., (2002), RXTE/OSSE Fits to the Hard State Spectrum of Cygnus X-1, MNRAS submitted, (astro-ph/0204235)
- . Maccarone T. J., Coppi P. S., (2003), Hysteresis in the light curves of soft X-ray transients, MNRAS, 338, 189-196
- . Machida M., Nakamura K. E., Matsumoto R., (2006), Formation of Magnetically Supported Disks during Hard-to-Soft Transitions in Black Hole Accretion Flows, PASJ, 58, 193-202
- . Malzac J., Beloborodov A. M., Poutanen J., (2001), X-ray spectra of accretion discs with dynamic coronae, MNRAS, 326, 417-427
- . Markoff S., Falcke H., Fender R., (2001), A jet model for the broadband spectrum of XTE J1118+480. Synchrotron emission from radio to X-rays in the Low/Hard spectral state, A&A, 372, L25-L28
- . Markoff S., Nowak M. A., Wilms J., (2005), Going with the Flow: Can the Base of Jets Subsume the Role of Compact Accretion Disk Coronae? ApJ, 635, 1203-1216
- . Mayer M., Pringle J. E., (2007), Time-dependent models of two-phase accretion discs around black holes, MNRAS, 376, 435-456
- . McConnell M. L., et al., (2000), A High-Sensitivity Measurement of the MeV Gamma-Ray Spectrum of Cygnus X-1, ApJ, 543, 928-937
- . Medvedev M. V., (2004), Boundary Layer Self-Similar Solution for the Hot Radiative Accretion onto a Rapidly Spinning Neutron Star, ApJ, 613, 506-511
- . Medvedev, M. V., & Narayan, R. (2001), Self-similar Hot Accretion Flow onto a Neutron Star, ApJ, 554, 1255-1267
- . Meier D. L., (2005), Magnetically Dominated Accretion Flows (MDAFS) and Jet Production in the Lowhard State, Ap&SS, 300, 55-65
- . Menou K., Quataert E., (2001), Ionization, Magnetorotational, and Gravitational Instabilities in Thin Accretion Disks Around Supermassive Black Holes, ApJ, 552, 204-208
- . Menou K., Narayan R., Lasota J.-P., (1999), A Population of Faint Nontransient Low-Mass Black Hole Binaries, ApJ, 513, 811-826
- . Merloni A., Nayakshin S., (2006), On the limit-cycle instability in magnetized accretion discs, MNRAS, 372, 728-734
- . Merloni A., (2003), Beyond the standard accretion disc model: coupled magnetic disc-corona solutions with a physically motivated viscosity law, MNRAS, 341, 1051-1056
- . Merloni A., Fabian A. C., Ross R. R., (2000), On the interpretation of the multicolour disc model for black hole candidates, MNRAS, 313, 193-197
- . Meyer, F., & Meyer-Hofmeister, E. (1994), Accretion disk evaporation by a coronal siphon flow, A&A, 288, 175-182
- . Miller J. M., Homan J., Steeghs D., Rupen M., Hunstead R. W., Wijnands R., Charles P. A., Fabian A. C., (2006), A Long, Hard Look at the Low/Hard State in Accreting Black Holes, ApJ, 653, 525-535
- . Miller J. M., Homan J., Miniutti G., (2006), A Prominent Accretion Disk in the Low-Hard State of the Black Hole Candidate SWIFT J1753.5-0127, ApJ, 652, L113-L116
- . Miller J. M., Raymond J., Fabian A., Steeghs D., Homan J., Reynolds C., van der Klis M., Wijnands R., (2006), The magnetic nature of disk accretion onto black holes, Natur, 441, 953-955
- . Mineshige S., Takeuchi M., Nishimori H., (1994), Is a black hole accretion disk in a self-organized critical state?, ApJ, 435, L125-L128
- . Mitsuda K., et al., (1984), Energy spectra of low-mass binary X-ray sources observed from TENMA, PASJ, 36, 741-759
- . Mitsuda K., Inoue H., Nakamura N., Tanaka Y., (1989), Luminosity-related changes of the energy spectrum of X1608-522, PASJ, 41, 97-111
- . Miyamoto, S., & Kitamoto, S. (1989), X-ray time variations from Cygnus X-1 and implications for the accretion process, Natur, 342, 773-774
- . Miyamoto S., Kimura K., Kitamoto S., Dotani T., Ebisawa K., (1991), X-ray variability of GX 339 - 4 in its very high state, ApJ, 383, 784-807

- . Miyamoto S., Iga S., Kitamoto S., Kamado Y., (1993), Another canonical time variation of X-rays from black hole candidates in the very high flare state?, *ApJ*, 403, L39-L42
- . Muno M. P., Remillard R. A., Chakrabarty D., (2002), How Do Z and Atoll X-Ray Binaries Differ? *ApJ*, 568, L35-L39
- . Ohsuga K., (2006), Two-dimensional Radiation-Hydrodynamic Model for Limit-Cycle Oscillations of Luminous Accretion Disks, *ApJ*, 640, 923-928
- . Ohsuga K., (2007), Feedback from Supercritical Disk Accretion Flows, *ApJ*, 659, 205-210
- . Narayan R., (2003), George Darwin Lecture: Evidence for the black hole event horizon, *A&G*, 44, 22-26 (astro-ph/0310692)
- . Narayan R., Yi I., (1995), Advection-dominated Accretion: Underfed Black Holes and Neutron Stars, *ApJ*, 452, 710-735
- . Nayakshin S., Kazanas D., Kallman T. R., (2000), Thermal Instability and Photoionized X-Ray Reflection in Accretion Disks, *ApJ*, 537, 833-852
- . Netzer H., (2006), A Thermal Wind Model for the X-Ray Outflow in GRO J1655-40, *ApJ*, 652, L117-L120
- . Nowak M. A., (1995), Toward a Unified View of Black-Hole High-Energy States, *PASP*, 107, 1207-1214
- . Nowak M. A., (2000), Are there three peaks in the power spectra of GX 339-4 and Cyg X-1? *MNRAS*, 318, 361-367
- . Orosz J. A., Jain R. K., Bailyn C. D., McClintock J. E., Remillard R. A., (1998), Orbital Parameters for the Soft X-Ray Transient 4U 1543-47: Evidence for a Black Hole, *ApJ*, 499, 375-384
- . Osaki Y., (1996), Dwarf-Nova Outbursts, *PASP*, 108, 39-60
- . Paizis A., et al., (2006), Average hard X-ray emission from NS LMXBs: observational evidence of different spectral states in NS LMXBs, *A&A*, 459, 187-197
- . Pereyra N. A., Hillier D. J., Turnshek D. A., (2006), On the Steady Nature of Line-driven Disk Winds: Application to Cataclysmic Variables, *ApJ*, 636, 411-425
- . Popham R., Sunyaev R., (2001), Accretion Disk Boundary Layers around Neutron Stars: X-Ray Production in Low-Mass X-Ray Binaries, *ApJ*, 547, 355-383
- . Pottschmidt K., et al., (2003), Long term variability of Cygnus X-1. I. X-ray spectral-temporal correlations in the hard state, *A&A*, 407, 1039-1058
- . Poutanen J., Krolik J. H., Ryde F., (1997), The nature of spectral transitions in accreting black holes - The case of CYG X-1, *MNRAS*, 292, L21-L25
- . Poutanen J., Fabian A. C., (1999), Spectral evolution of magnetic flares and time lags in accreting black hole sources, *MNRAS*, 306, L31-L37
- . Poutanen J., Lipunova G., Fabrika S., Butkevich A. G., Abolmasov P., (2007), Supercritically accreting stellar mass black holes as ultraluminous X-ray sources, *MNRAS*, 377, 1187-1194
- . Pringle J. E., (1976), Thermal instabilities in accretion discs, *MNRAS*, 177, 65-71
- . Proga D., (2003), Numerical Simulations of Mass Outflows Driven from Accretion Disks by Radiation and Magnetic Forces, *ApJ*, 585, 406-417
- . Proga D., (2000), Winds from Accretion Disks Driven by Radiation and Magnetocentrifugal Force, *ApJ*, 538, 684-690
- . Proga D., Kallman T. R., (2002), On the Role of the Ultraviolet and X-Ray Radiation in Driving a Disk Wind in X-Ray Binaries, *ApJ*, 565, 455-470
- . Psaltis D., Belloni T., van der Klis M., (1999), Correlations in Quasi-periodic Oscillation and Noise Frequencies among Neutron Star and Black Hole X-Ray Binaries, *ApJ*, 520, 262-270
- . Psaltis D., Norman C., (2000), On the Origin of Quasi-Periodic Oscillations and Broad-band Noise in Accreting Neutron Stars and Black Holes, (astro-ph/0001391)
- . Rees M. J., Phinney E. S., Begelman M. C., Blandford R. D., (1982), Ion-supported tori and the origin of radio jets, *Natur*, 295, 17-21
- . Reig P., Belloni T., van der Klis M., (2003), Does GRS 1915+105 exhibit “canonical” black-hole states?, *A&A*, 412, 229-233

- . Remillard R. A., McClintock J. E., (2006), X-Ray Properties of Black-Hole Binaries, *ARA&A*, 44, 49-92
- . Revnivtsev M., Gilfanov M., Churazov E., (1999), The frequency resolved spectroscopy of CYG X-1: fast variability of the Fe K α line, *A&A*, 347, L23-L26
- . Revnivtsev M., Gilfanov M., Churazov E., Sunyaev R., (2002), Super-Eddington outburst of V4641 Sgr, *A&A*, 391, 1013-1022
- . Revnivtsev M. G., Gilfanov M. R., (2006), Boundary layer emission and Z-track in the color-color diagram of luminous LMXBs, *A&A*, 453, 253-259
- . Rezzolla L., Yoshida S., Maccarone T. J., Zanotti O., (2003), A new simple model for high-frequency quasi-periodic oscillations in black hole candidates, *MNRAS*, 344, L37-L41
- . Rodriguez, J., Corbel, S., Hannikainen, D. C., Belloni, T., Paizis, A., Vilhu, O., (2004), Spectral Properties of Low-Frequency Quasi-periodic Oscillations in GRS 1915+105, *ApJ*, 615, 416-421
- . Ross R. R., Fabian A. C., (1993), The effects of photoionization on X-ray reflection spectra in active galactic nuclei, *MNRAS*, 261, 74-82
- . Ross R. R., Fabian A. C., Young A. J., (1999), X-ray reflection spectra from ionized slabs, *MNRAS*, 306, 461-466
- . Różańska A., Czerny B., (2000), Two-phase radiative/conductive equilibrium in active galactic nuclei and galactic black holes *MNRAS*, 316, 473-478
- . Rykoff E. S., Miller J. M., Steeghs D., Torres M. A. P., (2007), Swift Observations of the Cooling Accretion Disk of XTE J1817-330, *ApJ*, submitted (astro-ph/0703497)
- . Saz Parkinson P. M. S., et al., (2003), Long-Term X-Ray Variability of Circinus X-1, *ApJ*, 595, 333-341
- . Shafee, R., McClintock, J. E., Narayan, R., Davis, S. W., Li, L.-X., & Remillard, R. A. (2006), Estimating the Spin of Stellar-Mass Black Holes by Spectral Fitting of the X-Ray Continuum, *ApJ*, 636, L113-L116
- . Shahbaz T., Charles P. A., King A. R., (1998), Soft X-ray transient light curves as standard candles: exponential versus linear decays, *MNRAS*, 301, 382-388
- . Shakura N. I., Sunyaev R. A., (1973), Black holes in binary systems. Observational appearance, *A&A*, 24, 337-355
- . Shapiro S. L., Lightman A. P., Eardley D. M., (1976), A two-temperature accretion disk model for Cygnus X-1 - Structure and spectrum, *ApJ*, 204, 187-199
- . Shimura T., Takahara F., (1995), On the spectral hardening factor of the X-ray emission from accretion disks in black hole candidates, *ApJ*, 445, 780-788
- . Sibgatullin N. R., Sunyaev R. A., (2000), Energy Release During Disk Accretion onto a Rapidly Rotating Neutron Star, *AstL*, 26, 699
- . Suleimanov V., Poutanen J., (2006), Spectra of the spreading layers on the neutron star surface and constraints on the neutron star equation of state, *MNRAS*, 369, 2036-2048
- . Sidoli L., Oosterbroek T., Parmar A. N., Lumb D., Erd C., (2001), An XMM-Newton study of the X-ray binary MXB 1659-298 and the discovery of narrow X-ray absorption lines, *A&A*, 379, 540-550
- . Siemiginowska, A., Czerny, B., & Kostyunin, V., (1996), Evolution of an Accretion Disk in an Active Galactic Nucleus, *ApJ*, 458, 491-507
- . Smith D. M., Heindl W. A., Swank J. H., (2002), Two Different Long-Term Behaviors in Black Hole Candidates: Evidence for Two Accretion Flows? *ApJ*, 569, 362-380
- . Sobczak G. J., McClintock J. E., Remillard R. A., Bailyn C. D., Orosz J. A., (1999a), RXTE Spectral Observations of the 1996-1997 Outburst of the Microquasar GRO J1655-40, *ApJ*, 520, 776-787
- . Sobczak G. J., McClintock J. E., Remillard R. A., Levine A. M., Morgan E. H., Bailyn C. D., Orosz J. A., (1999b), X-Ray Nova XTE J1550-564: RXTE Spectral Observations, *ApJ*, 517, L121-L125
- . Sobolewska M. A., Życki P. T., (2006), Spectral and Fourier analyses of X-ray quasi-periodic oscillations in accreting black holes, *MNRAS*, 370, 405-414
- . Smak J., (1984), Outbursts of dwarf novae, *PASP*, 96, 5-18

- . Stella L., Rosner R., (1984), Magnetic field instabilities in accretion disks, *ApJ*, 277, 312-321
- . Stella, L., & Vietri, M. (1998), Lense-Thirring Precession and Quasi-periodic Oscillations in Low-Mass X-Ray Binaries, *ApJ*, 492, L59-L62
- . Stella, L., & Vietri, M. (1999), kHz Quasiperiodic Oscillations in Low-Mass X-Ray Binaries as Probes of General Relativity in the Strong-Field Regime, *Physical Review Letters*, 82, 17-20
- . Stella, L., Vietri, M., & Morsink, S. M. (1999), Correlations in the Quasi-periodic Oscillation Frequencies of Low-Mass X-Ray Binaries and the Relativistic Precession Model, *ApJ*, 524, L63-L66
- . Sunyaev R., Revnivtsev M., (2000), Fourier power spectra at high frequencies: a way to distinguish a neutron star from a black hole, *A&A*, 358, 617-623
- . Sunyaev R. A., Shakura N. I., (1986), Disk Accretion onto a Weak Field Neutron Star - Boundary Layer Disk Luminosity Ratio, *SvAL*, 12, 117-120
- . Szuszkiewicz E., Miller J. C., (2001), Non-linear evolution of thermally unstable slim accretion discs with a diffusive form of viscosity, *MNRAS*, 328, 36-44
- . Takahashi H., Makishima K., (2006), X-ray study of mass-accretion flows onto weakly-magnetized neutron stars, In: *Proceedings of the "The X-ray Universe 2005"*, 26-30 September 2005, El Escorial, Madrid, Spain. Ed. by A. Wilson. ESA SP-604, p. 309-310
- . Tanaka Y., Lewin W. H. G., (1995), in *X-ray Binaries*, eds. W. H. G. Lewin, J. van Paradijs, and W. P. J. van den Heuvel, Cambridge University Press
- . Takahashi, H., et al. (2007), Low/Hard State Spectra of GRO J1655-40 Observed with Suzaku, *PASJ*, in press (astro-ph/0707.3867)
- . Tomsick, J. A., Lapshov, I., & Kaaret, P. (1998), An X-Ray Dip in the X-Ray Transient 4U 1630-47, *ApJ*, 494, 747-752
- . Tremaine S., et al., (2002), The Slope of the Black Hole Mass versus Velocity Dispersion Correlation, *ApJ*, 574, 740-753
- . Ueda Y., Inoue H., Tanaka Y., Ebisawa K., Nagase F., Kotani T., Gehrels N., (1998), Detection of Absorption-Line Features in the X-Ray Spectra of the Galactic Superluminous Source GRO J1655-40, *ApJ*, 492, 782-787
- . Ueda Y., Asai K., Yamaoka K., Dotani T., Inoue H., (2001), Discovery of an Iron K Absorption Line in the Low-Mass X-Ray Binary GX 13+1, *ApJ*, 556, L87-L90
- . Uttley, P., McHardy, I. M., (2001), The flux-dependent amplitude of broadband noise variability in X-ray binaries and active galaxies, *MNRAS*, 323, L26-L30
- . Uttley, P., McHardy, I. M., Vaughan, S., (2005), Non-linear X-ray variability in X-ray binaries and active galaxies, *MNRAS*, 359, 345-362
- . van der Klis M., (2004), A review of rapid X-ray variability in X-ray binaries, (astro-ph/0410551)
- . Vadawale S. V., Rao A. R., Chakrabarti S. K., (2001), Spectral differences between the radio-loud and radio-quiet low-hard states of GRS 1915+105, *A&A*, 372, 793-802
- . Vadawale S. V., Rao A. R., Naik S., Yadav J. S., Ishwara-Chandra C. H., Pramesh Rao A., Pooley G. G., (2003), On the Origin of the Various Types of Radio Emission in GRS 1915+105, *ApJ*, 597, 1023-1035
- . van Straaten S., van der Klis M., Wijnands R., (2005), Relations Between Timing Features and Colors in Accreting Millisecond Pulsars, *ApJ*, 619, 455-482
- . van Paradijs J., (1996), On the Accretion Instability in Soft X-Ray Transients, *ApJ*, 464, L139-L141
- . Vaughan B. A., et al., (1994), Searches for millisecond pulsations in low-mass X-ray binaries, 2, *ApJ*, 435, 362-371
- . Watarai K.-Y., Fukue J., Takeuchi M., Mineshige S., (2000), Galactic Black-Hole Candidates Shining at the Eddington Luminosity, *PASJ*, 52, 133-141
- . White N. E., Stella L., Parmar A. N., (1988), The X-ray spectral properties of accretion discs in X-ray binaries *ApJ*, 324, 363-378
- . Wijnands R., van der Klis M., (1999), The Broadband Power Spectra of X-Ray Binaries, *ApJ*, 514, 939-944

-
- . Wilms J., Nowak M. A., Dove J. B., Fender R. P., di Matteo T., (1999), Low-Luminosity States of the Black Hole Candidate GX 339-4. I. ASCA and Simultaneous Radio/RXTE Observations, *ApJ*, 522, 460-475
 - . Woods D. T., Klein R. I., Castor J. I., McKee C. F., Bell J. B., (1996), X-Ray-heated Coronae and Winds from Accretion Disks: Time-dependent Two-dimensional Hydrodynamics with Adaptive Mesh Refinement, *ApJ*, 461, 767-804
 - . Yamaoka K., Ueda Y., Inoue H., Nagase F., Ebisawa K., Kotani T., Tanaka Y., Zhang S. N., (2001), ASCA Observation of the Superluminal Jet Source GRO J1655-40 in the 1997 Outburst, *PASJ*, 53, 179-188
 - . Yoshida K., Mitsuda K., Ebisawa K., Ueda Y., Fujimoto R., Yaqoob T., Done C., (1993), Low state properties of the low-mass X-ray binary X1608-522 observed with GINGA, *PASJ*, 45, 605-616
 - . Yuan F., (2001), Luminous hot accretion discs, *MNRAS*, 324, 119-127
 - . Yuan F., Zdziarski A. A., Xue Y., Wu X.-B., (2007), Modeling the Hard States of XTE J1550-564 during Its 2000 Outburst, *ApJ*, 659, 541-548
 - . Zdziarski A. A., Gierliński M., (2004), Radiative Processes, Spectral States and Variability of Black-Hole Binaries, *PThPS*, 155, 99-119
 - . Zdziarski A. A., Lubinski P., Smith D. A., (1999), Correlation between Compton reflection and X-ray slope in Seyferts and X-ray binaries, *MNRAS*, 303, L11-L15
 - . Zdziarski A. A., Grove J. E., Poutanen J., Rao A. R., Vadawale S. V., (2001), OSSE and RXTE Observations of GRS 1915+105: Evidence for Nonthermal Comptonization, *ApJ*, 554, L45-L48
 - . Zdziarski A. A., Lubinski P., Gilfanov M., Revnivtsev M., (2003), Correlations between X-ray and radio spectral properties of accreting black holes, *MNRAS*, 342, 355-372
 - . Zdziarski A. A., Gierliński M., Rao A. R., Vadawale S. V., Mikołajewska J., (2005), GRS 1915+105: the distance, radiative processes and energy-dependent variability, 360, 825-838
 - . Zhang S. N., Cui W., Harmon B. A., Paciesas W. S., Remillard R. E., van Paradijs J., (1997), The 1996 Soft State Transition of Cygnus X-1, *ApJ*, 477, L95-L98
 - . Zhang, S. N., Cui, W., & Chen, W. (1997), Black Hole Spin in X-Ray Binaries: Observational Consequences, *ApJ*, 482, L155-L158
 - . Zycki P. T., Czerny B., (1994), The Iron K-Alpha Line from a Partially Ionized Reflecting Medium in an Active Galactic Nucleus, *MNRAS*, 266, 653-668